

# Efficient data augmentation techniques for state space models

Linda S. L. Tan (statsll@nus.edu.sg)

National University of Singapore

## Abstract

In the first part of the article, we propose a data augmentation scheme for improving the rate of convergence of the EM algorithm in estimating Gaussian state space models. The scheme considers a linear transformation of the latent states in which two working parameters are introduced for rescaling and recentering. We derive optimal values of the working parameters by minimizing the fraction of missing information, and study their large sample properties and dependence on the persistence and signal-to-noise ratio. An alternating expectation-conditional maximization (AECM) algorithm is designed to take advantage of the proposed scheme, and shown to be a more attractive alternative to the centered parametrization (CP) or noncentered parametrization (NCP). In the second part, we extend earlier results to Bayesian Markov chain Monte Carlo (MCMC) algorithms for non-Gaussian state space models, focusing on the stochastic volatility and stochastic conditional duration models. A block-specific reparametrization (BSR) strategy for multi-block MCMC samplers is proposed which enables the EM data augmentation scheme to be applied to non-Gaussian models via a mixture of normals approximation. Applications on simulated data and benchmark real data sets indicate that the BSR strategy is able to yield improvements in simulation efficiency compared with the CP or NCP, and sometimes even over ASIS (which interweaves the CP and NCP).

**Keywords:** Gaussian state space models, EM algorithm, Rate of convergence, Stochastic volatility models, Stochastic conditional duration models, Model reparametrization, Bayesian Markov chain Monte Carlo algorithm.

## 1 Introduction

The expectation-maximization or EM algorithm ([Dempster et al., 1977](#)) is an iterative method for maximum likelihood estimation that is widely used in missing data problems. For state space models, the EM algorithm provides a natural approach for estimating the model parameters (e.g. [Shumway and Stoffer, 1982](#)), as the latent states can be taken as the missing data and the E-step can be performed using smoothed estimates from the

Kalman filter (Kalman, 1960). Compared with other techniques like scoring or Newton-Raphson, the EM algorithm has attractive features such as numerical stability (each iteration increases the observed data likelihood) and guaranteed convergence to a local maximum for exponential families (Wu, 1983). However, the EM algorithm may converge slowly in later stages of the iterative procedure despite moving quickly to a region close to the maximum (Watson and Engle, 1983; Harvey and Peters, 1990).

The rate of convergence of the EM algorithm is governed by the *fraction of missing information* in the data augmentation scheme. Let  $Y_{\text{aug}} = (Y_{\text{obs}}, Y_{\text{mis}})$  denote the augmented data, where  $Y_{\text{obs}}$  is the observed data and  $Y_{\text{mis}}$  is the missing data. Let  $\theta^*$  be the maximum likelihood estimate (MLE) of unknown parameter  $\theta$  and  $\nabla_{\theta}^2(\cdot) = \partial^2(\cdot)/\partial\theta\partial\theta^T$ . The (matrix) rate of convergence of the EM algorithm (Dempster et al., 1977) is

$$\text{DM} = I_{\text{aug}}(\theta^*)^{-1} I_{\text{mis}}(\theta^*) = I - I_{\text{aug}}(\theta^*)^{-1} I_{\text{obs}}(\theta^*), \quad (1)$$

where  $I_{\text{obs}}(\theta) = \nabla_{\theta}^2 \log p(Y_{\text{obs}} | \theta)$ ,  $I_{\text{aug}}(\theta) = -E_{Y_{\text{mis}}|Y_{\text{obs}},\theta}[\nabla_{\theta}^2 \log p(Y_{\text{aug}} | \theta)]$  and  $I_{\text{mis}}(\theta) = -E_{Y_{\text{mis}}|Y_{\text{obs}},\theta}[\nabla_{\theta}^2 \log p(Y_{\text{mis}} | Y_{\text{obs}}, \theta)]$ . The actual observed (global) rate of convergence is given by the largest eigenvalue of DM, and a larger value indicates slower convergence. The EM algorithm converges slowly (DM is close to identity) if the proportion of missing information relative to augmented information is large. Conversely, convergence is rapid (DM is close to zero) if the observed information is close to the augmented information. Thus, the rate of convergence can be optimized by minimizing the missing information. Meng and van Dyk (1997, 1998) develop augmentation schemes for the multivariate  $t$ -model and mixed effects models by rescaling the missing data, and introducing “working parameters” that control the portion of the scale factor shifted into the missing data. Optimal values of the working parameters are found by minimizing the fraction of missing information. A similar approach was considered by Tan et al. (2007) for quadratic optimization problems. The PX-EM algorithm (Liu et al., 1998) also seeks to reduce the fraction of missing information albeit by expanding the set of model parameters to adjust the covariance among parameters in the M-step.

In the first part of this article, we consider Gaussian state space models of the form:

$$\begin{aligned} y_t &= x_t + \sigma_{\epsilon}\epsilon_t, & t &= 1, \dots, n, \\ x_t &= \mu + \phi(x_{t-1} - \mu) + \sigma_{\eta}\eta_t, & t &= 2, \dots, n, \\ x_1 &\sim N(\mu, \sigma_{\eta}^2/(1 - \phi^2)), \end{aligned} \quad (2)$$

where  $\mathbf{y} = (y_1, \dots, y_n)^T$  are the observations,  $\mathbf{x} = (x_1, \dots, x_n)^T$  are the latent states,  $|\phi| < 1$ ,  $\sigma_{\epsilon} > 0$ ,  $\sigma_{\eta} > 0$  and  $\mu \in \mathbb{R}$ . The  $\{\epsilon_t\}$  and  $\{\eta_s\}$  sequences are distributed as standard normals, independent for all  $t$  and  $s$ , and of  $\{x_t\}$ . Let  $\theta = (\mu, \sigma_{\eta}^2, \phi, \sigma_{\epsilon}^2)$  be the model parameters. This model is called the AR(1) plus noise or ARMA(1,1) model in time

series analysis (Durbin and Koopman, 2012), and the signal-to-noise ratio is defined as  $\gamma = \sigma_\eta^2 / \sigma_\epsilon^2$ . We propose a data augmentation scheme that introduces working parameters,  $a$  and  $\mathbf{w} = (w_1, \dots, w_n)^T$  to rescale and recenter the latent states. For  $t = 1, \dots, n$ , we define transformed latent state  $\alpha_t$  as

$$\alpha_t = (x_t - w_t \mu) / \sigma_\eta^a, \quad a \in \mathbb{R}, w_t \in \mathbb{R}. \quad (3)$$

Let  $\mathbf{1}$  and  $\mathbf{0}$  denote the vectors of all ones and zeros respectively (dimension inferred from context). Suppose  $a = 0$ . In the context of Markov chain Monte Carlo (MCMC) algorithms, (3) is known as the noncentered parametrization (NCP) when  $\mathbf{w} = \mathbf{1}$  and centered parametrization (CP) when  $\mathbf{w} = \mathbf{0}$ . For random effect models (Gelfand et al., 1995, 1996), Gaussian state space models (Pitt and Shephard, 1999; Frühwirth-Schnatter, 2004) and a large class of hierarchical models (Papaspiliopoulos et al., 2003, 2007), it has been shown that the convergence rates of MCMC algorithms depend critically on the parametrization (Roberts and Sahu, 1997). In addition, the CP and NCP play complementary roles in that the Gibbs sampler often converges much faster under one parametrization than the other. To take advantage of this contrasting feature, Yu and Meng (2011) propose ASIS, an ancillarity-sufficiency strategy that interweaves these two parametrizations.

A less known alternative is the partially noncentered parametrization (PNCP), which is capable of yielding better convergence than both the CP and NCP, when fitting random effect models using Gibbs samplers (Papaspiliopoulos et al., 2003). Partial noncentering (of the mean) assumes the form of (3) with  $a = 0$  and  $0 < w_t < 1$ , and is regarded as lying on the continuum between the CP and NCP. In this article, we consider a data augmentation scheme or parametrization of the Gaussian state space model where *both* the location and scale are partially noncentered, and investigate how this scheme can be optimized to construct efficient EM algorithms. Optimal values of  $(a, \mathbf{w})$  are derived under different settings and their (large sample) properties are studied, which reveal features distinct from those in random effect models. To enable the optimal parametrization for inferring each parameter to be used, we designed an alternating expectation-conditional maximization (AECM) algorithm (Meng and van Dyk, 1997), which proves to be an attractive alternative to the CP and NCP for both simulated and real data.

The rate of convergence of EM algorithms and Gibbs samplers are closely linked (Sahu and Roberts, 1999), and in the second part of the paper, we demonstrate how the data augmentation schemes optimized for the EM algorithm can be transferred to Bayesian MCMC algorithms with similar benefits. We focus on two non-Gaussian state space models, the stochastic volatility (SV) model for financial returns (Taylor, 1982) and stochastic conditional duration (SCD) model (Bauwens and Veredas, 2004) for time intervals between transactions, which can be linked to Gaussian state space models via mixture of normals approximations (Kim et al., 1998). A block-specific reparametrization

(BSR) strategy for MCMC samplers is proposed, which allows the parametrization of the latent states to vary across blocks and the data augmentation schemes optimized for EM to be incorporated into the sampler. Comparison of the BSR strategy with the CP, NCP and ASIS on simulated data and several real applications indicate that BSR is always able to perform better than the worse of CP and NCP, and often able to surpass both and even ASIS. The BSR strategy is applicable quite generally, there remains much room in the search of "optimal" block-specific reparametrization schemes for MCMC samplers. It will also be interesting to explore how our data augmentation scheme can be extended to variational approximation methods, which we only touch on lightly in this article.

## 2 EM algorithm for partially noncentered Gaussian state space model

The Gaussians state space model in 2 can be re-expressed in terms of  $\{\alpha_t\}$  as

$$\begin{aligned} y_t &= \sigma_\eta^a \alpha_t + w_t \mu + \sigma_\epsilon \epsilon_t, \quad t = 1, \dots, n, \\ \sigma_\eta^a \alpha_t &= \bar{w}_t \mu + \phi(\sigma_\eta^a \alpha_{t-1} - \bar{w}_{t-1} \mu) + \sigma_\eta \eta_t, \quad t = 2, \dots, n, \\ \sigma_\eta^a \alpha_1 &\sim N(\bar{w}_1 \mu, \sigma_\eta^2 / (1 - \phi^2)), \end{aligned} \quad (4)$$

where  $\bar{w}_t = 1 - w_t$ . Now  $\mu$  and  $\sigma_\eta$  appear in both the observation and state equations. Let  $\boldsymbol{\alpha} = (\alpha_1, \dots, \alpha_n)^T$  and  $\bar{\mathbf{w}} = (\bar{w}_1, \dots, \bar{w}_n)^T$ . When  $a = 0$  and  $\mathbf{w} = \mathbf{0}$ , we recover the fully centered parametrization (CP) in (2), so called as the latent state  $x_t$  is centered around the a priori expected value  $\mu$  and the parameters  $\mu, \sigma_\eta^2$  appear only in the state equation. The fully noncentered parametrization (NCP) is obtained when  $a = 1$  and  $\mathbf{w} = \mathbf{1}$ . In matrix notation, (4) can be expressed as

$$\mathbf{y} \mid \boldsymbol{\alpha}, \boldsymbol{\theta} \sim N(\sigma_\eta^a \boldsymbol{\alpha} + \mu \mathbf{w}, \sigma_\epsilon^2 I), \quad \sigma_\eta^a \boldsymbol{\alpha} \mid \boldsymbol{\theta} \sim N(\mu \bar{\mathbf{w}}, \sigma_\eta^2 \Lambda^{-1}), \quad (5)$$

where  $\Lambda$  is a symmetric *tridiagonal* matrix with off-diagonal elements equal to  $-\phi$  and the diagonal given by  $(1, 1 + \phi^2, \dots, 1 + \phi^2, 1)^T$ . For  $|\phi| < 1$ ,  $\Lambda$  is invertible. Let  $\Lambda_1 = \partial \Lambda / \partial \phi$ , which is also a symmetric tridiagonal matrix with diagonal  $(0, 2\phi, \dots, 2\phi, 0)^T$  and off-diagonal elements equal to  $-1$ . Regardless of the parametrization, the marginal distribution of  $\mathbf{y}$  is  $N(\mu \mathbf{1}, S)$  where  $S = \sigma_\epsilon^2 I + \sigma_\eta^2 \Lambda^{-1}$ .

Suppose we wish to find the MLE,  $\boldsymbol{\theta}^* = (\mu^*, \sigma_\eta^{2*}, \phi^*, \sigma_\epsilon^{2*})$ , that maximizes the observed data log-likelihood  $\log p(\mathbf{y} \mid \boldsymbol{\theta}) = \log \int p(\boldsymbol{\alpha}, \mathbf{y} \mid \boldsymbol{\theta}) d\boldsymbol{\alpha}$  using an EM algorithm. We consider the latent states  $\boldsymbol{\alpha}$  as missing data and  $(\mathbf{y}, \boldsymbol{\alpha})$  as augmented data. Given an initial estimate  $\boldsymbol{\theta}^{(0)}$ , the algorithm performs an E-step and M-step at each iteration  $i$ , where the E-step computes  $Q(\boldsymbol{\theta} \mid \boldsymbol{\theta}^{(i)}) = E_{\boldsymbol{\alpha} \mid \mathbf{y}, \boldsymbol{\theta}^{(i)}}[\log p(\boldsymbol{\alpha}, \mathbf{y} \mid \boldsymbol{\theta})]$ , and the M-step maximizes  $Q(\boldsymbol{\theta} \mid \boldsymbol{\theta}^{(i)})$  with

respect to  $\boldsymbol{\theta}$ . The conditional distribution  $p(\boldsymbol{\alpha} \mid \mathbf{y}, \boldsymbol{\theta})$  is  $N(\mathbf{m}_{a\mathbf{w}}, V_a)$ , where

$$V_a = \sigma_\eta^{-2a}(\sigma_\epsilon^{-2}I + \sigma_\eta^{-2}\Lambda)^{-1}, \quad \mathbf{m}_{a\mathbf{w}} = \sigma_\eta^a V_a [(\mathbf{y} - \mu\mathbf{w})/\sigma_\epsilon^2 + \mu\sigma_\eta^{-2}\Lambda\bar{\mathbf{w}}]. \quad (6)$$

The subscripts of  $V_a$  and  $\mathbf{m}_{a\mathbf{w}}$  represent their dependence on the values of  $a$  and  $\mathbf{w}$  in the scheme. For instance, when  $a = 0$  and  $\mathbf{w} = \mathbf{1}$ ,

$$V_0 = (\sigma_\epsilon^{-2}I + \sigma_\eta^{-2}\Lambda)^{-1}, \quad \mathbf{m}_{0\mathbf{1}} = V_0(\mathbf{y} - \mu\mathbf{1})/\sigma_\epsilon^2. \quad (7)$$

It can be derived that

$$\begin{aligned} Q(\boldsymbol{\theta} \mid \boldsymbol{\theta}^{(i)}) = & \frac{1}{2} [\log(1 - \phi^2) - (\mathbf{y} - \mu\mathbf{w} - \sigma_\eta^a \mathbf{m}_{a\mathbf{w}}^{(i)})^T (\mathbf{y} - \mu\mathbf{w} - \sigma_\eta^a \mathbf{m}_{a\mathbf{w}}^{(i)}) / \sigma_\epsilon^2 \\ & - \sigma_\eta^{2a} \text{tr}(V_a^{(i)}) / \sigma_\epsilon^2 - n \log \sigma_\epsilon^2 - n(1 - a) \log \sigma_\eta^2 - \sigma_\eta^{2(a-1)} \text{tr}(\Lambda V_a^{(i)}) \\ & - \sigma_\eta^{-2} (\sigma_\eta^a \mathbf{m}_{a\mathbf{w}}^{(i)} - \mu\bar{\mathbf{w}})^T \Lambda (\sigma_\eta^a \mathbf{m}_{a\mathbf{w}}^{(i)} - \mu\bar{\mathbf{w}})] - n \log(2\pi), \end{aligned}$$

where  $\mathbf{m}_{a\mathbf{w}}^{(i)}$  and  $V_a^{(i)}$  are evaluated at  $\boldsymbol{\theta}^{(i)}$ . At each iteration, the EM algorithm updates  $\mathbf{m}_{a\mathbf{w}}$  and  $V_a$  given  $\boldsymbol{\theta}^{(i)}$  and sets  $\boldsymbol{\theta}^{(i+1)} = \arg \max_{\boldsymbol{\theta}} Q(\boldsymbol{\theta} \mid \boldsymbol{\theta}^{(i)})$ . The expectation-conditional maximization (ECM) algorithm (Meng and Rubin, 1993) reduces the complexity of the M-step by replacing it with a sequence of conditional maximization steps. If we maximize  $Q(\boldsymbol{\theta} \mid \boldsymbol{\theta}^{(i)})$  with respect to each element  $\theta_s$  of  $\boldsymbol{\theta}$  with the remaining elements held fixed at current values, then the update of  $\theta_s$  can be obtained by setting  $\partial Q(\boldsymbol{\theta} \mid \boldsymbol{\theta}^{(i)}) / \partial \theta_s = 0$ . This yields the following closed form updates for  $\mu$  and  $\sigma_\epsilon^2$ :

$$\begin{aligned} \mu = & \frac{\sigma_\epsilon^{-2}(\mathbf{y} - \sigma_\eta^a \mathbf{m}_{a\mathbf{w}}^{(i)})^T \mathbf{w} + \sigma_\eta^{a-2} \mathbf{m}_{a\mathbf{w}}^{(i)T} \Lambda \bar{\mathbf{w}}}{\sigma_\epsilon^{-2} \mathbf{w}^T \mathbf{w} + \sigma_\eta^{-2} \bar{\mathbf{w}}^T \Lambda \bar{\mathbf{w}}}, \\ \sigma_\epsilon^2 = & \frac{1}{n} [\sigma_\eta^{2a} \text{tr}(V_a^{(i)}) + (\mathbf{y} - \mu\mathbf{w} - \sigma_\eta^a \mathbf{m}_{a\mathbf{w}}^{(i)})^T (\mathbf{y} - \mu\mathbf{w} - \sigma_\eta^a \mathbf{m}_{a\mathbf{w}}^{(i)})]. \end{aligned} \quad (8)$$

Setting  $\partial Q(\boldsymbol{\theta} \mid \boldsymbol{\theta}^{(i)}) / \partial \sigma_\eta^2 = 0$  yields

$$\begin{aligned} (1 - a) \{ n \sigma_\eta^2 - \sigma_\eta^{2a} [\text{tr}(\Lambda V_a^{(i)}) + \mathbf{m}_{a\mathbf{w}}^{(i)T} \Lambda \mathbf{m}_{a\mathbf{w}}^{(i)}] \} + (2 - a) \mu \sigma_\eta^a \mathbf{m}_{a\mathbf{w}}^{(i)T} \Lambda \bar{\mathbf{w}} \\ = \mu^2 \bar{\mathbf{w}}^T \Lambda \bar{\mathbf{w}} + a \sigma_\eta^{2+a} \sigma_\epsilon^{-2} \{ (\mathbf{y} - \mu\mathbf{w})^T \mathbf{m}_{a\mathbf{w}}^{(i)} - \sigma_\eta^a [\text{tr}(V_a^{(i)}) + \mathbf{m}_{a\mathbf{w}}^{(i)T} \mathbf{m}_{a\mathbf{w}}^{(i)}] \}. \end{aligned} \quad (9)$$

Closed form updates are available for the CP and NCP:

$$\sigma_\eta^2 = \begin{cases} [(\mathbf{m}_{00}^{(i)} - \mu\mathbf{1})^T \Lambda (\mathbf{m}_{00}^{(i)} - \mu\mathbf{1}) + \text{tr}(\Lambda V_0^{(i)})] / n & \text{if CP } (a = 0, \mathbf{w} = \mathbf{0}), \\ \{(\mathbf{y} - \mu\mathbf{1})^T \mathbf{m}_{11}^{(i)}\}^2 / \{ \text{tr}(V_1^{(i)}) + \mathbf{m}_{11}^{(i)T} \mathbf{m}_{11}^{(i)} \}^2 & \text{if NCP } (a = 1, \mathbf{w} = \mathbf{1}). \end{cases}$$

There are no closed form updates for  $\sigma_\eta^2$  and  $\phi$  for arbitrary values of  $(a, \mathbf{w})$ . For  $\phi$ , closed form updates do not exist for the CP and NCP as well. We use the `optimize` function

from the `Optim` package (Mogensen and Riseth, 2018) in `Julia` to maximize  $Q(\boldsymbol{\theta} \mid \boldsymbol{\theta}^{(i)})$  with respect to these parameters. Brent's method is used to find  $\phi \in (-1, 1)$  while the unconstrained L-BFGS method is used to find  $\nu = \log \sigma_\eta^2$ .

We are interested in finding values of  $(a, \mathbf{w})$  that optimize the rate of convergence of the EM algorithm. From (1),  $I_{\text{obs}}(\boldsymbol{\theta}^*)$  depends only on the observed data and is independent of the parametrization. Hence it is sufficient to minimize  $I_{\text{aug}}(\boldsymbol{\theta}^*)$  with respect to  $(a, \mathbf{w})$ . Let  $I_{\theta_i, \theta_j}$  denote the  $(i, j)$  element in  $I_{\text{aug}}(\boldsymbol{\theta}^*)$ . We first consider cases where only the location  $\mu$  or scale  $\sigma_\eta^2$  is unknown, followed by the case where all parameters are unknown.

## 2.1 Unknown location parameter

Suppose  $\sigma_\eta^2$ ,  $\phi$  and  $\sigma_\epsilon^2$  are known and  $\mu$  is the only unknown parameter. The EM algorithm for this case (Algorithm 1) alternately updates  $\mathbf{m}_{a\mathbf{w}}^{(i)}$  and  $\mu$  as in (6) and (8).

**Theorem 1.** *The rate of convergence of Algorithm 1 is*

$$1 - (\mathbf{1}^T S^{-1} \mathbf{1}) / \tau(\mathbf{w}) = \rho(\mathbf{w})^T V_0 \rho(\mathbf{w}) / \tau(\mathbf{w}),$$

where  $\tau(\mathbf{w}) = \sigma_\epsilon^{-2} \mathbf{w}^T \mathbf{w} + \sigma_\eta^{-2} \bar{\mathbf{w}}^T \Lambda \bar{\mathbf{w}}$  and  $\rho(\mathbf{w}) = V_0^{-1} \mathbf{w} - \sigma_\eta^{-2} \Lambda \mathbf{1}$ . This rate is minimized to zero at

$$\mathbf{w}^{\text{opt}} = \sigma_\eta^{-2} V_0 \Lambda \mathbf{1} \quad \text{or} \quad \bar{\mathbf{w}}^{\text{opt}} = \sigma_\epsilon^{-2} V_0 \mathbf{1}. \quad (10)$$

*Proof.* It is shown in Section S1 and S3 of the supplementary material that  $I_{\text{obs}} = \mathbf{1}^T S^{-1} \mathbf{1}$  and  $I_{\text{aug}} = \tau(\mathbf{w})$ . From (1), the rate of convergence is  $1 - I_{\text{obs}} I_{\text{aug}}^{-1}$ . Since  $\rho(\mathbf{w}) = 0$  only at  $\mathbf{w} = \sigma_\eta^{-2} V_0 \Lambda \mathbf{1}$ , the convergence rate is minimized to zero at  $\mathbf{w}^{\text{opt}}$ .  $\square$

From Theorem 1, the rate of convergence of Algorithm 1 for the CP ( $\mathbf{w} = \mathbf{0}$ ) and NCP ( $\mathbf{w} = \mathbf{1}$ ) are  $(\mathbf{1}^T \Lambda V_0 \Lambda \mathbf{1}) / (\sigma_\eta^2 \mathbf{1}^T \Lambda \mathbf{1})$  and  $(\mathbf{1}^T V_0 \mathbf{1}) / (n \sigma_\epsilon^2)$  respectively. However, when  $\mathbf{w} = \mathbf{w}^{\text{opt}}$ , Algorithm 1 converges instantly to

$$\mu^* = \frac{\mathbf{y}^T S^{-1} \mathbf{1}}{\mathbf{1}^T S^{-1} \mathbf{1}}.$$

This can be seen by plugging  $\mathbf{w}^{\text{opt}}$  into the update in (8). It is possible to compute  $\mathbf{w}^{\text{opt}}$  in advance for Algorithm 1 as  $\mathbf{w}^{\text{opt}}$  does not depend on  $\mu$ , and the rate of convergence is also independent of  $a$ , so that  $a$  can be set to any convenient value.

We investigate the range of elements in  $\mathbf{w}^{\text{opt}}$  and their dependence on  $(\sigma_\eta^2, \phi, \sigma_\epsilon^2)$  by deriving an explicit expression for  $\mathbf{w}^{\text{opt}}$ . From (10),  $\bar{\mathbf{w}}^{\text{opt}}$  is simply the row sums of  $V_0$  divided by  $\sigma_\epsilon^2$ . We first present an expression for  $V_0$  and some important properties. Recall that  $V_0^{-1} = \sigma_\epsilon^{-2} I + \sigma_\eta^{-2} \Lambda$  and  $\sigma_\eta^2 V_0^{-1} = \gamma I + \Lambda$ . If  $\phi \neq 0$ , let

$$Q = \sigma_\eta^2 V_0^{-1} / |\phi|,$$

so that  $Q$  is a symmetric tridiagonal matrix with diagonal  $(d, c, \dots, c, d)^T$  and off-diagonal elements equal to  $-b$ , where  $b = \phi/|\phi|$ ,  $d = (\gamma + 1)/|\phi|$  and  $c = d + |\phi|$ . Note that  $b = \pm 1$ ,  $d > 1$  and  $c > 2$ . From Corollary 2, Property 2 and Theorems 2 and 5 of Tan (2019), we have the following properties of  $Q^{-1}$  respectively.

**Property 1.** If  $\phi \neq 0$ ,  $Q_{ij}^{-1} = u_i v_j$  for  $i \leq j$ , where

$$\begin{aligned} v_i &= b^{i-1} \kappa_{n-i} / \kappa, & u_i &= b^{i-1} \kappa_{i-1} / \kappa_0 \quad (i = 1, \dots, n), \\ \kappa &= \varphi_+^2 r_+^{n-1} - \varphi_-^2 r_-^{n-1}, & \kappa_i &= \varphi_+ r_+^i - \varphi_- r_-^i \quad (i = 0, \dots, n-1), \\ \varphi_{\pm} &= r_{\pm} - |\phi|, & r_{\pm} &= (c \pm \sqrt{c^2 - 4})/2. \end{aligned}$$

**Property 2.** If  $0 < \phi < 1$ ,  $u_i$  and  $v_i$  are positive for  $i = 1, \dots, n$ , and all elements of  $Q^{-1}$  are positive.

**Property 3.** The sum of the  $i$ th row of  $Q^{-1}$  is  $s_i = \{1 - b(1 - \phi)(v_i + v_{n-i+1})\}/(c - 2b)$ . If  $0 < \phi < 1$ ,  $(d - \phi)^{-1} < s_i < (c - 2)^{-1}$ . If  $-1 < \phi < 0$ ,  $2/(c + 2) - (d + \phi)^{-1} < s_i < (d + \phi)^{-1}$ .

**Theorem 2.** Let  $w_t^{\text{opt}}$  be the  $t^{\text{th}}$  element of  $\mathbf{w}^{\text{opt}}$ . If  $\phi = 0$ ,  $w_t^{\text{opt}} = (1 + \gamma)^{-1}$  and

$$w_t^{\text{opt}} = \frac{(1 - \phi)^2 + b\gamma(1 - \phi)(v_t + v_{n-t+1})}{(1 - \phi)^2 + \gamma} \quad \text{if } \phi \neq 0. \quad (11)$$

*Proof.* If  $\phi = 0$ ,  $\Lambda = I$  and  $V_0 = \sigma_\eta^2/(1 + \gamma)I$ . Hence  $\mathbf{w}^{\text{opt}} = 1/(1 + \gamma)\mathbf{1}$ . If  $\phi \neq 0$ ,  $\bar{\mathbf{w}}^{\text{opt}} = \gamma/|\phi|Q^{-1}\mathbf{1}$  and  $w_t^{\text{opt}} = 1 - \gamma s_t/|\phi|$ . Substituting the expression for  $s_t$  from Property 3 and noting that  $|\phi|(c - 2b) = (1 - \phi)^2 + \gamma$  yields the result in (11).  $\square$

As  $u_1 = 1$  and  $Q_{1j}^{-1} = v_j$  from Property 1, Theorem 2 implies that  $\mathbf{w}^{\text{opt}}$  can be computed using only elements from the first row of  $Q^{-1}$ . In addition,  $\mathbf{w}^{\text{opt}}$  is symmetric since  $w_t^{\text{opt}} = w_{n-t+1}^{\text{opt}}$  for each  $t$ . It is clear that  $\mathbf{w}^{\text{opt}}$  depends on  $\phi$ , and on  $\sigma_\eta^2$  and  $\sigma_\epsilon^2$  only through the signal-to-noise ratio  $\gamma$ . Corollary 1 presents bounds for  $\mathbf{w}^{\text{opt}}$  which are tight when  $\phi = 0$ , showing that  $0 < w_t^{\text{opt}} < 1$  if  $\phi \in [0, 1)$  and  $0 < w_t^{\text{opt}} < 2$  if  $\phi \in (-1, 0)$ . If  $\phi > 0$ , Corollary 2 shows that the location centered parametrization ( $\mathbf{w} = \mathbf{0}$ ) is increasingly preferred as  $\phi$  and  $\gamma$  increase.

**Corollary 1.** For  $t = 1, \dots, n$ ,

$$\begin{aligned} 0 < 1 - B_1 &\leq w_t^{\text{opt}} \leq 1 - B_2 < 1 \quad (0 \leq \phi < 1), \\ 0 < 1 - B_2 &\leq w_t^{\text{opt}} \leq 1 + B_2 - 2B_1 < 2 \quad (-1 < \phi < 0), \end{aligned}$$

where  $B_1 = \gamma/\{(1 - \phi)^2 + \gamma\}$  and  $B_2 = \gamma/(1 - \phi^2 + \gamma)$ . When  $0 \leq \phi < 1$ ,  $0 < B_2 \leq B_1 < 1$  and when  $-1 < \phi < 0$ ,  $0 < B_1 < B_2 < 1$ .

*Proof.* From Theorem 2,  $w_t^{\text{opt}} = (1 + \gamma)^{-1}$  if  $\phi = 0$  which is the value of the lower and upper bounds. If  $0 < \phi < 1$ ,  $b = 1$  and  $v_t > 0$  for  $t = 1, \dots, n$  from Property 2. Hence

$w_t^{\text{opt}} > 1 - B_1$  from (11). From Property 3,  $s_t > (d - \phi)^{-1}$  implies that  $w_t^{\text{opt}} = 1 - \gamma s_t / |\phi| < 1 - \gamma / \{\phi(d - \phi)\} = 1 - B_2$ . If  $-1 < \phi < 0$ ,  $b = -1$  and  $\phi = -|\phi|$ . From Property 3,  $2/(c + 2) - 1/(d + \phi) < s_t < 1/(d + \phi)$  implies  $1 - B_2 \leq w_t^{\text{opt}} \leq 1 + B_2 - 2B_1$ .  $\square$

**Corollary 2.** *If  $0 < \phi < 1$ , each element of  $\mathbf{w}^{\text{opt}}$  decreases strictly as  $\phi$  and the signal-to-noise ratio  $\gamma$  increase. As  $\phi$  approaches 1,  $\mathbf{w}^{\text{opt}}$  approaches  $\mathbf{0}$ .*

*Proof.* Writing  $\mathbf{w}^{\text{opt}} = (\gamma \Lambda^{-1} + I)^{-1} \mathbf{1}$ ,

$$\frac{\partial \mathbf{w}^{\text{opt}}}{\partial \gamma} = -\frac{Q^{-1} \mathbf{w}^{\text{opt}}}{|\phi|}, \quad \frac{\partial \mathbf{w}^{\text{opt}}}{\partial \phi} = \frac{Q^{-1} \Lambda_1 \bar{\mathbf{w}}^{\text{opt}}}{|\phi|}.$$

From Property 2 and Corollary 1, all elements of  $Q^{-1}$  and  $\mathbf{w}^{\text{opt}}$  are positive. Hence each element of  $\partial \mathbf{w}^{\text{opt}} / \partial \gamma$  is negative and  $w_t^{\text{opt}}$  decreases strictly with  $\gamma$  for all  $t$ . To show that each element of  $\partial \mathbf{w}^{\text{opt}} / \partial \phi$  is negative, it suffices to show that each element of  $\Lambda_1 \bar{\mathbf{w}}_{\text{opt}}$  (a symmetric vector) is negative. The first and last elements are equal to  $-\bar{w}_2^{\text{opt}}$ , which is negative from Corollary 1. For  $t = 2, \dots, n - 1$ , the  $t^{\text{th}}$  element of  $\Lambda_1 \bar{\mathbf{w}}_{\text{opt}}$  is

$$2\phi \bar{w}_t^{\text{opt}} - \bar{w}_{t-1}^{\text{opt}} - \bar{w}_{t+1}^{\text{opt}} = \frac{\gamma}{\phi} [2\phi s_t - s_{t-1} - s_{t+1}] < 0$$

from Lemma S3 in the Supplementary material. It is clear from (11) that as  $\phi$  approaches 1,  $\mathbf{w}^{\text{opt}}$  approaches  $\mathbf{0}$ .  $\square$

Figure 1 illustrates the values of the elements in  $\mathbf{w}_{\text{opt}}$  when  $n = 10$  for different values of  $\gamma$  and  $\phi$ . As highlighted in Corollary 2, the location centered parametrization ( $\mathbf{w} = \mathbf{0}$ ) is increasingly preferred as  $\phi$  and  $\gamma$  increase when  $0 < \phi < 1$ . However, when  $-1 < \phi < 0$ ,  $w_t^{\text{opt}}$  may not be strictly decreasing with either  $\phi$  or  $\gamma$ .

From Theorem 1, the instant convergence rate of zero is achievable only if the portion of  $\mu$  subtracted from  $x_t$  in (3) is allowed to vary with  $t$ . However, in Theorem 3, we show that for large  $n$ , the convergence rate of Algorithm 1 goes to zero even if we assume  $w_t$  is common for all  $t$ , that is,  $\mathbf{w} = w\mathbf{1}$ . The optimal value  $w^{\text{opt}}$  is fast and easy to compute and reduces storage when  $n$  is large. Figure 2 shows how the rate of convergence of Algorithm 1 converges to zero as  $n$  increases if  $\mathbf{w} = w^{\text{opt}}\mathbf{1}$  for  $\phi \in \{-0.9, 0.9\}$  and  $\gamma \in \{0.1, 1, 10\}$ .

**Theorem 3.** *Assuming  $\mathbf{w} = w\mathbf{1}$ , the rate of convergence of Algorithm 1 is optimized at  $w^{\text{opt}} = 1/(1 + u)$ , where  $u = n\gamma/(\mathbf{1}^T \Lambda \mathbf{1})$ . As  $n \rightarrow \infty$ ,  $w^{\text{opt}} \rightarrow 1/(1 + u^*)$  where  $u^* = \gamma/(1 - \phi)^2$  and the optimized rate of convergence of Algorithm 1 goes to zero.*

*Proof.* If  $\mathbf{w} = w\mathbf{1}$ ,  $\nabla_w \tau(w\mathbf{1}) = 2[(\mathbf{1}^T V_0^{-1} \mathbf{1})w - \mathbf{1}^T \Lambda \mathbf{1} / \sigma_\eta^2]$  and  $\nabla_w^2 \tau(w\mathbf{1}) = 2(\mathbf{1}^T V_0^{-1} \mathbf{1}) > 0$ . Hence  $\tau(w\mathbf{1})$  is minimized at  $w^{\text{opt}} = 1/(1 + u)$  where  $u = n\gamma/(\mathbf{1}^T \Lambda \mathbf{1})$ , and  $\tau(w^{\text{opt}}\mathbf{1}) = n/[\sigma_\epsilon^2(1 + u)]$ . Since  $\mathbf{1}^T \Lambda \mathbf{1} = n(1 - \phi)^2 + 2\phi(1 - \phi)$ ,  $u \rightarrow u^*$  and hence  $w^{\text{opt}} \rightarrow 1/(1 + u^*)$  as  $n \rightarrow \infty$ . The rate of convergence of Algorithm 1 at  $w^{\text{opt}}$  is

$$1 - \sigma_\epsilon^2(1 + u)\mathbf{1}^T S^{-1} \mathbf{1} / n = 1 - (1 + u)(\mathbf{1}^T \mathbf{w}^{\text{opt}}) / n,$$

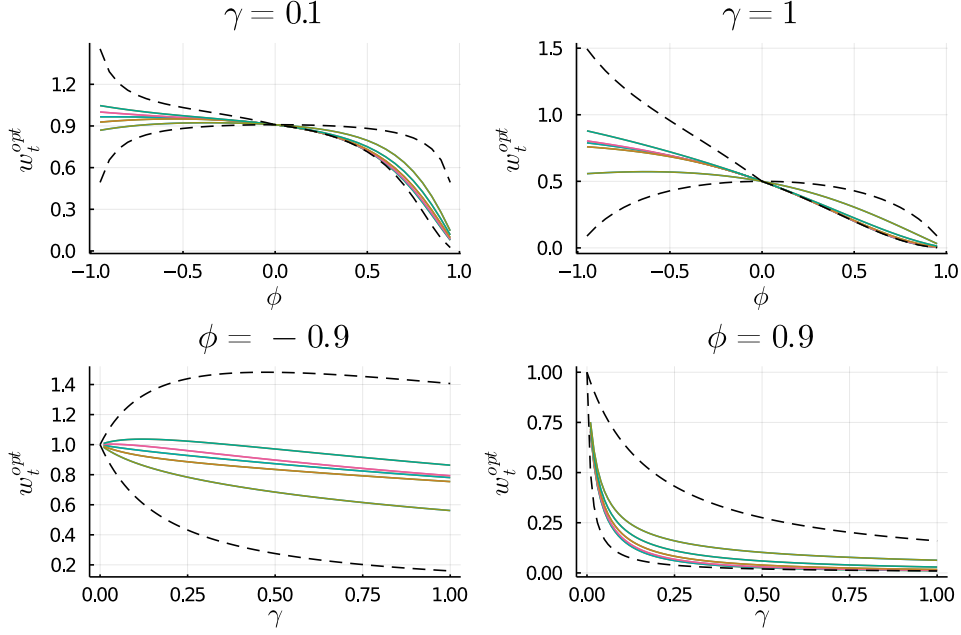


Figure 1: Plots of  $\mathbf{w}^{\text{opt}}$  for different values of  $\phi$  and  $\gamma$  when  $n = 10$ . Each solid line corresponds to an element in  $\mathbf{w}^{\text{opt}}$ . Only 5 distinct lines can be seen as  $\mathbf{w}^{\text{opt}}$  is symmetric. Dashed lines represent bounds in Corollary 1.

since  $\sigma_\epsilon^2 S^{-1} = I - V_0/\sigma_\epsilon^2$  implies  $\sigma_\epsilon^2 \mathbf{1}^T S^{-1} \mathbf{1} = n - \mathbf{1}^T \bar{\mathbf{w}}^{\text{opt}} = \mathbf{1}^T \mathbf{w}^{\text{opt}}$  where  $\bar{\mathbf{w}}^{\text{opt}} = V_0 \mathbf{1}/\sigma_\epsilon^2$ . From Lemma S4 in the supplementary material,  $\lim_{n \rightarrow \infty} (\mathbf{1}^T \mathbf{w}^{\text{opt}})/n = 1/(1 + u^*)$ . Hence the rate of convergence of Algorithm 1 goes to zero.  $\square$

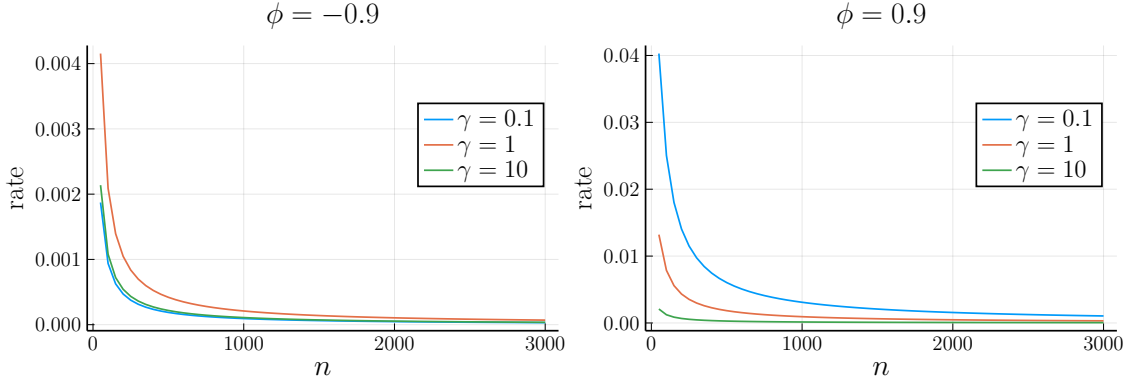


Figure 2: Convergence rate of Algorithm 1 when  $\mathbf{w} = w^{\text{opt}} \mathbf{1}$ .

## 2.2 Unknown scale parameter

Now suppose  $(\mu, \phi, \sigma_\epsilon^2)$  are known and  $\sigma_\eta^2$  is the only unknown parameter. We assume  $\mu \neq 0$  as this is the case of interest. The EM algorithm for this case (Algorithm 2), alternately updates  $\mathbf{m}_{a\mathbf{w}}$  and  $V_a$  at the E-step as in (6) and  $\sigma_\eta^2$  at the M-step

**Theorem 4.** If  $\mu \neq 0$ , the rate of convergence of Algorithm 2 is jointly minimized at

$$a^{\text{opt}} = \frac{\text{tr}(V_0\Lambda)}{n\sigma_\eta^2} = 1 - \frac{\text{tr}(V_0)}{n\sigma_\epsilon^2} \quad \text{and} \quad \bar{\mathbf{w}}^{\text{opt}} = \frac{1}{\mu} \left( \frac{2V_0\Lambda}{a^{\text{opt}}\sigma_\eta^2} - I \right) \mathbf{m}_{01}, \quad (12)$$

where  $\sigma_\eta^2 = \sigma_\eta^{2*}$ .

*Proof.* The rate of convergence of Algorithm 2 can be optimized by minimizing  $I_{\sigma_\eta^2, \sigma_\eta^2}$  with respect to  $a$  and  $\mathbf{w}$ . In Section S3 of the Supplementary material, we show that

$$I_{\sigma_\eta^2, \sigma_\eta^2} = \frac{1}{2\sigma_\eta^4} \left\{ n(a-1)^2 + \frac{a^2}{2} \mathbf{m}_{0\mathbf{w}}^T V_0^{-1} \mathbf{m}_{0\mathbf{w}} - \frac{2a\mu}{\sigma_\eta^2} \mathbf{m}_{01}^T \Lambda \bar{\mathbf{w}} \right\}.$$

From (6),  $\mathbf{m}_{0\mathbf{w}} = V_0(\mathbf{y} - \mu\mathbf{1})/\sigma_\epsilon^2 + \mu\bar{\mathbf{w}} = \mathbf{m}_{01} + \mu\bar{\mathbf{w}}$ , where  $V_0$  and  $\mathbf{m}_{01}$  are defined in (7). Note that  $I_{\sigma_\eta^2, \sigma_\eta^2}$  is evaluated at the MLE,  $\sigma_\eta^2 = \sigma_\eta^{2*}$ . Setting  $\partial I_{\sigma_\eta^2, \sigma_\eta^2} / \partial a = 0$  and  $\partial I_{\sigma_\eta^2, \sigma_\eta^2} / \partial \bar{\mathbf{w}} = 0$  yields

$$a = \frac{2n + 2\mu\sigma_\eta^{-2} \bar{\mathbf{w}}^T \Lambda \mathbf{m}_{01}}{2n + \mathbf{m}_{0\mathbf{w}}^T V_0^{-1} \mathbf{m}_{0\mathbf{w}}} \quad \text{and} \quad \bar{\mathbf{w}} = \frac{1}{\mu} \left( \frac{2V_0\Lambda}{a\sigma_\eta^2} \mathbf{m}_{01} - \mathbf{m}_{01} \right) \quad (13)$$

respectively. Solving the two equations simultaneously, we obtain

$$a^{\text{opt}} = 1 - \frac{\mathbf{m}_{01}^T \Lambda \mathbf{m}_{01}}{n\sigma_\eta^2} = \frac{\text{tr}(V_0\Lambda)}{n\sigma_\eta^2} = 1 - \frac{\text{tr}(V_0)}{n\sigma_\epsilon^2}.$$

The last two equalities follows from (9) as  $\mathbf{m}_{01}^T \Lambda \mathbf{m}_{01} = n\sigma_\eta^2 - \text{tr}(V_0\Lambda) = \gamma \text{tr}(V_0)$  at the MLE. The corresponding value of  $\bar{\mathbf{w}}$  is given in (12). The Hessian of  $I_{\sigma_\eta^2, \sigma_\eta^2}$  can be verified to be positive definite at  $(a^{\text{opt}}, \bar{\mathbf{w}}^{\text{opt}})$ , and hence  $I_{\sigma_\eta^2, \sigma_\eta^2}$  is minimized at  $(a^{\text{opt}}, \bar{\mathbf{w}}^{\text{opt}})$ . Details are given in Section S5 of the Supplementary material.  $\square$

From Theorem 4,  $(a^{\text{opt}}, \mathbf{w}^{\text{opt}})$  depend on the unknown  $\sigma_\eta^{2*}$ , while  $\mathbf{w}^{\text{opt}}$  also depends on the observed data  $\mathbf{y}$ . Even if the true  $\sigma_\eta^{2*}$  is known,  $\mathbf{w}^{\text{opt}}$  will still vary across datasets generated from model (4) due to sampling variability. We recommend updating  $(a^{\text{opt}}, \mathbf{w}^{\text{opt}})$  based on the latest update of  $\sigma_\eta^2$ . In Corollary 3, we show that  $a^{\text{opt}}$  is bounded in  $(0, 1)$ . However, the same does not apply to  $w_t^{\text{opt}}$ , which has been observed to be negative or exceed 1 in simulations.

**Corollary 3.**  $a^{\text{opt}}$  depends on  $\phi$ , and on  $\sigma_\eta^2$  and  $\sigma_\epsilon^2$  only through the signal-to-noise ratio  $\gamma$ . In addition,  $a^{\text{opt}} \in (0, 1)$  and decreases strictly as  $\gamma$  increases.

*Proof.*  $a^{\text{opt}} = \text{tr}(C^{-1})/n$  where  $C = \gamma\Lambda^{-1} + I$ . Hence  $a^{\text{opt}}$  is a function of  $\phi$  and  $\gamma$  only. The eigenvalues  $\{\lambda_i\}$  of  $\gamma\Lambda^{-1}$  are positive since  $\Lambda^{-1}$  is a symmetric positive definite matrix. Thus the eigenvalues of  $C$  are  $\{\lambda_i + 1\}$  and  $\text{tr}(C^{-1}) = \sum_{i=1}^n 1/(\lambda_i + 1) \in (0, n)$ . It follows that  $a^{\text{opt}} \in (0, 1)$ .  $\partial a^{\text{opt}} / \partial \gamma = -\text{tr}(C^{-1}\Lambda^{-1}C^{-1})/n < 0$  since  $C^{-1}\Lambda^{-1}C^{-1}$  is positive definite.  $\square$

**Corollary 4.** For  $\mathbf{w}^{\text{opt}}$  defined in (12),  $E(\mathbf{w}^{\text{opt}}) = \mathbf{1}$  and  $\text{cov}(\mathbf{w}^{\text{opt}}) = AS^{-1}A/\mu^2$ , where  $A = 2V_0/a^{\text{opt}} - \sigma_\eta^2\Lambda^{-1}$ .

*Proof.* From (12),  $\bar{\mathbf{w}}^{\text{opt}} = AS^{-1}(y/\mu - \mathbf{1})$ . As  $y \sim N(\mu\mathbf{1}, S)$ ,  $E(\bar{\mathbf{w}}^{\text{opt}}) = \mathbf{0}$  and  $\text{cov}(\bar{\mathbf{w}}^{\text{opt}}) = AS^{-1}SS^{-1}A/\mu^2 = AS^{-1}A/\mu^2$ .  $\square$

Theorem 5 derives a large-sample estimate  $\hat{a}^{\text{opt}}$  of  $a^{\text{opt}}$ , which improves as  $n$  increases. The proof requires the trace of  $Q^{-1}$  which is stated in Property 4 (Theorem 3, Tan, 2019). The trace of  $Q^{-2}$ , which is required for deriving the rate of convergence of Algorithm 2 in Theorem 6 is also given in Property 4.

**Property 4.** The trace of  $Q^{-1}$  is  $(\kappa_0^2\kappa)^{-1}[n\kappa_0(\varphi_+^2r_+^{n-1} + \varphi_-^2r_-^{n-1}) + 2\gamma(r_+^n - r_-^n)]$  and the trace of  $Q^{-2}$  is  $(\kappa_0^2\kappa^2)^{-1}\mathcal{S}$ , where

$$\begin{aligned} \mathcal{S} = & 4n^2\gamma^2 + 8n\gamma(\phi^2 - 1) + \kappa_0^{-1}nc(\varphi_+^4r_+^{2n-2} - \varphi_-^4r_-^{2n-2}) - 4\gamma(1 + \phi^2) + 2(\phi^2 - 1)^2 \\ & + 4\gamma\kappa_0^{-2}\{4\gamma + c(\varphi_+^2r_+^{2n-1} + \varphi_-^2r_-^{2n-1})\} + 2\kappa_0^{-1}(\phi^2 - 1)(\varphi_+^2r_+^{2n-1} - \varphi_-^2r_-^{2n-1}). \end{aligned}$$

**Theorem 5.** As  $n \rightarrow \infty$ ,  $a^{\text{opt}}$  converges to

$$\hat{a}^{\text{opt}} = 1 - \gamma/\sqrt{\{(1 - \phi)^2 + \gamma\}\{(1 + \phi)^2 + \gamma\}}. \quad (14)$$

*Proof.* We have  $a^{\text{opt}} = 1 - \text{tr}(V_0)/(n\sigma_\epsilon^2) = 1 - \gamma\text{tr}(Q^{-1})/(n|\phi|)$ . From Property 4,  $\lim_{n \rightarrow \infty} \text{tr}(Q^{-1})/n$  is

$$\frac{1}{\kappa_0} \lim_{n \rightarrow \infty} \frac{\varphi_+^2 + \varphi_-^2(r_-/r_+)^{n-1}}{\varphi_+^2 - \varphi_-^2(r_-/r_+)^{n-1}} + \frac{2\gamma}{\kappa_0^2} \lim_{n \rightarrow \infty} \frac{1 - (r_-/r_+)^n}{n\{\varphi_+^2/r_+ - (\varphi_-^2/r_+)(r_-/r_+)^{n-1}\}},$$

which reduces to  $\kappa_0^{-1}$  since  $0 < r_-/r_+ < 1$ . Moreover  $\kappa_0 = r_+ - r_- = \sqrt{c^2 - 4} = \sqrt{\{(1 - \phi)^2 + \gamma\}\{(1 + \phi)^2 + \gamma\}}/|\phi|$ . Thus we obtain the large-sample limit of  $a^{\text{opt}}$ .  $\square$

The large-sample limit in Theorem 5 lends insight on how  $a^{\text{opt}}$  varies with  $\gamma$  and  $\phi$ . From (14),  $\hat{a}_{\text{opt}}$  is symmetric about  $\phi = 0$  and decreases strictly with  $\gamma$  as  $\partial\hat{a}^{\text{opt}}/\partial\gamma < 0$ , but the relationship of  $\hat{a}_{\text{opt}}$  with  $|\phi|$  is not monotone. Figure 3 shows the values of  $a^{\text{opt}}$  and  $\hat{a}^{\text{opt}}$  under different parameter settings. We see that  $a^{\text{opt}}$  is almost indistinguishable from  $\hat{a}^{\text{opt}}$  for  $n \geq 200$ . In addition,  $a^{\text{opt}}$  decreases as  $\gamma$  increases, is symmetric about  $\phi = 0$ , and varies with  $\phi$  in the form of a (sometimes inverted) U-shaped curve. We can compute  $a^{\text{opt}} = 1 - \text{tr}(V_0)/(n\sigma_\epsilon^2)$  efficiently using a Kalman filter and smoother using  $\mathcal{O}(n)$  time steps, but  $\hat{a}^{\text{opt}}$  is even easier to compute and can be used in place of  $a^{\text{opt}}$  for large  $n$ .

To investigate the dependence of  $\mathbf{w}^{\text{opt}}$  on  $\phi$  and signal-to-noise ratio  $\gamma$ , we compute  $\mathbf{w}^{\text{opt}}$  for 1000 data sets simulated under different parameter settings. We set  $\mu = 1$ ,  $\sigma_\epsilon^2 = 0.1$ ,  $\sigma_\eta^2 \in \{0.01, 0.1, 1\}$ ,  $\phi \in \{-0.95, -0.90, \dots, 0.95\}$  and  $n \in \{50, 200, 1000\}$ . Figure 4 shows the mean, 5th and 95th quantiles of the first element of  $\mathbf{w}^{\text{opt}}$  evaluated across 1000 simulated data sets. Plots of other elements look similar and are not shown.

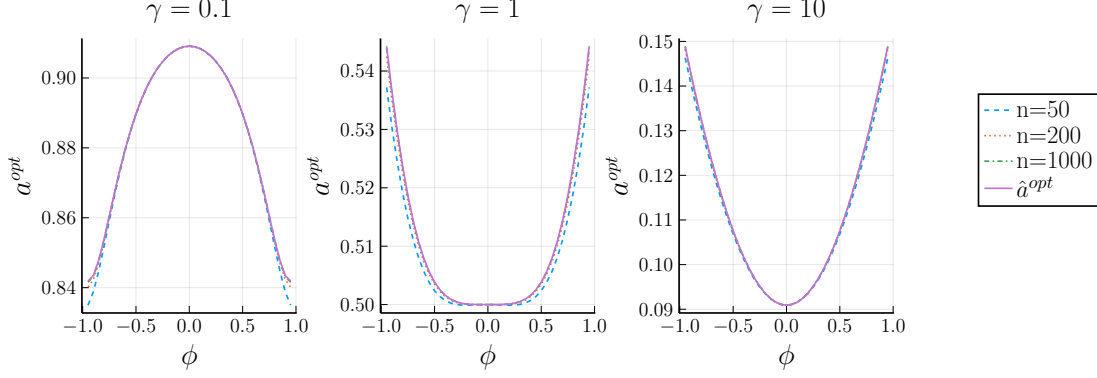


Figure 3: Values of  $a^{\text{opt}}$  and  $\hat{a}^{\text{opt}}$  under different parameter settings.

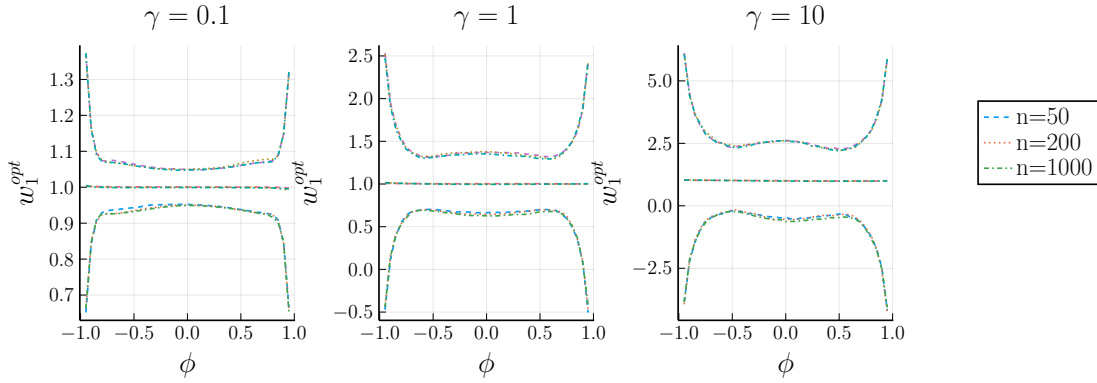


Figure 4: Mean, 5th and 95th quantiles of  $w_1^{\text{opt}}$  over 1000 simulated datasets.

The mean is approximately 1 as is consistent with Corollary 4, but the variance increases with  $\gamma$  and as  $|\phi| \rightarrow 1$ . The behavior of  $\mathbf{w}^{\text{opt}}$  does not appear to vary with  $n$ .

Theorem 6 gives the approximate rate of convergence of Algorithm 2 for large  $n$  and the proof is given in Section S5.3 of the supplementary material. The asymptotic rate of convergence is less than 0.5 and symmetric about  $\phi = 0$ . Algorithm 2 converges faster for smaller values of  $|\phi|$  and larger signal-to-noise ratio  $\gamma$ . Figure 5 shows the asymptotic convergence rate for different combinations of  $\gamma$  and  $\phi$ . We can see that Algorithm 2 converges most slowly when  $|\phi|$  is close to 1 and  $\gamma$  is close to 0.

**Theorem 6.** *The asymptotic rate of convergence of Algorithm 2 as  $n \rightarrow \infty$  is approximately  $(c - \kappa_0)/(2c - \kappa_0)$ , where  $\kappa_0 = \sqrt{c^2 - 4}$  and  $c = (1 + \gamma + \phi^2)/|\phi|$ . This rate decreases as  $\gamma$  increases and  $|\phi|$  decreases.*

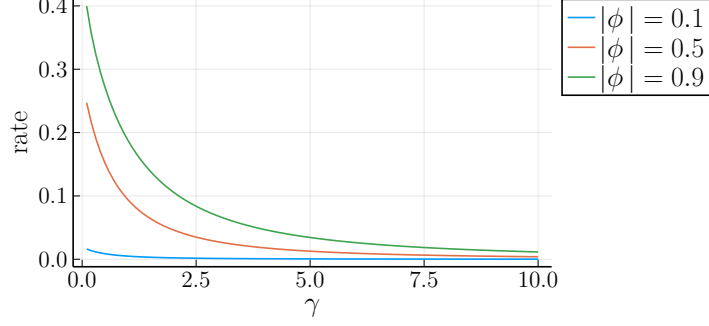


Figure 5: Asymptotic rate of convergence of Algorithm 2.

### 2.3 All parameters are unknown (AECM Algorithm)

When all four parameters are unknown, the augmented information matrix is

$$I_{\text{aug}}(\boldsymbol{\theta}^*) = \begin{bmatrix} I_{\mu, \mu}(\mathbf{w}) & I_{\mu, \sigma_{\eta}^2}(a, \mathbf{w}) & I_{\mu, \phi}(\mathbf{w}) & I_{\mu, \sigma_{\epsilon}^2}(\mathbf{w}) \\ \cdot & I_{\sigma_{\eta}^2, \sigma_{\eta}^2}(a, \mathbf{w}) & I_{\sigma_{\eta}^2, \phi}(a, \mathbf{w}) & I_{\sigma_{\eta}^2, \sigma_{\epsilon}^2}(a, \mathbf{w}) \\ \cdot & \cdot & I_{\phi, \phi} & I_{\phi, \sigma_{\epsilon}^2} \\ \cdot & \cdot & \cdot & I_{\sigma_{\epsilon}^2, \sigma_{\epsilon}^2} \end{bmatrix}.$$

Each element is dependent only on the working parameters stated in brackets and explicit expressions are given in the Supplementary material Section S3. For instance,  $I_{\mu, \mu}$  is independent of  $a$  while  $I_{\sigma_{\eta}^2, \sigma_{\eta}^2}$  depends on both  $a$  and  $\mathbf{w}$ . Note that  $I_{\phi, \sigma_{\epsilon}^2} = 0$ , and  $I_{\phi, \phi}$ ,  $I_{\sigma_{\epsilon}^2, \sigma_{\epsilon}^2}$  are both independent of  $(a, \mathbf{w})$ . We further prove that  $I_{\mu, \phi}/n$ ,  $I_{\mu, \sigma_{\epsilon}^2}/n$ ,  $I_{\sigma_{\eta}^2, \phi}/n$  and  $I_{\sigma_{\eta}^2, \sigma_{\epsilon}^2}/n$  converge to 0 almost surely as  $n \rightarrow \infty$  (see Section S3 of Supplementary material). Hence these elements do not change substantially with  $(a, \mathbf{w})$  for large  $n$ , and it is sufficient to focus on minimizing

$$\widetilde{I}_{\text{aug}}(\boldsymbol{\theta}^*) = \begin{bmatrix} I_{\mu, \mu}(\mathbf{w}) & I_{\mu, \sigma_{\eta}^2}(a, \mathbf{w}) \\ \cdot & I_{\sigma_{\eta}^2, \sigma_{\eta}^2}(a, \mathbf{w}) \end{bmatrix},$$

when optimizing the rate of convergence of the EM algorithm.

From Sections 2.1 and 2.2, the parametrization optimal for inferring  $\mu$  is not optimal for inferring  $\sigma_{\eta}^2$ , and it is impossible to find  $(a, \mathbf{w})$  that jointly minimizes  $I_{\mu, \mu}$  and  $I_{\sigma_{\eta}^2, \sigma_{\eta}^2}$ . Hence when all parameters are unknown, we employ the *alternating expectation-conditional maximization* (AECM, Meng and van Dyk, 1997) algorithm, which inserts an E-step before each conditional update, thus allowing the data augmentation scheme to vary across parameters. This enables us to use the optimal augmentation scheme for each parameter while conditioning on the rest, at the cost of more computation per iteration. To minimize the number of additional E-steps, we group  $(\phi, \sigma_{\epsilon}^2)$  with  $\sigma_{\eta}^2$  and perform only one E-step based on the optimal parametrization for  $\sigma_{\eta}^2$  before the conditional updates of  $(\sigma_{\eta}^2, \phi, \sigma_{\epsilon}^2)$ . This is feasible as any convenient parametrization can be used for  $(\phi, \sigma_{\epsilon}^2)$ . The updates of  $(\phi, \sigma_{\epsilon}^2)$  is considered a joint update as  $\phi$  and  $\sigma_{\epsilon}^2$  are independent in  $Q(\boldsymbol{\theta} | \boldsymbol{\theta}^{(i)})$ .

After that, we update  $\mu$  using its optimal parametrization. Instead of performing the E-step and M-step separately, we note that the update for  $\mu$  in (8) for  $\mathbf{w}^{\text{opt}} = \sigma_\eta^{-2} V_0 \Lambda \mathbf{1}$  simplifies to  $(\mathbf{y}^T S^{-1} \mathbf{1}) / (\mathbf{1}^T S^{-1} \mathbf{1})$ , and  $S^{-1} \mathbf{1} = \sigma_\epsilon^{-2} \mathbf{w}^{\text{opt}}$ . Hence we can compute  $\mathbf{w}^{\text{opt}}$  followed by the  $\mu$  update directly without computing  $\mathbf{m}_{a\mathbf{w}}$ . This choice of  $\mathbf{w}$  corresponds to having no missing data since the  $\mu$  update is that obtained by maximizing  $p(\mathbf{y} \mid \boldsymbol{\theta})$  directly with respect to  $\mu$ . The AECM Algorithm 3 for inferring all the parameters is outlined below, and each iteration has two cycles. Algorithm 1 (for inferring  $\mu$  only) omits step 2 while Algorithm 2 (for inferring  $\sigma_\eta^2$  only) omits step 3 and updates of  $(\phi, \sigma_\epsilon^2)$  in step 2(iii). We say that Algorithms 1, 2 and 3 are using the partially noncentered parametrization (PNCP) as both the mean and scale are partially noncentered.

---

#### AECM Algorithm 3

---

Initialize  $\boldsymbol{\theta}^{(0)}$ ,  $i = 0$  and  $r = 1$ . While  $i \leq M$  and  $r < \delta$ ,

1.  $i \leftarrow i + 1$ .
  2. (i) Set  $a = 1 - \text{tr}(V_0)/(n\sigma_\epsilon^2)$  and  $\bar{\mathbf{w}} = \{2V_0\Lambda/(a\sigma_\eta^2) - I\}\mathbf{m}_{01}/\mu$ .  
(ii) Update  $\mathbf{m}_{a\mathbf{w}}^{(i)}$  and  $V_a^{(i)}$  as in (6).  
(iii) Update  $\sigma_\eta^2$ ,  $\sigma_\epsilon^2$  and  $\phi$ .
  3. (i) Set  $\mathbf{w} = \sigma_\eta^{-2} V_0 \Lambda \mathbf{1}$ .  
(ii) Update  $\mu = (\mathbf{y}^T \mathbf{w}) / (\mathbf{1}^T \mathbf{w})$ .
  4. Let  $\boldsymbol{\theta}^{(i)}$  denote current estimate of  $(\mu, \sigma_\eta^2, \phi, \sigma_\epsilon^2)$ . Compute  $L^{(i)} = \log p(\mathbf{y} \mid \boldsymbol{\theta}^{(i)})$ .  
If  $i \geq 2$ , compute  $r = (L^{(i)} - L^{(i-1)}) / L^{(i-1)}$ .
- 

## 2.4 Initialization and diagnosing convergence

The EM algorithm can be sensitive to initialization and there is also a risk of getting stuck in local modes. To aid convergence, we initialize using the strategy described below. Recall that  $\mathbf{y}$  is marginally distributed as  $N(\mu \mathbf{1}, S)$ , where  $S = \sigma_\epsilon^2 I + \sigma_\eta^2 \Lambda^{-1}$ . Hence

$$S_{tt} = \sigma_\epsilon^2 + \frac{\sigma_\eta^2}{1 - \phi^2}, \quad S_{t,t+h} = \frac{\phi^h \sigma_\eta^2}{1 - \phi^2}, \quad \text{for } t = 1, \dots, n, \ 1 \leq h \leq n - t.$$

We initialize  $\mu$  as  $\bar{y} = \sum_{t=1}^n y_t / n$ . Let  $\hat{\gamma}_h = \sum_{t=h+1}^n (y_t - \bar{y})(y_{t-h} - \bar{y}) / n$  be the sample autocovariance at lag  $h$ . Shumway and Stoffer (2017) suggest initializing  $\phi$  as  $\hat{\gamma}_2 / \hat{\gamma}_1$ . This strategy works well if  $|\phi|$  is close to 1 but can be poor if  $|\phi|$  is close to 0. Let  $\hat{\rho}_1 = \hat{\gamma}_1 / \hat{\gamma}_0$ . We consider values of  $\phi$  sharing the sign of  $\hat{\gamma}_1$ , such that  $|\phi| \in \{0.1, 0.2, \dots, 0.9\}$  and  $|\phi| > |\hat{\rho}_1|$ . If this set is empty, we consider  $\phi = (\hat{\rho}_1 + \text{sign}(\hat{\rho}_1)) / 2$ . For each plausible value of  $\phi$ , we compute  $\sigma_\eta^2 = \hat{\gamma}_1(1 - \phi^2) / \phi$  and  $\sigma_\epsilon^2 = \hat{\gamma}_0 - \hat{\gamma}_1 / \phi$ . Then we evaluate the log-likelihood at each set of values  $(\mu, \sigma_\eta^2, \phi, \sigma_\epsilon^2)$  and choose the set that maximizes the

likelihood as initial values. For diagnosing convergence, we consider the relative increment  $r$  in the log-likelihood as defined in Algorithm 3, and terminate the algorithm when  $r$  is less than a tolerance  $\delta$  or if the maximum number of iterations  $M$  is reached. We set  $\delta = 10^{-9}$  and  $M = 10^5$  in all experiments unless stated otherwise. Efficient computation of the log-likelihood and optimal values of  $(a, \mathbf{w})$  (using the Kalman filter) are discussed in the Supplementary material Sections S1 and S6 respectively.

### 3 Experimental results for EM algorithm

We compare Algorithms 1–3 with the ECM algorithms using the CP ( $a = 0, \mathbf{w} = 0$ ) or NCP ( $a = 1, \mathbf{w} = 1$ ). For the ECM algorithms, only one E-step is used at the beginning of each iteration followed by the CM-steps. In contrast, the AECM algorithm requires more computation in each iteration to update working parameters,  $a$  and  $\bar{\mathbf{w}}$  (twice), and find numerically the value of  $\sigma_\eta^2$  that maximizes  $Q(\boldsymbol{\theta} \mid \boldsymbol{\theta}^{(i)})$ . To make Algorithms 2 and 3 more competitive, the updates in steps 2(i) and 3 are performed only in the first five iterations and thereafter only at  $i = 1000, 2000, \dots$ . After convergence, we perform a final update of  $\mu$  and the log-likelihood. These modifications do not affect the convergence rate of Algorithms 2 and 3 but are very helpful in reducing the computation cost.

#### 3.1 Simulations

First, we simulate data from the Gaussian state space model under different settings. We set  $n = 10^4$ ,  $\mu = -1$ ,  $\sigma_\epsilon^2 = 0.1$ ,  $\phi \in \{-0.9, -0.6, -0.3, 0.3, 0.6, 0.9\}$  and  $\sigma_\eta^2 \in \{0.01, 0.1, 1\}$ . Twenty datasets are generated in each setting.

Algorithm 1 considers  $\mu$  as the only unknown. When  $\mu$  is initialized as  $\bar{y}$  and  $\delta = 10^{-9}$ , all the algorithms (NCP, CP, PNCP) converge on average in less than five iterations within one hundredth of a second. The averaged estimates of  $\mu$  in each setting are also identical (up to 3 decimal places), except when  $\phi = 0.9$  and  $\gamma = 10$  (PNCP and CP return  $-0.976$  while NCP returns  $-0.977$ ). Thus, it is difficult to differentiate among different parametrizations. To magnify the differences, we reduce  $\delta$  to  $10^{-11}$ . With this lower tolerance, NCP achieves the same averaged estimates of  $\mu$  as CP and PNCP in all cases. The average number of iterations NCP and CP take to converge are shown in Figure 6, whereas Algorithm 1 converges instantly. Figure 6 shows that NCP becomes increasingly inefficient as  $\gamma$  increases from 0.1 to 10, and especially as  $\phi$  approaches 1. On the other hand, CP is least efficient when  $\gamma = 0.1$  and  $\phi = -0.9$ . It improves as  $\gamma$  increases and  $\phi \rightarrow 1$ . Hence the performance of NCP and CP are complementary to each other. These observations can also be explained using Theorem 3, where it is stated that  $w^{\text{opt}} \rightarrow (1 - \phi)^2 / \{\gamma + (1 - \phi)^2\}$  as  $n \rightarrow \infty$ . From this expression,  $w^{\text{opt}} \rightarrow 0$  as  $\phi \rightarrow 1$  and  $\gamma \rightarrow +\infty$ . Hence the CP ( $\mathbf{w} = \mathbf{0}$ ) is strongly preferred in these conditions.

	NCP				CP		
$\phi$	0.1	1	10	$\phi$	0.1	1	10
-0.9	2.0	3.5	11.4	-0.9	36.2	12.8	4.0
-0.6	2.0	3.0	9.4	-0.6	6.9	6.9	2.9
-0.3	2.0	2.3	7.5	-0.3	2.2	3.8	2.4
0.3	2.0	2.8	12.3	0.3	3.4	2.8	2.0
0.6	2.2	3.7	55.5	0.6	4.7	2.7	2.0
0.9	2.9	3.8	666.8	0.9	3.0	2.2	2.0

Figure 6: (Unknown  $\mu$ ) Average number of iterations required for convergence.

For Algorithm 2 where  $\sigma_\eta^2$  is the only unknown parameter, the average number of iterations required for each algorithm to converge are shown in Figure 7. The average runtime in seconds is also given in brackets. The rate of convergence appears to be symmetric about  $\phi = 0$  for each parametrization. As is consistent with Theorem 6, PNCP becomes more efficient as  $\gamma$  increases and  $|\phi|$  decreases. The efficiency of CP worsens as  $\gamma \rightarrow 0$  and  $|\phi| \rightarrow 0$ . On the other hand, NCP performs best when  $\gamma$  is close to 1 and worsens as  $|\phi|$  increases. The estimates of  $\sigma_\eta^2$  obtained using different parametrizations are virtually identical except where  $\phi \in \{-0.9, -0.6, 0.9\}$  and  $\gamma = 10$ . NCP converges slowly in these cases and yields estimates slightly different from CP and PNCP.

	NCP				CP				PNCP		
$\phi$	0.1	1	10	$\phi$	0.1	1	10	$\phi$	0.1	1	10
-0.9	13.7 (0.01)	42.1 (0.03)	144.4 (0.11)	-0.9	46.0 (0.04)	16.7 (0.02)	5.6 (0.00)	-0.9	6.2 (0.01)	4.7 (0.01)	2.9 (0.01)
-0.6	17.1 (0.02)	12.8 (0.01)	41.4 (0.03)	-0.6	187.3 (0.17)	16.4 (0.02)	4.8 (0.01)	-0.6	6.8 (0.01)	3.9 (0.01)	2.5 (0.01)
-0.3	32.8 (0.03)	12.1 (0.01)	36.2 (0.03)	-0.3	511.0 (0.46)	23.0 (0.02)	5.2 (0.01)	-0.3	5.8 (0.02)	3.8 (0.01)	2.3 (0.01)
0.3	33.9 (0.03)	12.8 (0.01)	35.8 (0.03)	0.3	563.3 (0.52)	24.6 (0.03)	5.2 (0.01)	0.3	5.8 (0.01)	3.7 (0.01)	2.6 (0.01)
0.6	16.8 (0.02)	12.2 (0.02)	46.2 (0.04)	0.6	186.3 (0.18)	15.7 (0.02)	5.1 (0.01)	0.6	6.7 (0.01)	4.0 (0.01)	2.8 (0.01)
0.9	14.9 (0.02)	47.3 (0.04)	146.2 (0.11)	0.9	50.9 (0.05)	18.4 (0.02)	5.4 (0.00)	0.9	6.5 (0.01)	5.0 (0.01)	2.8 (0.01)

Figure 7: (Unknown  $\sigma_\eta^2$ ) Average number of iterations required for convergence, and average runtime in seconds in brackets.

Algorithm 3 treats all parameters as unknown. The average number of iterations required for convergence and runtime of each algorithm are shown in Figure 8. Again, there is some symmetry about  $\phi = 0$ . In each setting, PNCP converges on average using the least number of iterations. Its average runtime is always close to, if not faster than the better of NCP and CP, and it also achieves on average a higher log-likelihood. Table 1 shows that PNCP is able to provide speedup over CP and NCP in most cases, of

NCP				CP				PNCP						
$\phi$	$\gamma$			$\phi$	$\gamma$			$\phi$	$\gamma$					
	0.1	1	10		0.1	1	10		0.1	1	10			
	-0.9	55.6 (0.07)	102.3 (0.12)		685.9 (0.82)	-0.9	153.4 (0.21)		52.7 (0.08)	431.4 (0.63)	-0.9	29.1 (0.05)	29.6 (0.05)	423.5 (0.59)
	-0.6	339.2 (0.44)	154.0 (0.19)		1214.4 (1.52)	-0.6	1041.9 (1.59)		169.9 (0.25)	1127.0 (1.76)	-0.6	296.5 (0.45)	98.7 (0.15)	1115.5 (1.65)
	-0.3	3598.3 (4.57)	1153.0 (1.60)		4026.9 (5.73)	-0.3	4371.3 (6.89)		1276.3 (2.22)	3910.3 (6.87)	-0.3	3142.5 (4.70)	1002.4 (1.65)	3857.8 (6.42)
	0.3	3706.9 (5.20)	1281.7 (1.84)		3177.5 (4.74)	0.3	4404.1 (7.72)		1393.7 (2.52)	3089.2 (5.71)	0.3	3208.6 (5.31)	1114.9 (1.91)	3040.4 (5.32)
	0.6	318.4 (0.53)	172.2 (0.29)		1406.5 (2.62)	0.6	964.8 (1.93)		192.8 (0.41)	1304.0 (3.02)	0.6	278.9 (0.53)	109.3 (0.23)	1290.0 (2.80)
	0.9	53.5 (0.10)	107.9 (0.21)		692.2 (1.44)	0.9	147.5 (0.37)		54.1 (0.14)	429.2 (1.12)	0.9	28.0 (0.08)	29.9 (0.08)	421.3 (1.04)

Figure 8: (All parameters unknown) Average number of iterations required for convergence, and average runtime in seconds in brackets.

up to 4.9 times. In the worst case scenario, it is at least 90% as fast as the better of

$\phi$	-0.9			-0.6			-0.3			0.3			0.6			0.9		
$\gamma$	0.1	1	10	0.1	1	10	0.1	1	10	0.1	1	10	0.1	1	10	0.1	1	10
NCP	1.3	2.3	1.4	1.0	1.3	0.9	1.0	1.0	0.9	1.0	1.0	0.9	1.0	1.3	0.9	1.4	2.6	1.4
CP	4.2	1.6	1.1	3.5	1.7	1.1	1.5	1.3	1.1	1.5	1.3	1.1	3.6	1.8	1.1	4.9	1.6	1.1

Table 1: (All parameters unknown) Speedup factor in average runtime provided by PNCP over NCP and CP.

NCP and CP. These properties make PNCP a great option as it is always faster than the worst of CP and NCP, often able to provide speedup and achieves a higher log likelihood on average. Table 2 shows the averaged estimates obtained at convergence and any differences have been highlighted in bold. In most cases, the estimates obtained using different parametrizations are practically identical. The greatest differences arise when  $|\phi| = 0.3$  and  $\gamma = 0.1$ . For these settings, NCP is preferred to CP as it converges faster and achieves a higher log-likelihood on average. PNCP leans towards NCP automatically in these case and its estimates are closer to that of NCP than CP. However, PNCP is able to achieve a higher average log-likelihood than NCP, suggesting that its estimates are closer on average to the true MLEs.

### 3.2 Real data

The first data set contains IBM stock prices from 1962 to 1965 ( $n = 1008$ ), and it is available at <https://github.com/PacktPublishing/Practical-Time-Series-Analysis/tree/master/Data>. The second data set involves an industrial robot making a sequence of movements and the time series ( $n = 324$ ) records the distance in inches from a final target. It is available from the R package TSA (Cryer and Chan, 2008) as `data(robot)`. We scale all measurements in `robot` up by 1000 before applying the algorithms.

$\phi$	$\gamma$	NCP	CP	PNCP
-0.9	0.1	(-1.000, 0.010, -0.897, 0.100)	(-1.000, 0.010, -0.897, 0.100)	(-1.000, 0.010, -0.897, 0.100)
	1	(-1.000, 0.101, -0.899, 0.100)	(-1.000, 0.101, -0.899, 0.100)	(-1.000, 0.101, -0.899, 0.100)
	10	(-0.999, 1.005, -0.900, 0.099)	(-0.999, 1.005, -0.900, 0.099)	(-0.999, 1.005, -0.900, 0.099)
-0.6	0.1	(-1.000, 0.011, -0.581, 0.099)	(-1.000, 0.011, -0.581, 0.099)	(-1.000, 0.011, -0.581, 0.099)
	1	(-1.000, 0.102, -0.599, 0.099)	(-1.000, 0.102, -0.599, 0.099)	(-1.000, 0.102, -0.599, 0.099)
	10	(-0.999, 1.002, -0.601, 0.100)	(-0.999, 1.002, -0.601, 0.100)	(-0.999, 1.002, -0.601, 0.100)
-0.3	0.1	(-1.000, <b>0.025</b> , - <b>0.285</b> , <b>0.085</b> )	(-1.000, <b>0.023</b> , - <b>0.291</b> , <b>0.087</b> )	(-1.000, <b>0.027</b> , - <b>0.283</b> , <b>0.083</b> )
	1	(-1.000, 0.109, -0.299, 0.092)	(-1.000, 0.109, -0.299, 0.092)	(-1.000, 0.109, -0.299, 0.092)
	10	(-0.999, 0.969, -0.311, 0.129)	(-0.999, 0.969, -0.311, 0.129)	(-0.999, 0.969, -0.311, 0.129)
0.3	0.1	(-1.000, <b>0.026</b> , <b>0.276</b> , <b>0.085</b> )	(-1.000, <b>0.024</b> , <b>0.282</b> , <b>0.087</b> )	(-1.000, <b>0.027</b> , <b>0.274</b> , <b>0.083</b> )
	1	(-0.999, 0.109, <b>0.296</b> , 0.091)	(-0.999, 0.109, <b>0.296</b> , 0.091)	(-0.999, 0.109, <b>0.297</b> , 0.091)
	10	(-0.997, 0.956, 0.313, <b>0.142</b> )	(-0.997, 0.956, 0.313, <b>0.141</b> )	(-0.997, 0.956, 0.313, <b>0.141</b> )
0.6	0.1	(-1.000, 0.011, <b>0.578</b> , 0.100)	(-1.000, 0.011, <b>0.578</b> , 0.100)	(-1.000, 0.011, <b>0.579</b> , 0.100)
	1	(-0.999, 0.100, 0.601, 0.101)	(-0.999, 0.100, 0.601, 0.101)	(-0.999, 0.100, 0.601, 0.101)
	10	(-0.995, 0.992, 0.603, 0.107)	(-0.995, 0.992, 0.603, 0.107)	(-0.995, 0.992, 0.603, 0.107)
0.9	0.1	(-0.998, 0.010, 0.901, 0.100)	(-0.998, 0.010, 0.901, 0.100)	(-0.998, 0.010, 0.901, 0.100)
	1	(-0.993, 0.100, 0.901, 0.101)	(-0.993, 0.100, 0.901, 0.101)	(-0.993, 0.100, 0.901, 0.101)
	10	(- <b>0.977</b> , 0.996, 0.901, 0.103)	(- <b>0.976</b> , 0.996, 0.901, 0.103)	(- <b>0.976</b> , 0.996, 0.901, 0.103)

Table 2: (All parameters unknown) Averaged estimates of  $(\mu, \sigma_\eta^2, \phi, \sigma_\epsilon^2)$ .

Table 3 shows the results for the IBM data. The estimate of  $\phi = 0.995$  is very close to 1, while  $\gamma = 44.275/0.135$  is large. From Figure 8, we expect CP to perform better than NCP and this is indeed the case. PNCP automatically leans towards CP and provides a speedup of about 2.2 compared to NCP. The log-likelihood attained by NCP is lower than CP and PNCP, and the estimates of  $(\mu, \sigma_\eta^2, \sigma_\epsilon^2)$  also differ noticeably.

NCP	CP	PNCP
23504	9036	9030
4.86	2.30	2.25
-3346.113	-3345.929	-3345.929
(463.125, 43.946, 0.995, 0.153)	(482.043, 44.275, 0.995, 0.135)	(482.043, 44.275, 0.995, 0.135)

Table 3: IBM data. First row: number of iterations to converge, second row: runtime (in seconds), third row: log-likelihood, last row: estimates of  $(\mu, \sigma_\eta^2, \phi, \sigma_\epsilon^2)$ .

Table 4 shows the results for the robot data. The estimate of  $\phi = 0.947$  is also close to 1, but  $\gamma = 0.209/5.062 = 0.041$  is small, and NCP is expected to perform better based on Figure 8. Indeed, NCP converges faster than CP, while PNCP reduces the number of iterations of NCP further by about half. The estimates returned by NCP and PNCP are identical while CP differs slightly.

Figure 9 tracks the log-likelihood at each iteration, and optimization of the working parameters has provided PNCP with a good headstart. Overall, PNCP provides an attractive alternative to NCP and CP as it automatically gravitates towards the better parametrization and is often able to outperform both in terms of speed and accuracy.

NCP	CP	PNCP
93	326	42
0.00	0.03	0.00
-748.809	-748.809	-748.809
(1.486, 0.209, 0.947, 5.062)	(1.486, 0.210, 0.947, 5.061)	(1.486, 0.209, 0.947, 5.062)

Table 4: Robot data. First row: number of iterations to converge, second row: runtime (in seconds), third row: log-likelihood, last row: estimates of  $(\mu, \sigma_\eta^2, \phi, \sigma_\epsilon^2)$ .

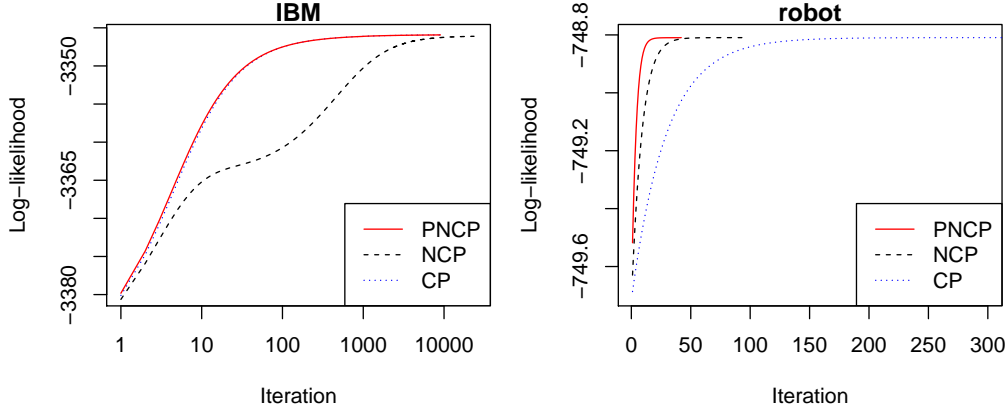


Figure 9: Log-likelihood at each iteration.

## 4 Extensions

We have proposed a data augmentation scheme for the Gaussian state space model in which working parameters  $(a, \mathbf{w})$  are introduced for rescaling and recentering. Optimal values of  $(a, \mathbf{w})$  that optimize the convergence of the EM algorithm in maximum likelihood estimation have been derived. However, the EM algorithm can also be used in the Bayesian framework to find the mode of a posterior distribution. Will the optimal values of  $(a, \mathbf{w})$  vary depending on the prior specified on  $\boldsymbol{\theta}$ ? It is known that the rate of convergence of the Gibbs sampler is closely linked to the EM algorithm. Will the proposed data augmentation scheme also improve convergence for the Gibbs sampler? We seek to address these issues in this section and also touch briefly on the connection to variational Bayes.

### 4.1 EM Algorithm for finding posterior mode

Suppose a prior  $p(\boldsymbol{\theta})$  is placed on  $\boldsymbol{\theta}$ , and we wish to use the EM algorithm to find the posterior mode  $\boldsymbol{\theta}^*$ . That is, we wish to find  $\boldsymbol{\theta}$  maximizing  $\log p(\mathbf{y}, \boldsymbol{\theta}) = \log p(\mathbf{y} | \boldsymbol{\theta}) + \log p(\boldsymbol{\theta})$ . As before, let  $\boldsymbol{\alpha}$  denote the latent states dependent on  $(a, \mathbf{w})$ . In this case,

$$Q(\boldsymbol{\theta} | \boldsymbol{\theta}^{(i)}) = \mathbb{E}_{\boldsymbol{\alpha} | \mathbf{y}, \boldsymbol{\theta}^{(i)}} [\log p(\mathbf{y}, \boldsymbol{\alpha}, \boldsymbol{\theta})] = \mathbb{E}_{\boldsymbol{\alpha} | \mathbf{y}, \boldsymbol{\theta}^{(i)}} [\log p(\mathbf{y}, \boldsymbol{\alpha} | \boldsymbol{\theta})] + \log p(\boldsymbol{\theta}).$$

As  $Q(\boldsymbol{\theta} | \boldsymbol{\theta}^{(i)})$  only has an additional term  $\log p(\boldsymbol{\theta})$ , the E-step is unchanged but the M-step must be modified to accommodate  $\log p(\boldsymbol{\theta})$ . As  $p(\boldsymbol{\theta}, \boldsymbol{\alpha} | \mathbf{y}) = p(\boldsymbol{\alpha} | \boldsymbol{\theta}, \mathbf{y})p(\boldsymbol{\theta} | \mathbf{y}) =$

$p(\boldsymbol{\theta} \mid \boldsymbol{\alpha}, \mathbf{y}) p(\boldsymbol{\alpha} \mid \mathbf{y})$ , taking the logarithm, differentiating twice with respect to  $\boldsymbol{\theta}$  and taking expectation with respect to  $p(\boldsymbol{\alpha} \mid \boldsymbol{\theta}, \mathbf{y})$  leads to

$$-E_{\boldsymbol{\alpha} \mid \boldsymbol{\theta}, \mathbf{y}}[\nabla_{\boldsymbol{\theta}}^2 \log p(\boldsymbol{\alpha} \mid \boldsymbol{\theta}, \mathbf{y})] - \nabla_{\boldsymbol{\theta}}^2 \log p(\boldsymbol{\theta} \mid \mathbf{y}) = -E_{\boldsymbol{\alpha} \mid \boldsymbol{\theta}, \mathbf{y}}[\nabla_{\boldsymbol{\theta}}^2 \log p(\boldsymbol{\theta} \mid \boldsymbol{\alpha}, \mathbf{y})].$$

This yields the Bayesian analogue of the missing information principle,

$$I_{\text{mis}}(\boldsymbol{\theta}) + I_{\text{obs}}^B(\boldsymbol{\theta}) = I_{\text{aug}}^B(\boldsymbol{\theta}),$$

where  $I_{\text{obs}}^B(\boldsymbol{\theta}) = -\nabla_{\boldsymbol{\theta}}^2 \log p(\boldsymbol{\theta} \mid \mathbf{y}) = -\nabla_{\boldsymbol{\theta}}^2 \log p(\mathbf{y} \mid \boldsymbol{\theta}) - \nabla_{\boldsymbol{\theta}}^2 \log p(\boldsymbol{\theta})$  and

$$\begin{aligned} I_{\text{aug}}^B(\boldsymbol{\theta}) &= -E_{\boldsymbol{\alpha} \mid \boldsymbol{\theta}, \mathbf{y}}[\nabla_{\boldsymbol{\theta}}^2 \log p(\boldsymbol{\theta} \mid \boldsymbol{\alpha}, \mathbf{y})] = -E_{\boldsymbol{\alpha} \mid \boldsymbol{\theta}, \mathbf{y}}[\nabla_{\boldsymbol{\theta}}^2 \log p(\mathbf{y}, \boldsymbol{\alpha} \mid \boldsymbol{\theta})] - \nabla_{\boldsymbol{\theta}}^2 \log p(\boldsymbol{\theta}) \\ &= I_{\text{aug}}(\boldsymbol{\theta}) - \nabla_{\boldsymbol{\theta}}^2 \log p(\boldsymbol{\theta}). \end{aligned}$$

To optimize the rate of convergence of the EM algorithm, we seek values of  $(a, \mathbf{w})$  that minimizes  $I_{\text{aug}}^B(\boldsymbol{\theta}^*)$ . Since  $p(\boldsymbol{\theta})$  is independent of  $(a, \mathbf{w})$ , it suffices to minimize  $I_{\text{aug}}(\boldsymbol{\theta}^*)$  with respect to  $(a, \mathbf{w})$ . The only difference here is that  $I_{\text{aug}}(\boldsymbol{\theta})$  is evaluated at the posterior mode  $\boldsymbol{\theta}^*$  instead of the MLE  $\boldsymbol{\theta}^*$ . As  $I_{\mu, \mu}$  is independent of  $\mu$ , the optimal value of  $\mathbf{w}$  derived in Section 2.1 remains valid. As for  $I_{\sigma_{\eta}^2, \sigma_{\eta}^2}$ , it is shown in Section S7 of the supplementary material that the optimal values of  $(a, \mathbf{w})$  derived in Section 2.2 miraculously remain valid for any prior distribution  $p(\sigma_{\eta}^2)$ . Thus we can still make use of the optimal values of  $(a, \mathbf{w})$  derived in Sections 2.1 and 2.2 to optimize the rate of convergence of the EM algorithm when finding the posterior mode of the Gaussian state space model.

## 4.2 Gibbs sampler and variational Bayes

It is well known that the convergence rates of the EM algorithm and Gibbs sampler are closely related. When the target distribution  $p(\boldsymbol{\theta}, \mathbf{x} \mid \mathbf{y})$  is Gaussian, [Sahu and Roberts \(1999\)](#) showed that the rate of convergence of the Gibbs sampler that alternately updates  $\boldsymbol{\theta}$  and  $\mathbf{x}$  is equal to that of the corresponding EM algorithm. Specifically, if the precision matrix of  $p(\boldsymbol{\theta}, \mathbf{x} \mid \mathbf{y})$  is

$$H = \begin{bmatrix} H_{11} & H_{12} \\ H_{12}^T & H_{22} \end{bmatrix},$$

where  $H_{11}$  and  $H_{22}$  are the blocks corresponding to  $\boldsymbol{\theta}$  and  $\mathbf{x}$  respectively, then the common rate of convergence is  $H_{11}^{-1} H_{12} H_{22}^{-1} H_{21}$ .

As illustration, suppose  $\mu$  is the only unknown parameter and a flat prior  $p(\mu) \propto 1$  is used. We show that the strategy of partially noncentering  $\mu$  and results in Section 2.1 can be transferred to the Gibbs sampler corresponding to Algorithm 1 given below.

Initialize  $\mu^{(0)}$ . For  $i = 1, \dots, N$ ,

Step 1. Sample  $\boldsymbol{\alpha}^{(i)}$  from  $p(\boldsymbol{\alpha} \mid \mu^{(i-1)}, \mathbf{y})$ .

Step 2. Sample  $\mu^{(i)}$  from  $p(\mu \mid \boldsymbol{\alpha}^{(i)}, \mathbf{y})$ .

The conditional distribution  $p(\boldsymbol{\alpha} \mid \mu, \mathbf{y})$  is given in (6) and

$$\mu \mid \boldsymbol{\alpha}, \mathbf{y} \sim \mathcal{N}(\tau(\mathbf{w})^{-1}\{\sigma_\epsilon^{-2}\mathbf{y}^T\mathbf{w} - \sigma_\eta^a\boldsymbol{\alpha}^T\rho(\mathbf{w})\}, \tau(\mathbf{w})^{-1}).$$

The joint posterior density  $p(\mu, \boldsymbol{\alpha} \mid \mathbf{y})$  is Gaussian with precision matrix  $H$ , where  $H_{11} = \tau(\mathbf{w})$ ,  $H_{12} = \sigma_\eta^a\rho(\mathbf{w})^T$  and  $H_{22} = \sigma_\eta^{2a}V_0^{-1}$ . By Sahu and Roberts (1999), the rate of convergence of the Gibbs sampler is  $\tau(\mathbf{w})^{-1}\rho(\mathbf{w})^TV_0\rho(\mathbf{w})$ , the same as that stated in Theorem 1. Hence the Gibbs sampler converges instantly and produces independent draws when  $\mathbf{w} = \mathbf{w}^{\text{opt}}$ . Alternatively, if we combine the updates in steps 1 and 2, the update of  $\mu$  at the  $i$ th iteration is

$$\mu^{(i)} = \tau(\mathbf{w})^{-1} \left[ \mathbf{y}^TS^{-1}\mathbf{1} + \rho(\mathbf{w})^TV_0\rho(\mathbf{w})\mu^{(i-1)} + \sqrt{\rho(\mathbf{w})^TV_0\rho(\mathbf{w}) + \tau(\mathbf{w})}Z \right],$$

where  $Z \sim \mathcal{N}(0, 1)$ . The rate of convergence can be optimized by minimizing the autocorrelation at lag 1,  $\tau(\mathbf{w})^{-1}\rho(\mathbf{w})^TV_0\rho(\mathbf{w})$ , and the result in Theorem 1 follows.

Next, we demonstrate that variational Bayes (Attias, 1999) can also benefit from partial noncentering. Consider a variational Bayes approximation to  $p(\mu, \boldsymbol{\alpha} \mid \mathbf{y})$  of the form  $q(\boldsymbol{\alpha}, \mu) = q(\boldsymbol{\alpha})q(\mu)$ . Subjected to this product density restriction, the optimal  $q(\boldsymbol{\alpha})$  and  $q(\mu)$ , obtained by minimizing the Kullback-Leibler divergence from  $p(\mu, \boldsymbol{\alpha} \mid \mathbf{y})$  to  $q(\boldsymbol{\alpha}, \mu)$ , are  $\mathcal{N}(m_\alpha^q, \sigma_\eta^{-2a}V_0)$  and  $\mathcal{N}(m_\mu^q, \tau(\mathbf{w})^{-1})$  respectively (see, e.g. Ormerod and Wand, 2010), where

$$m_\alpha^q = \sigma_\eta^{-a}V_0\{\sigma_\epsilon^{-2}\mathbf{y} - \rho(\mathbf{w})m_\mu^q\}, \quad m_\mu^q = \tau(\mathbf{w})^{-1}\{\sigma_\epsilon^{-2}\mathbf{y}^T\mathbf{w} - \sigma_\eta^a\rho(\mathbf{w})^Tm_\alpha^q\}.$$

The variational Bayes algorithm thus iterates between updating  $m_\alpha^q$  and  $m_\mu^q$ . Combining the two updates, we have at the  $i$ th iteration,

$$m_\mu^{q(i)} = \tau(\mathbf{w})^{-1}(\mathbf{y}^TS^{-1}\mathbf{1} + \rho(\mathbf{w})^TV_0\rho(\mathbf{w})m_\mu^{q(i-1)}).$$

Hence the rate of convergence is also  $\tau(\mathbf{w})^{-1}\rho(\mathbf{w})^TV_0\rho(\mathbf{w})$ , which is minimized to zero when  $\mathbf{w} = \mathbf{w}^{\text{opt}}$ . Moreover,  $\tau(\mathbf{w}^{\text{opt}}) = (\mathbf{1}^TS^{-1}\mathbf{1})^{-1}$ . Hence  $m_\mu^q = (\mathbf{y}^TS^{-1}\mathbf{1})/(\mathbf{1}^TS^{-1}\mathbf{1})$  and  $q(\mu)$  is able to capture the true marginal distribution of  $\mu$ .

In summary, when  $\mu$  is the only unknown parameter, the rate of convergence of the EM algorithm, Gibbs sampler and variational Bayes are all equal to  $\tau(\mathbf{w})^{-1}\rho(\mathbf{w})^TV_0\rho(\mathbf{w})$ , which is optimized at  $\mathbf{w}^{\text{opt}}$ . This outcome is in line with the result of Tan and Nott (2014), who showed the equivalence of the rates of convergence between the EM algorithm, Gibbs sampler and variational Bayes, when the target density is Gaussian. Intuitively,  $\mathbf{w}^{\text{opt}}$  minimizes the fraction of missing information for the EM algorithm, and the autocorrelation at lag 1 for the Gibbs sampler. For variational Bayes,  $\mathbf{w}^{\text{opt}}$ , besides optimizing the rate

of convergence, also produces a more accurate posterior approximation. This is because  $\text{cov}(\boldsymbol{\alpha}, \mu | \mathbf{y})$  is zero when  $\mathbf{w} = \mathbf{w}^{\text{opt}}$ , and  $q(\boldsymbol{\alpha}, \mu) = q(\boldsymbol{\alpha})q(\mu)$  is then an accurate reflection of the dependence structure between  $\boldsymbol{\alpha}$  and  $\mu$ .

## 5 Non-Gaussian state space models

In the second part of this paper, we consider Bayesian MCMC algorithms for some non-Gaussian state space models and demonstrate how the optimal parametrizations derived in Section 2 for the Gaussian state space model can be used to improve the mixing and convergence of MCMC sampler. We focus on for two non-Gaussian state space models, the stochastic volatility (SV) model and the stochastic conditional duration (SCD) model.

### 5.1 Stochastic volatility (SV) model

The returns of financial time series often have variances that vary with time. The SV model (Taylor, 1982) seeks to capture this behavior by modeling the logarithm of the squared volatility as a hidden first order autoregressive process. It can be specified as

$$\begin{aligned} y_t &= e^{x_t/2} \epsilon_t, \quad t = 1, \dots, n, \\ x_t &= \mu + \phi(x_{t-1} - \mu) + \sigma_\eta \eta_t, \quad t = 2, \dots, n, \\ x_1 &\sim N(\mu, \sigma_\eta^2 / (1 - \phi^2)), \end{aligned} \tag{15}$$

where  $e^{x_t/2}$  represents the volatility, and  $\{\epsilon_t\}$  and  $\{\eta_s\}$  are independent sequences distributed as standard normal. The unknown parameters are  $\boldsymbol{\theta} = (\mu, \sigma_\eta^2, \phi)$ . We can transform the SV model into a linear model by writing

$$\tilde{y}_t = \log y_t^2 = x_t + \log \epsilon_t^2,$$

where  $\log \epsilon_t^2$  follows a  $\log \chi_1^2$  distribution with mean,  $\psi(0.5) - \log 0.5 \approx -1.27$ , and variance,  $\pi^2/2 \approx 4.93$ . Harvey et al. (1994) approximate the distribution of  $\log \epsilon_t^2$  using  $N(-1.27, 4.93)$ , thereby recovering the Gaussian state space model in (2) with  $y_t$  replaced by  $\tilde{y}_t + 1.2704$  and  $\sigma_\epsilon^2 = 4.93$ . They then estimated the parameters  $\boldsymbol{\theta}$  by maximizing the quasi-likelihood using Kalman filtering. However, Kim et al. (1998) showed that the distribution of  $\log \epsilon_t^2$  is highly skewed and poorly approximated by a normal distribution, and they approximate it using a 7-component mixture of normal densities instead. Here we consider the improved mixture approximation with  $K = 10$  components by Omori et al. (2007). Let  $r_t \in \{1, \dots, K\}$  be mixture component indicators such that  $P(r_t = k) = p_k$  and  $\log \epsilon_t^2 | r_t = k \sim N(m_k, s_k^2)$  for  $t = 1, \dots, n$ . Conditional on the mixture indicator  $r_t$ ,

$$\tilde{y}_t - m_{r_t} = x_t + s_{r_t} \varepsilon_t,$$

where  $\varepsilon_t \sim N(0, 1)$  and the state space model in (2) is recovered with  $y_t$  replaced by  $\tilde{y}_t - m_{r_t}$  and  $\sigma_\varepsilon$  replaced by  $s_{r_t}$ .

## 5.2 Stochastic conditional duration (SCD) model

The timing of transactions is central to the study of the microstructure of financial markets. As time intervals between transactions are highly irregular, Engle and Russell (1998) formulated the autoregressive conditional duration model to analyze such data, treating arrival times as a point process and allowing the conditional intensity to be dependent on past durations. As an extension, Bauwens and Veredas (2004) propose the SCD model, which treats the logarithm of the conditional mean of durations as a latent variable following a first order autoregression. The latent states of the SCD model are defined in the same way as the SV model. However the duration  $y_t$  in the SCD model has positive support, and the observation equation is given by

$$y_t = e^{x_t} \epsilon_t, \quad t = 1, \dots, n,$$

where  $\epsilon_t$  is assumed to follow the exponential distribution with mean 1. Other possible choices for the distribution of  $\epsilon_t$  include Weibull and Gamma (Strickland et al., 2006). Applying a similar technique, we transform the SCD model into a linear one by writing

$$\tilde{y}_t = \log y_t = x_t + \log \epsilon_t,$$

where  $\log \epsilon_t$  has mean,  $\psi(1) \approx -0.58$ , and variance,  $\pi^2/6 \approx 1.64$ . The distribution of  $\log \epsilon_t$  is also poorly approximated by  $N(-0.58, 1.64)$  and we approximate it using a mixture of normal densities. Carter and Kohn (1997) provide the parameters of a 5-component mixture approximation for  $\log \epsilon_t$ , but we prefer to use an improved 10-component mixture approximation that we found using the R package `mixtools` (Benaglia et al., 2009). The parameters of the mixture approximation for the SV and SCD models are given in Table 5. Figure 10 shows the true densities of  $\log \chi_1^2$  and  $\log \exp(1)$  (blue solid lines), Gaussian approximation based on the mean and variance of the original variables (green dotted lines) and 10-component mixture approximations (red dashed lines).

Using the mixture of normals approximation, we can construct Bayesian MCMC algorithms for the SV and SCD models similarly, with the only difference being  $\tilde{y}_t = \log y_t^2$  for the SV model, while  $\tilde{y}_t = \log y_t$  for the SCD model. Let  $\tilde{\mathbf{y}} = (\tilde{y}_1, \dots, \tilde{y}_n)^T$ ,  $\mathbf{r} = (r_1, \dots, r_n)^T$ ,  $\mathbf{m}_{\mathbf{r}} = (m_{r_1}, \dots, m_{r_n})^T$  and  $\mathbf{s}_{\mathbf{r}}^2 = (s_{r_1}^2, \dots, s_{r_n}^2)^T$ . In matrix notation,

$$\tilde{\mathbf{y}} - \mathbf{m}_{\mathbf{r}} \mid \mathbf{r}, \mathbf{x} \sim N(\mathbf{x}, D_{\mathbf{r}}), \quad \mathbf{x} \mid \boldsymbol{\theta} \sim N(\mu \mathbf{1}, \sigma_\eta^2 \Lambda^{-1}),$$

where  $D_{\mathbf{r}} = \text{diag}(\mathbf{s}_{\mathbf{r}}^2)$ . As before, we introduce the latent states  $\boldsymbol{\alpha} = (\mathbf{x} - \mu \mathbf{w})/\sigma_\eta^a$ . Then

$k$	SV model			SCD model		
	$p_k$	$m_k$	$s_k^2$	$p_k$	$m_k$	$s_k^2$
1	0.00609	1.92677	0.11265	0.02855	-3.58113	2.10124
2	0.04775	1.34744	0.17788	0.05885	-1.93950	0.34798
3	0.13057	0.73504	0.26768	0.29083	-0.86004	0.36818
4	0.20674	0.02266	0.40601	0.11277	-2.17891	1.14959
5	0.22715	-0.85173	0.62699	0.07446	-0.53312	0.10306
6	0.18842	-1.97278	0.98583	0.01375	-0.29681	0.03879
7	0.12047	-3.46788	1.57469	0.16382	0.05911	0.10076
8	0.05591	-5.55246	2.54498	0.00281	-5.39508	4.88222
9	0.01575	-8.68384	4.16591	0.17465	0.56731	0.12503
10	0.00115	-14.65000	7.33342	0.07951	1.07227	0.14771

Table 5: Parameters of mixture of normals for SV model and SCD model.

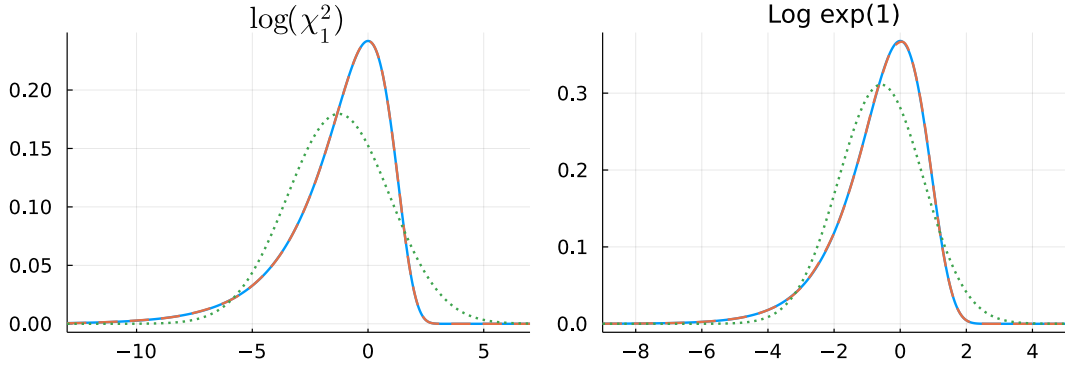


Figure 10: Densities of  $\log \chi_1^2$  and  $\log \exp(1)$  (blue solid lines),  $N(-1.27, 4.93)$  and  $N(-0.58, 1.64)$  approximations (green dotted lines) and 10-component mixture approximations (red dashed lines).

the model can be written as

$$\tilde{\mathbf{y}} - \mathbf{m}_{\mathbf{r}} \mid \mathbf{r}, \boldsymbol{\alpha}, \boldsymbol{\theta} \sim N(\sigma_{\eta}^a \boldsymbol{\alpha} + \mu \mathbf{w}, D_{\mathbf{r}}), \quad \sigma_{\eta}^a \boldsymbol{\alpha} \mid \boldsymbol{\theta} \sim N(\mu \bar{\mathbf{w}}, \sigma_{\eta}^2 \Lambda^{-1}).$$

For Bayesian inference, a prior  $p(\boldsymbol{\theta})$  is placed on the unknown parameters  $\boldsymbol{\theta}$ . Following [Kastner and Frühwirth-Schnatter \(2014\)](#), we specify independent priors for the components of  $\boldsymbol{\theta}$ , namely,  $\mu \sim N(b_{\mu}, B_{\mu})$ ,  $\sigma_{\eta}^2 \sim \text{Gamma}(0.5, 0.5B_{\sigma})$  such that  $E(\sigma_{\eta}^2) = B_{\sigma}$ , and  $\text{Beta}(b_{\phi}, B_{\phi})$  for  $(\phi + 1)/2$  ([Kim et al., 1998](#)). The joint posterior distribution is

$$p(\boldsymbol{\alpha}, \boldsymbol{\theta}, \mathbf{r} \mid \mathbf{y}) \propto p(\mathbf{y} \mid \mathbf{r}, \boldsymbol{\alpha}, \boldsymbol{\theta}) p(\boldsymbol{\alpha} \mid \boldsymbol{\theta}) p(\boldsymbol{\theta}) p(\mathbf{r}).$$

The choice of a gamma prior for  $\sigma_{\eta}^2$  instead of the conventional inverse-gamma prior reduces sensitivity to the prior hyperparameters ([Frühwirth-Schnatter and Wagner, 2010](#)).

## 6 MCMC Algorithms

First we outline a baseline MCMC algorithm for the SV and SCD models which can be run using the CP ( $a = 0$ ,  $\mathbf{w} = \mathbf{0}$ ), NCP ( $a = 1$ ,  $\mathbf{w} = \mathbf{1}$ ), or any fixed values of  $(a, \mathbf{w})$ . It is based largely on the MCMC sampler for the SV model constructed in [Kastner and Frühwirth-Schnatter \(2014\)](#) with some differences. In particular, the updates may be used with any arbitrary values of  $(a, \mathbf{w})$ , and not just the CP or NCP.

---

### MCMC Algorithm for SV and SCD models

---

Initialize  $\boldsymbol{\theta}^{(0)}$  and  $\mathbf{r}^{(0)}$ . For  $i = 0, \dots, M - 1$ ,

1. Sample  $\boldsymbol{\alpha}^{(i+1)}$  from  $p(\boldsymbol{\alpha} \mid \mathbf{y}, \boldsymbol{\theta}^{(i)}, \mathbf{r}^{(i)})$ ,
2. Sample  $\boldsymbol{\theta}^{(i+1)}$  from  $p(\boldsymbol{\theta} \mid \mathbf{y}, \boldsymbol{\alpha}^{(i+1)}, \mathbf{r}^{(i)})$ ,
3. Sample  $\mathbf{r}^{(i+1)}$  from  $p(\mathbf{r} \mid \mathbf{y}, \boldsymbol{\alpha}^{(i+1)}, \boldsymbol{\theta}^{(i+1)})$ .

Return the draws  $\{\boldsymbol{\theta}^{(i)}, \mathbf{r}^{(i)} \mid i = 1, \dots, M\}$ .

---

The sampling of  $\boldsymbol{\alpha}$  and  $\mathbf{r}$  from their conditional posterior distributions in steps 1 and 3 are performed using Gibbs. To sample  $\boldsymbol{\theta} = (\mu, \sigma_\eta^2, \phi)$  in step 2, [Kastner and Frühwirth-Schnatter \(2014\)](#) investigated 1-block, 2-block and 3-block samplers, all requiring some use of Metropolis-Hastings updates. Conditional on the parametrization, the simulation efficiency for  $(\mu, \sigma_\eta^2, \phi)$  was found to be similar across different blocking strategies, except that the 3-block sampler is lower in simulation efficiency for  $\phi$  compared to the 1-block and 2-block samplers under the CP. Here we only consider the 3-block sampler for  $\boldsymbol{\theta}$ . The updates in each step are derived below for arbitrary values of  $(a, \mathbf{w})$ . Updates for the CP and NCP can be obtained simply by substituting appropriate values of  $(a, \mathbf{w})$ .

The conditional posterior distribution for the latent states  $\boldsymbol{\alpha}$  is

$$p(\boldsymbol{\alpha} \mid \mathbf{y}, \boldsymbol{\theta}, \mathbf{r}) \propto \exp\{-[(\tilde{\mathbf{y}} - \mathbf{m}_\mathbf{r} - \mu\mathbf{w} - \sigma_\eta^a \boldsymbol{\alpha})^T D_\mathbf{r}^{-1} (\tilde{\mathbf{y}} - \mathbf{m}_\mathbf{r} - \mu\mathbf{w} - \sigma_\eta^a \boldsymbol{\alpha}) + \sigma_\eta^{-2} (\sigma_\eta^a \boldsymbol{\alpha} - \mu\bar{\mathbf{w}})^T \Lambda (\sigma_\eta^a \boldsymbol{\alpha} - \mu\bar{\mathbf{w}})]/2\} \propto \exp\{-(\boldsymbol{\alpha}^T C_\alpha \boldsymbol{\alpha} - 2\boldsymbol{\alpha}^T \mathbf{c}_\alpha)/2\},$$

where  $C_\alpha = \sigma_\eta^{2a} (D_\mathbf{r}^{-1} + \sigma_\eta^{-2} \Lambda)$  and  $\mathbf{c}_\alpha = \sigma_\eta^a (D_\mathbf{r}^{-1} (\tilde{\mathbf{y}} - \mathbf{m}_\mathbf{r} - \mu\mathbf{w}) + \sigma_\eta^{-2} \mu \Lambda \bar{\mathbf{w}})$ . Hence  $\boldsymbol{\alpha} \mid \mathbf{y}, \boldsymbol{\theta}, \mathbf{r} \sim N(C_\alpha^{-1} \mathbf{c}_\alpha, C_\alpha^{-1})$ . As  $C_\alpha$  is a symmetric tridiagonal matrix, we first compute the  $LDL^T$  decomposition of  $C_\alpha$ , where  $D$  is a diagonal matrix and  $L$  is a unit lower triangular matrix with only the first lower diagonal nonzero.  $C_\alpha^{-1} \mathbf{c}_\alpha$  is then computed using backward substitution. To generate  $\boldsymbol{\alpha}$ , a random vector  $\mathbf{z}$  is first simulated from  $N(0, I)$  so that  $\boldsymbol{\alpha} = C_\alpha^{-1} \mathbf{c}_\alpha + L^{-T} D^{-1/2} \mathbf{z}$ .

For the indicators  $\mathbf{r}$ ,  $p(\mathbf{r} \mid \mathbf{y}, \boldsymbol{\alpha}, \boldsymbol{\theta}) \propto \prod_{t=1}^n p(y_t \mid r_t, \alpha_t, \boldsymbol{\theta}) p(r_t)$ . Thus, the  $\{r_t\}$  are conditionally independent a posteriori. For  $t = 1, \dots, n$ ,  $k = 1, \dots, K$ ,

$$P(r_t = k \mid y_t, \alpha_t, \boldsymbol{\theta}) \propto \exp\{\log p_k - \log(s_k^2)/2 - (\tilde{y}_t - \mu w_t - \sigma_\eta^a \alpha_t - m_k)^2 / (2s_k^2)\},$$

where  $p_k = P(r_t = k)$  is given in Table 5. Hence, we can sample each  $r_t$  according to the conditional posterior probabilities (normalized to sum to one) across  $k = 1, \dots, K$ .

For the parameter  $\mu$ ,

$$p(\mu \mid \mathbf{y}, \boldsymbol{\alpha}, \mathbf{r}, \sigma_\eta^2, \phi) \propto \exp\{ -[(\tilde{\mathbf{y}} - \mathbf{m}_\mathbf{r} - \mu \mathbf{w} - \sigma_\eta^a \boldsymbol{\alpha})^T D_\mathbf{r}^{-1} (\tilde{\mathbf{y}} - \mathbf{m}_\mathbf{r} - \mu \mathbf{w} - \sigma_\eta^a \boldsymbol{\alpha}) + (\mu - b_\mu)^2 / B_\mu + \sigma_\eta^{-2} (\sigma_\eta^a \boldsymbol{\alpha} - \mu \bar{\mathbf{w}})^T \Lambda (\sigma_\eta^a \boldsymbol{\alpha} - \mu \bar{\mathbf{w}})] / 2 \} \propto \exp\{ -(C_\mu \mu^2 - 2c_\mu \mu) / 2 \}.$$

Hence  $\mu \mid \mathbf{y}, \boldsymbol{\alpha}, \mathbf{r}, \sigma_\eta^2, \phi \sim N(C_\mu^{-1} c_\mu, C_\mu^{-1})$ , where

$$C_\mu = B_\mu^{-1} + \mathbf{w}^T D_\mathbf{r}^{-1} \mathbf{w} + \sigma_\eta^{-2} \bar{\mathbf{w}}^T \Lambda \bar{\mathbf{w}}, \quad c_\mu = B_\mu^{-1} b_\mu + \sigma_\eta^{a-2} \boldsymbol{\alpha}^T \Lambda \bar{\mathbf{w}} + (\tilde{\mathbf{y}} - \mathbf{m}_\mathbf{r} - \sigma_\eta^a \boldsymbol{\alpha})^T D_\mathbf{r}^{-1} \mathbf{w}.$$

For the parameter  $\phi$ , let  $h_t = \sigma_\eta^a \alpha_t - \mu \bar{w}_t$  for  $t = 1, \dots, n$ . Then

$$\begin{aligned} p(\phi \mid \mathbf{y}, \boldsymbol{\alpha}, \mathbf{r}, \mu, \sigma_\eta^2) &\propto \exp\{ [\log(1 - \phi^2) - \sigma_\eta^{-2} (\sigma_\eta^a \boldsymbol{\alpha} - \mu \bar{\mathbf{w}})^T \Lambda (\sigma_\eta^a \boldsymbol{\alpha} - \mu \bar{\mathbf{w}})] / 2 \\ &\quad + (b_\phi - 1) \log(1 + \phi) + (B_\phi - 1) \log(1 - \phi) \} \\ &\propto \exp\left\{ g_\phi(\phi) - \sum_{t=2}^n (h_t - \phi h_{t-1})^2 / (2\sigma_\eta^2) \right\}, \end{aligned} \quad (16)$$

where

$$g_\phi(\phi) = \left(b_\phi - \frac{1}{2}\right) \log(1 + \phi) + \left(B_\phi - \frac{1}{2}\right) \log(1 - \phi) + \frac{\phi^2 h_1}{2\sigma_\eta^2}.$$

We perform a Metropolis-Hastings step (Kim et al., 1998), where a proposal  $\phi^{\text{new}}$  is generated from  $N(\{\sum_{t=1}^{n-1} h_t^2\}^{-1} \{\sum_{t=1}^{n-1} h_t h_{t+1}\}, \{\sum_{t=1}^{n-1} h_t^2\}^{-1} \sigma_\eta^2)$ , based on a normal approximation to the last term in (16). If  $|\phi^{\text{new}}| < 1$ , then  $\phi^{\text{new}}$  is accepted with probability equal to  $\min(1, \exp\{g_\phi(\phi^{\text{new}}) - g_\phi(\phi^{\text{old}})\})$ .

Lastly, for the parameter  $\sigma_\eta^2$ ,

$$\begin{aligned} p(\sigma_\eta^2 \mid \mathbf{y}, \boldsymbol{\alpha}, \mathbf{r}, \mu, \phi) &\propto \exp\left\{ -\sigma_\eta^{2a} \boldsymbol{\alpha}^T (D_\mathbf{r}^{-1} + \sigma_\eta^{-2} \Lambda) \boldsymbol{\alpha} / 2 + \sigma_\eta^a \boldsymbol{\alpha}^T [D_\mathbf{r}^{-1} (\tilde{\mathbf{y}} - \mathbf{m}_\mathbf{r} - \mu \mathbf{w})] \right. \\ &\quad \left. + \mu \Lambda \bar{\mathbf{w}} / \sigma_\eta^2 - \mu^2 \bar{\mathbf{w}}^T \Lambda \bar{\mathbf{w}} / (2\sigma_\eta^2) - [n(1 - a) + 1] (\log \sigma_\eta^2) / 2 - \sigma_\eta^2 / (2B_\sigma) \right\}. \end{aligned}$$

First, we discuss updates for the CP and NCP before proposing an update for arbitrary values of  $(a, \mathbf{w})$ . For the CP ( $a = 0, \mathbf{w} = 0$ ),  $p(\sigma_\eta^2 \mid \mathbf{y}, \boldsymbol{\alpha}, \mathbf{r}, \mu, \phi) \propto \exp\{f_\sigma(\sigma_\eta^2)\}$ , where

$$f_\sigma(\sigma_\eta^2) = -C_\sigma / \sigma_\eta^2 - (c_\sigma + 1) \log(\sigma_\eta^2) - \sigma_\eta^2 / (2B_\sigma),$$

$C_\sigma = (\boldsymbol{\alpha} - \mu \mathbf{1})^T \Lambda (\boldsymbol{\alpha} - \mu \mathbf{1}) / 2$  and  $c_\sigma = (n - 1) / 2$ . Kastner and Frühwirth-Schnatter (2014) propose a Metropolis-Hastings step, where a proposal  $\sigma_\eta^{2\text{new}}$  is generated from the inverse gamma distribution,  $\text{IG}(c_\sigma, C_\sigma)$ , and is accepted with a probability of  $\min(1, \exp[(\sigma_\eta^{2\text{old}} - \sigma_\eta^{2\text{new}}) / (2B_\sigma)])$ . For the NCP ( $a = 1, \mathbf{w} = 1$ ),

$$p(\sigma_\eta \mid \mathbf{y}, \boldsymbol{\alpha}, \mathbf{r}, \mu, \phi) \propto \exp\{c'_\sigma \sigma_\eta - C'_\sigma \sigma_\eta^2 / 2\},$$

where  $C'_\sigma = \boldsymbol{\alpha}^T D_{\mathbf{r}}^{-1} \boldsymbol{\alpha} + B_\sigma^{-1}$  and  $c'_\sigma = \boldsymbol{\alpha}^T D_{\mathbf{r}}^{-1} (\tilde{\mathbf{y}} - \mathbf{m}_{\mathbf{r}} - \mu \mathbf{1})$ . Thus we can generate a proposal  $\sigma_\eta^{\text{new}}$  from  $N(C_\sigma'^{-1} c'_\sigma, C_\sigma'^{-1})$ , which is accepted if  $\sigma_\eta^{\text{new}} > 0$ . For arbitrary values of  $(a, \mathbf{w})$ , we consider a transformation  $\sigma_\eta^2 = e^\nu$  so that  $\nu$  is unconstrained. We have  $p(\nu \mid \mathbf{y}, \boldsymbol{\alpha}, \mathbf{r}, \mu, \phi) \propto \exp\{f_\nu(\nu)\}$ , where

$$f_\nu(\nu) = A_1 e^{a\nu} + A_2 e^{(a-1)\nu} + A_3 e^{a\nu/2} + A_4 e^{(a/2-1)\nu} + A_5 e^{-\nu} + A_6 e^\nu + A_7 \nu,$$

$$A_1 = -\boldsymbol{\alpha}^T D_{\mathbf{r}}^{-1} \boldsymbol{\alpha} / 2, A_2 = -\boldsymbol{\alpha}^T \Lambda \boldsymbol{\alpha} / 2, A_3 = \boldsymbol{\alpha}^T D_{\mathbf{r}}^{-1} (\tilde{\mathbf{y}} - \mathbf{m}_{\mathbf{r}} - \mu \mathbf{w}), A_4 = \mu \boldsymbol{\alpha}^T \Lambda \bar{\mathbf{w}}, A_5 = -\mu^2 \bar{\mathbf{w}}^T \Lambda \bar{\mathbf{w}} / 2, A_6 = -1 / (2B_\sigma) \text{ and } A_7 = -[n(1-a) - 1] / 2.$$

$$\begin{aligned} f'_\nu(\nu) &= aA_1 e^{a\nu} + (a-1)A_2 e^{(a-1)\nu} + \frac{aA_3}{2} e^{\frac{a\nu}{2}} + \frac{(a-2)A_4}{2} e^{\frac{(a-2)\nu}{2}} - A_5 e^{-\nu} + A_6 e^\nu + A_7. \\ f''_\nu(\nu) &= a^2 A_1 e^{a\nu} + (a-1)^2 A_2 e^{(a-1)\nu} + \frac{a^2 A_3}{4} e^{\frac{a\nu}{2}} + \frac{(a-2)^2 A_4}{4} e^{\frac{(a-2)\nu}{2}} + A_5 e^{-\nu} + A_6 e^\nu. \end{aligned}$$

Let  $\hat{\nu} = \arg \max_\nu f_\nu(\nu)$  denote the posterior mode, which is found using the L-BFGS algorithm. Then  $f_\nu(\nu) \approx f_\nu(\hat{\nu}) + f''_\nu(\hat{\nu})(\nu - \hat{\nu})^2 / 2$  since  $f'_\nu(\hat{\nu}) = 0$ , and a normal approximation to the conditional posterior is  $N(\hat{\nu}, -1/f''_\nu(\hat{\nu}))$ . A proposal  $\nu^{\text{new}}$  generated from this normal density is accepted with probability  $\min(1, \exp\{g_\nu(\nu^{\text{new}}) - g_\nu(\nu^{\text{old}})\})$ , where

$$g_\nu(\nu) = f_\nu(\nu) - f''_\nu(\hat{\nu})(\nu - \hat{\nu})^2 / 2.$$

## 6.1 Ancillarity-sufficiency interweaving strategy (ASIS)

The mixing and convergence of the baseline MCMC sampler depends heavily on the parametrization chosen for the data at hand. For any given parametrization, the simulation efficiency may also differ across model parameters. As the behavior of the CP and NCP are often complementary to each other (one converges quickly if the other is slow), [Yu and Meng \(2011\)](#) proposed an ancillarity-sufficiency interweaving strategy (ASIS), that takes advantage of the contrasting features of the CP and NCP. This strategy interweaves a *sufficient* augmentation scheme where the missing data is a sufficient statistic for  $\boldsymbol{\theta}$  (usually the CP), and an *ancillary* augmentation scheme where the missing data is an ancillary statistic independent of  $\boldsymbol{\theta}$  (usually the NCP). [Yu and Meng \(2011\)](#) prove that interweaving these two schemes leads to an algorithm that is at least better than the worse of the two. Applying ASIS to the SV model, [Kastner and Frühwirth-Schnatter \(2014\)](#) found that it led to a significant improvement in the simulation efficiency of all parameters across different parameter settings, as compared to the baseline MCMC sampler using either the CP or NCP. While ASIS can be implemented using either the CP or NCP as the baseline, [Kastner and Frühwirth-Schnatter \(2014\)](#) report that choice of the baseline is immaterial. Hence, we will compare our proposed method only with ASIS using CP as baseline. The steps in this algorithm are outlined below.

Initialize  $\boldsymbol{\theta}^{(0)}$  and  $\mathbf{r}^{(0)}$ . For  $i = 0, \dots, M - 1$ ,

1. Under the CP (set  $a = 0$ ,  $\mathbf{w} = \mathbf{0}$ ):
  - (a) Sample  $\boldsymbol{\alpha}^{(i)}$  from  $p(\boldsymbol{\alpha} \mid \mathbf{y}, \boldsymbol{\theta}^{(i)}, \mathbf{r}^{(i)})$ .
  - (b) Sample  $\boldsymbol{\theta}^{(i+0.5)}$  from  $p(\boldsymbol{\theta} \mid \mathbf{y}, \boldsymbol{\alpha}^{(i)}, \mathbf{r}^{(i)})$ .
2. Move to the NCP (set  $a = 1$ ,  $\mathbf{w} = \mathbf{1}$ ):
  - (a) Compute  $\tilde{\boldsymbol{\alpha}}^{(i+1)} = (\boldsymbol{\alpha}^{(i)} - \mu^{(i+0.5)}) / \sigma_{\eta}^{(i+0.5)}$ .
  - (b) Sample  $\boldsymbol{\theta}^{(i+1)}$  from  $p(\boldsymbol{\theta} \mid \mathbf{y}, \tilde{\boldsymbol{\alpha}}^{(i+1)}, \mathbf{r}^{(i)})$ .
3. Move back to the CP (set  $a = 0$ ,  $\mathbf{w} = \mathbf{0}$ ):
  - (a) Compute  $\boldsymbol{\alpha}^{(i+1)} = \mu^{(i+1)} + \sigma_{\eta}^{(i+1)} \tilde{\boldsymbol{\alpha}}^{(i+1)}$ .
  - (b) Sample  $\mathbf{r}^{(i+1)}$  from  $p(\mathbf{r} \mid \mathbf{y}, \boldsymbol{\alpha}^{(i+1)}, \boldsymbol{\theta}^{(i+1)})$ .

Return the draws  $\{\boldsymbol{\theta}^{(i)}, \mathbf{r}^{(i)} \mid i = 1, \dots, M\}$ .

---

## 6.2 Block-specific reparametrization (BSR) strategy

To optimize the convergence rate of the EM algorithm for the Gaussian state space model, we have employed the AEEM algorithm so that the optimal parametrization for each parameter can be used while conditioning on the rest. As the convergence rate of the Gibbs sampler is equal to the corresponding EM algorithm when the target density is well approximated by a Gaussian (Sahu and Roberts, 1999), tailoring the data augmentation scheme to each block in a Gibbs sampler may yield similar improvements in convergence rates as in the EM algorithm. This is important as the simulation efficiency of a parametrization may be good for certain parameters but poor for others. Hence we propose a *block-specific reparametrization* (BSR) strategy that allows one to adopt a different parametrization for sampling from each block in a multi-block MCMC sampler. This yields flexibility in choosing a parametrization optimal for sampling from each block.

First, we outline the steps of an MCMC sampler adopting the BSR strategy and verify that the sampler will converge to the target density, before discussing the reparametrizations for each block. For simplicity, we limit the discussion to two blocks although BSR can be applied more generally to multiple blocks. Suppose the parameters are split into two blocks,  $\boldsymbol{\theta} = (\boldsymbol{\theta}_1, \boldsymbol{\theta}_2)$ , and consider two augmentation schemes with missing data  $\boldsymbol{\alpha}_1$  and  $\boldsymbol{\alpha}_2$  such that their joint distribution  $p(\boldsymbol{\alpha}_1, \boldsymbol{\alpha}_2 \mid \boldsymbol{\theta}, \mathbf{y})$  is well defined. This joint distribution may be degenerate, e.g. if  $\boldsymbol{\alpha}_2$  is a deterministic function of  $\boldsymbol{\alpha}_1$ . Consider an MCMC algorithm that initializes  $\boldsymbol{\theta}$  and then performs the following steps at the  $i$ th iteration for  $i = 0, \dots, M - 1$  (explicit conditioning on  $\mathbf{y}$  has been omitted for simplicity):

1. Sample  $\boldsymbol{\alpha}_1^{(i+1)}$  from  $p(\boldsymbol{\alpha}_1 \mid \boldsymbol{\theta}^{(i)})$ .

2. Sample  $\boldsymbol{\theta}_1^{(i+1)}$  from  $p(\boldsymbol{\theta}_1 | \boldsymbol{\alpha}_1^{(i+1)}, \boldsymbol{\theta}_2^{(i)})$ .
3. Sample  $\boldsymbol{\alpha}_2^{(i+1)}$  from  $p(\boldsymbol{\alpha}_2 | \boldsymbol{\alpha}_1^{(i+1)}, \boldsymbol{\theta}_1^{(i+1)}, \boldsymbol{\theta}_2^{(i)})$ .
4. Sample  $\boldsymbol{\theta}_2^{(i+1)}$  from  $p(\boldsymbol{\theta}_2 | \boldsymbol{\alpha}_2^{(i+1)}, \boldsymbol{\theta}_1^{(i+1)})$ .

The draws  $\{\boldsymbol{\theta}^{(i)} | i = 1, \dots, M\}$  are retained. The transition density of the above chain is

$$k(\boldsymbol{\theta}' | \boldsymbol{\theta}) = \int p(\boldsymbol{\theta}'_2 | \boldsymbol{\alpha}_2, \boldsymbol{\theta}'_1) p(\boldsymbol{\alpha}_2 | \boldsymbol{\alpha}_1, \boldsymbol{\theta}'_1, \boldsymbol{\theta}_2) p(\boldsymbol{\theta}'_1 | \boldsymbol{\alpha}_1, \boldsymbol{\theta}_2) p(\boldsymbol{\alpha}_1 | \boldsymbol{\theta}) d\boldsymbol{\alpha}_1 d\boldsymbol{\alpha}_2.$$

Let  $p(\boldsymbol{\theta})$  denote the stationary density. We have

$$\begin{aligned} \int k(\boldsymbol{\theta}' | \boldsymbol{\theta}) p(\boldsymbol{\theta}) d\boldsymbol{\theta} &= \int p(\boldsymbol{\theta}'_2 | \boldsymbol{\alpha}_2, \boldsymbol{\theta}'_1) p(\boldsymbol{\alpha}_2 | \boldsymbol{\alpha}_1, \boldsymbol{\theta}'_1, \boldsymbol{\theta}_2) p(\boldsymbol{\theta}'_1 | \boldsymbol{\alpha}_1, \boldsymbol{\theta}_2) \left( \int p(\boldsymbol{\alpha}_1, \boldsymbol{\theta}) d\boldsymbol{\theta}_1 \right) d\boldsymbol{\theta}_2 d\boldsymbol{\alpha}_1 d\boldsymbol{\alpha}_2 \\ &= \int p(\boldsymbol{\theta}'_2 | \boldsymbol{\alpha}_2, \boldsymbol{\theta}'_1) p(\boldsymbol{\alpha}_2 | \boldsymbol{\alpha}_1, \boldsymbol{\theta}'_1, \boldsymbol{\theta}_2) p(\boldsymbol{\theta}'_1, \boldsymbol{\alpha}_1, \boldsymbol{\theta}_2) d\boldsymbol{\theta}_2 d\boldsymbol{\alpha}_1 d\boldsymbol{\alpha}_2 \\ &= \int p(\boldsymbol{\theta}'_2 | \boldsymbol{\alpha}_2, \boldsymbol{\theta}'_1) \left( \int p(\boldsymbol{\alpha}_2, \boldsymbol{\alpha}_1, \boldsymbol{\theta}'_1, \boldsymbol{\theta}_2) d\boldsymbol{\theta}_2 d\boldsymbol{\alpha}_1 \right) d\boldsymbol{\alpha}_2 \\ &= \int p(\boldsymbol{\theta}'_2, \boldsymbol{\alpha}_2, \boldsymbol{\theta}'_1) d\boldsymbol{\alpha}_2 = p(\boldsymbol{\theta}). \end{aligned}$$

Hence the stationary density is preserved by the BSR strategy. If  $\boldsymbol{\alpha}_2$  is a deterministic function (say  $f$ ) of  $\boldsymbol{\alpha}_1$  given  $\boldsymbol{\theta}$ , then we can just compute  $\boldsymbol{\alpha}_2^{(i+1)} = f(\boldsymbol{\alpha}_1^{(i+1)} | \boldsymbol{\theta}_1^{(i+1)}, \boldsymbol{\theta}_2^{(i)})$  without having to sample  $\boldsymbol{\alpha}_2$  in step 3. This feature is particularly important in models where  $\boldsymbol{\alpha}$  is high-dimensional (e.g. state space models) and sampling of  $\boldsymbol{\alpha}$  is time-consuming.

Next, we discuss how the BSR strategy can be applied to the SV and SCD models. Conditional on  $\mathbf{r}$ ,  $\boldsymbol{\alpha}$  and  $\boldsymbol{\theta}$ ,  $\tilde{\mathbf{y}} - \mathbf{m}_{\mathbf{r}} \sim N(\sigma_{\eta}^2 \boldsymbol{\alpha} + \mu \mathbf{w}, D_{\mathbf{r}})$ . Comparing this distribution with (5), the differences are,  $\mathbf{y}$  is replaced by  $\tilde{\mathbf{y}} - \mathbf{m}_{\mathbf{r}}$ , and  $\sigma_{\epsilon}^2 I$  is replaced by  $D_{\mathbf{r}}^{-1}$ . In Section 4.1, we have shown that when using the EM algorithm to find the posterior mode of the unknown parameters, the optimal parametrizations for  $\mu$  and  $\sigma_{\eta}^2$  remain unchanged and are independent of the priors. In addition, it can be verified that for the Gaussian state space model, if  $\sigma_{\epsilon}^2$  is not constant across time, then it suffices to replace  $\sigma_{\epsilon}^{-2} I$  in the expressions of  $a$  and  $\mathbf{w}$  by a diagonal matrix filled with the variances at different time points (see Supplementary material Section S9). Applying these results to the SV and SCD models using a mixture of normals approximation, we propose to divide the parameters into two blocks,  $\mu$  and  $(\sigma_{\eta}^2, \phi, \mathbf{r})$ , and use the optimal schemes for  $\mu$  and  $\sigma_{\eta}^2$  respectively in these two blocks. Based on the EM algorithm, the augmented information matrix element  $I_{\phi, \phi}$  is independent of  $(a, \mathbf{w})$ . Hence it is not possible to choose  $(a, \mathbf{w})$  to optimize the convergence of  $\phi$ , and we just sample it along with  $\sigma_{\eta}^2$  under the second scheme. For convenience,  $\mathbf{r}$  is sampled in the second scheme as well. Conditional on the mixture indicators  $\mathbf{r}$ , the values of  $(a, \mathbf{w})$  in the first scheme are

$$a_1 = 0, \quad \bar{\mathbf{w}}_1 = V_0 D_{\mathbf{r}}^{-1} \mathbf{1}, \quad (17)$$

where  $V_0 = (D_{\mathbf{r}}^{-1} + \sigma_{\eta}^{-2}\Lambda)^{-1}$  and we have chosen  $a_1 = 0$  for simplicity. For the second scheme,

$$a_2 = 1 - \text{tr}(V_0 D_{\mathbf{r}}^{-1})/n, \quad \bar{\mathbf{w}}_2 = \frac{1}{\mu} \left( \frac{2V_0\Lambda}{a_2\sigma_{\eta}^2} - I \right) \mathbf{m}_{01}, \quad (18)$$

where  $\mathbf{m}_{01} = V_0 D_{\mathbf{r}}^{-1}(\tilde{\mathbf{y}} - \mathbf{m}_{\mathbf{r}} - \mu\mathbf{1})$ . Since  $\boldsymbol{\alpha}_s = (\mathbf{x} - \mu\mathbf{w}_s)/\sigma_{\eta}^{a_s}$  for  $s = 1, 2$ , we can simply set  $\boldsymbol{\alpha}_2 = \{\boldsymbol{\alpha}_1 + \mu(\bar{\mathbf{w}}_2 - \bar{\mathbf{w}}_1)\}/\sigma_{\eta}^{a_2}$  when switching from the first to second scheme. The key steps in the MCMC sampler using the BSR strategy are outlined below.

---

BSR Algorithm for SV and SCD models

---

Initialize  $\boldsymbol{\theta}^{(0)}$  and  $\mathbf{r}^{(0)}$ . For  $i = 0, \dots, M - 1$ ,

1. First scheme (set  $a = a_1$ ,  $\mathbf{w} = \mathbf{w}_1$ ):

- (a) Sample  $\boldsymbol{\alpha}_1^{(i+1)}$  from  $p(\boldsymbol{\alpha} \mid \mathbf{y}, \boldsymbol{\theta}_1^{(i)}, \boldsymbol{\theta}_2^{(i)})$ .
- (b) Sample  $\mu^{(i+1)}$  from  $p(\mu \mid \mathbf{y}, \boldsymbol{\alpha}_1^{(i+1)}, \sigma_{\eta}^{2(i)}, \phi^{(i)}, \mathbf{r}^{(i)})$ .

2. Switch to second scheme (set  $a = a_2$ ,  $\mathbf{w} = \mathbf{w}_2$ ):

- (a) Compute  $\boldsymbol{\alpha}_2^{(i+1)} = \{\boldsymbol{\alpha}_1^{(i+1)} + \mu^{(i+1)}(\bar{\mathbf{w}}_2 - \bar{\mathbf{w}}_1)\}/\sigma_{\eta}^{(i)a_2}$ .
- (b) Sample  $\sigma_{\eta}^{2(i+1)}$  from  $p(\sigma_{\eta}^2 \mid \mathbf{y}, \boldsymbol{\alpha}_2^{(i+1)}, \mu^{(i+1)}, \phi^{(i)}, \mathbf{r}^{(i)})$ .
- (c) Sample  $\phi^{(i+1)}$  from  $p(\phi \mid \mathbf{y}, \boldsymbol{\alpha}_2^{(i+1)}, \mu^{(i+1)}, \sigma_{\eta}^{2(i+1)}, \mathbf{r}^{(i)})$ .
- (d) Sample  $\mathbf{r}^{(i+1)}$  from  $p(\mathbf{r} \mid \mathbf{y}, \boldsymbol{\alpha}_2^{(i+1)}, \boldsymbol{\theta}^{(i+1)})$ .

Return the draws  $\{\boldsymbol{\theta}^{(i)}, \mathbf{r}^{(i)} \mid i = 1, \dots, M\}$ .

---

The values of  $(a, \mathbf{w})$  in (17) and (18) depend on the true values of the parameters  $\boldsymbol{\theta}$  and mixture indicators  $\mathbf{r}$ , which are unknown. Hence we propose the following procedure to overcome this difficulty. To initialize  $\boldsymbol{\theta}^{(0)}$ ,  $\bar{\mathbf{w}}_1$ ,  $\bar{\mathbf{w}}_2$  and  $a_2$ , we run AECM Algorithm 3 on transformed responses  $\tilde{\mathbf{y}}_t$ , by approximating the distribution of  $\log \epsilon_t^2$  in the SV model by  $N(-1.27, 4.93)$ , and  $\log \epsilon_t$  in the SCD model by  $N(-0.58, 1.64)$ . The MLE  $\hat{\boldsymbol{\theta}}$  obtained using the AECM algorithm is taken as  $\boldsymbol{\theta}^{(0)}$ , while  $\mathbf{r}^{(0)}$  is simulated randomly from its prior distribution. This initialization procedure is also used for the baseline MCMC algorithm (using the CP or NCP) and ASIS. We use  $\hat{\boldsymbol{\theta}}$  to compute  $(\bar{\mathbf{w}}_1, \bar{\mathbf{w}}_2, a_2)$  by assuming  $\sigma_{\epsilon}^2$  is constant across  $t$  (equal to 4.93 and 1.64 for the SV and SCD models respectively). These values of  $(\bar{\mathbf{w}}_1, \bar{\mathbf{w}}_2, a_2)$  are held fixed for the first two-thirds of the burn-in period. We compute rough estimates of the posterior means of  $\boldsymbol{\theta}$  and  $\mathbf{r}$  using draws after the first one-third till the first two-thirds of burn-in, and these are used to update the values of  $(\bar{\mathbf{w}}_1, \bar{\mathbf{w}}_2, a_2)$  after the first two-thirds of burn-in. For the remainder of the sampling period,  $(\bar{\mathbf{w}}_1, \bar{\mathbf{w}}_2, a_2)$  are held fixed at these updated values. Our experiments indicate that the BSR strategy works well even with rather crude estimates of  $(\bar{\mathbf{w}}_1, \bar{\mathbf{w}}_2, a_2)$ .

For the SV model, it may be of interest to estimate the volatility at time  $t$ ,  $\exp(x_t/2)$ . Since  $p(\mathbf{x} \mid \mathbf{y}) = \int p(\mathbf{x} \mid \boldsymbol{\theta}, \mathbf{r}, \mathbf{y})p(\boldsymbol{\theta}, \mathbf{r} \mid \mathbf{y})d\boldsymbol{\theta}d\mathbf{r}$ , we can generate draws of  $\mathbf{x}$  by sampling

from  $p(\mathbf{x} \mid \boldsymbol{\theta}, \mathbf{r}, \mathbf{y})$ , which is  $N(C_{\boldsymbol{\alpha}}^{-1}\mathbf{c}_{\boldsymbol{\alpha}}, C_{\boldsymbol{\alpha}}^{-1})$  under the CP ( $a = 0, \mathbf{w} = 0$ ), for each draw of  $(\boldsymbol{\theta}, \mathbf{r})$  from  $p(\boldsymbol{\theta}, \mathbf{r} \mid \mathbf{y})$ . The MCMC samplers presented are based on a mixture of normals approximation of the  $\log \chi_1^2$  and  $\log \exp(1)$  distributions, and hence the samples are strictly speaking not drawn from the true posterior. This minor approximation error can be corrected by reweighting the sampled draws (see [Kim et al., 1998](#)). As the mixture approximation used is very accurate, [Kim et al. \(1998\)](#) and [Omori et al. \(2007\)](#) report that the effect of reweighting is very small and estimates of posterior means are not significantly different statistically. There is however, some improvement in the Monte Carlo standard errors. In this article, we focus on comparison of different MCMC samplers, and do not perform this reweighting in our experiments.

## 7 Experimental results

We compare the proposed BSR strategy with the baseline MCMC algorithm using the CP or NCP, and ASIS, using simulated data and several benchmark real data sets. Following [Kim et al. \(1998\)](#) and [Kastner and Frühwirth-Schnatter \(2014\)](#), we use the inefficiency factor to assess simulation efficiency. The inefficiency factor or integrated autocorrelation time is estimated as the ratio of the variance of the sample mean from the MCMC sampler, to the variance of the sample mean based on independent draws. It can be computed using the R package `coda` ([Plummer et al., 2006](#)) as number of draws/effective sample size. Smaller inefficiency factors indicate better mixing in the chain and lower autocorrelation among draws. Each MCMC sampler is run for a total of 30,000 iterations of which the first 10,000 are discarded as burn-in. All code is written in Julia Version 1.6.1 ([Bezanson et al., 2017](#)) and R ([R Core Team, 2020](#)). All experiments are run on an Intel Core i9-9900K CPU @3.60 Ghz with 16 GB RAM.

### 7.1 Simulations

First, we present results from data simulated from the SV and SCD models. For each model, we consider  $\mu = -10$ ,  $\phi \in \{0.4, 0.7, 0.95\}$  and  $\sigma_{\eta}^2 \in \{0.05, 0.5, 5\}$ , which yields nine parameter settings. In each setting,  $n = 3000$  observations are generated and each experiment is repeated ten times. For the priors, following [Kastner and Frühwirth-Schnatter \(2014\)](#), we set  $b_{\mu} = -10$ ,  $B_{\mu} = 10$ ,  $B_{\sigma} = \sigma_{\eta_{\text{true}}}^2$ ,  $b_{\phi} = 40$  and  $B_{\phi} = 80/(1 + \phi_{\text{true}}) - 40$  (this represents a prior on  $\phi$  with mean equal to  $\phi_{\text{true}}$ ).

The inefficiency factors averaged over ten repetitions for each parameter setting are shown in [Tables 6 and 7](#) for the SV and SCD models respectively. The BSR strategy worked very well for the SV model, and the inefficiency factors are always better than the worst of NCP and CP in each setting. It is even able to yield improvements over ASIS in many cases. From [Table 6](#), we also observe that in a given setting, neither the

$\phi$	$\sigma_\eta^2$	$\mu$				$\sigma_\eta^2$				$\phi$			
		NCP	CP	ASIS	BSR	NCP	CP	ASIS	BSR	NCP	CP	ASIS	BSR
0.4	0.05	18	79	17	20	63	710	63	66	109	111	116	112
	0.5	17	16	9	9	42	68	32	31	51	54	52	48
	5	67	4	4	4	40	17	15	13	16	13	13	12
0.7	0.05	14	26	11	13	72	471	73	68	110	128	114	112
	0.5	32	7	5	5	54	64	37	31	43	43	34	28
	5	226	2	2	2	70	17	16	13	19	9	9	8
0.95	0.05	99	2	2	2	69	136	51	30	48	75	36	21
	0.5	823	1	1	1	114	28	24	13	33	9	8	5
	5	5994	1	1	1	330	12	12	9	13	3	2	2

Table 6: SV model: Inefficiency factors averaged over ten repetitions.

$\phi$	$\sigma_\eta^2$	$\mu$				$\sigma_\eta^2$				$\phi$			
		NCP	CP	ASIS	BSR	NCP	CP	ASIS	BSR	NCP	CP	ASIS	BSR
0.4	0.05	18	37	18	16	83	408	75	105	109	109	114	109
	0.5	29	9	7	8	45	46	30	36	38	33	33	32
	5	166	2	2	2	59	8	8	12	8	6	6	6
0.7	0.05	18	14	10	10	101	296	84	110	102	121	96	107
	0.5	78	4	3	3	66	40	31	32	39	24	23	22
	5	601	1	1	1	109	9	9	14	10	4	4	5
0.95	0.05	275	1	1	1	105	83	50	35	55	39	28	19
	0.5	2145	1	1	1	207	22	20	17	33	6	5	5
	5	9024	1	1	1	620	8	8	13	7	2	2	2

Table 7: SCD model: Inefficiency factors averaged over ten repetitions.

CP or NCP may be superior to the other in terms of simulation efficiency across all parameters. E.g. when  $\phi = 0.95$  and  $\sigma_\eta^2 = 0.05$ , the CP is much better than the NCP for  $\mu$ , but worse than the NCP for  $(\sigma_\eta^2, \phi)$ . Hence BSR can yield benefits beyond the CP and NCP by tailoring the parametrization to each block. For the SCD model, BSR is also always better than the worst of NCP and CP. Its performance is weaker than ASIS for  $\sigma_\eta^2$  when  $\phi = 0.4, 0.7$ . However, it is either on par with or better than ASIS in the rest of the settings. The optimal parametrization identified for  $\sigma_\eta^2$  in Section 2 was not able to reduce the convergence rate of the EM algorithm to zero unlike for  $\mu$ , and it is worth investigating whether allowing  $a$  to vary across time can lead to further improvements. We have also performed experiments for negative values of  $\phi$  and the results (not shown here) are similar to that of positive values of  $\phi$  (much like a reflection about  $\phi = 0$ ).

The average runtime of each MCMC sampler is given in Table 8. The amount of computation required by NCP and CP are about the same, while BSR requires slightly more computation (for updating the working parameters once and switching to the second scheme in each iteration). ASIS requires the most computation due to switching of schemes and multiple simulation of certain parameters at each iteration, but the increase in runtime of BSR and ASIS compared to CP and NCP are not significant.

	NCP	CP	ASIS	BSR
SV	238	238	245	241
SCD	202	202	210	206

Table 8: Runtimes averaged over all parameter settings and repetitions.

## 7.2 Real data

We consider three data sets on exchange rates, US consumer price index (CPI) and IBM transactions. For each data set, we set the priors as  $b_\phi = 20$ ,  $B_\phi = 1.5$  (following Kim et al., 1998),  $B_\sigma = 0.5$  and  $B_\mu = 100$ . For the exchange rate data, we set  $b_\mu = -10$ , while for the CPI and IBM transaction data, we set  $b_\mu = 0$ .

The exchange rate data is downloaded from the European Central Bank’s Statistical Data Warehouse (<https://sdw.ecb.europa.eu/home.do>). Kastner and Frühwirth-Schnatter (2014) analyzed  $n = 3140$  observations of the daily Euro exchange rates of 23 currencies in the period 3 Jan 2000 to 4 Apr 2012 using the SV model. Of these, we select three currencies, the Danish krone, New Zealand dollar and US dollar, which are representative of currencies among the 23 with the lowest, moderate and highest persistence respectively. Let  $r_t$  denote the exchange rate at time  $t$ . The response  $y_t$  is the mean-corrected differenced log return, that is,  $y_t = \log(r_t/r_{t-1}) - \sum_{t=2}^n \log(r_t/r_{t-1})/(n-1)$ . We use the MCMC samplers to fit the SV model to the exchange rate data and obtained the inefficiency factors in Table 9. The simulation efficiency of CP is higher than NCP for  $\mu$  but lower than NCP for  $(\sigma_\eta^2, \phi)$ . Hence, neither is a good option. ASIS achieves much better results but BSR is the clear winner here, as it has the lowest inefficiency factors across all currencies and parameters.

Table 10 shows the parameter estimates and runtimes of each MCMC sampler. The Danish krone has the lowest modal instantaneous volatility ( $\mu = -18$ ) and the highest volatility of the log-volatility ( $\sigma_\eta = 0.38$ ), while the US dollar has the highest persistence in volatility ( $\phi = 0.99$ ). In terms of runtime, a similar pattern as in the simulated data is observed. NCP is the fastest, followed by CP, BSR and ASIS, but the runtime of all the MCMC samplers are essentially about the same. Figure 11 shows the trace plots, sample autocorrelation function and marginal posterior densities of  $(\mu, \sigma_\eta, \phi)$  for the US dollar. There is better mixing in BSR’s  $\sigma_\eta$  chain than ASIS’s, and the sample autocorrelation for  $\sigma_\eta$  and  $\phi$  also decay more quickly for BSR than ASIS. These observations are consistent

	$\mu$				$\sigma_\eta^2$				$\phi$			
	NCP	CP	ASIS	BSR	NCP	CP	ASIS	BSR	NCP	CP	ASIS	BSR
Danish	91	3	3	3	97	143	64	43	71	87	52	32
NZ	110	3	2	2	189	461	129	72	147	345	113	58
US	455	1	1	1	123	354	78	28	84	114	39	14

Table 9: Inefficiency factors from SV model for exchange rate data.

		$\mu$	$\sigma_\eta$	$\phi$	runtime
Danish	NCP	$-18.05 \pm 0.09$	$0.377 \pm 0.037$	$0.916 \pm 0.015$	260
	CP	$-18.04 \pm 0.09$	$0.372 \pm 0.038$	$0.918 \pm 0.016$	265
	ASIS	$-18.04 \pm 0.09$	$0.374 \pm 0.037$	$0.917 \pm 0.015$	272
	BSR	$-18.04 \pm 0.09$	$0.378 \pm 0.038$	$0.916 \pm 0.016$	269
NZ	NCP	$-10.03 \pm 0.10$	$0.172 \pm 0.031$	$0.964 \pm 0.012$	291
	CP	$-10.02 \pm 0.10$	$0.171 \pm 0.035$	$0.964 \pm 0.014$	296
	ASIS	$-10.02 \pm 0.10$	$0.172 \pm 0.031$	$0.964 \pm 0.012$	302
	BSR	$-10.02 \pm 0.10$	$0.175 \pm 0.031$	$0.963 \pm 0.012$	296
US	NCP	$-10.18 \pm 0.20$	$0.065 \pm 0.011$	$0.994 \pm 0.003$	260
	CP	$-10.14 \pm 0.25$	$0.064 \pm 0.011$	$0.994 \pm 0.003$	264
	ASIS	$-10.13 \pm 0.24$	$0.065 \pm 0.011$	$0.994 \pm 0.003$	272
	BSR	$-10.14 \pm 0.24$	$0.066 \pm 0.010$	$0.993 \pm 0.003$	268

Table 10: Parameter estimates and runtimes from SV model for exchange rate data.

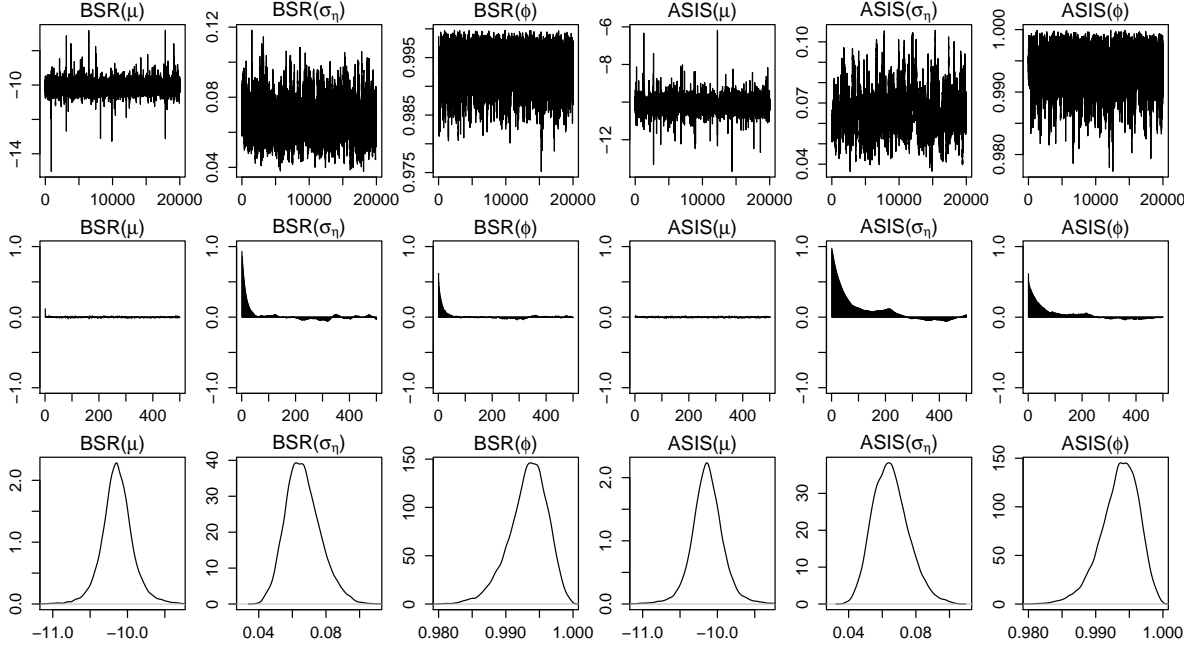


Figure 11: US dollar exchange rates. First row: Trace plots. Second row: Sample autocorrelation functions. Third row: Estimated marginal posterior densities.

with the inefficiency factors. Figure 12 shows the 0.05, 0.5 and 0.95 quantiles of volatilities estimated using 20000 samples from BSR, and a similar pattern with  $|y_t|$  can be detected.

The second data set, which can be downloaded from <https://people.smp.uq.edu.au/DirkKroese/statbook/Depvar/>, concerns US consumer price index (CPI) inflation rate from the second quarter of 1947 to the third quarter of 2011 (Kroese and Chan, 2014). There are  $n = 258$  observations and a SV model is fitted to the mean-corrected rates. The parameter estimates and inefficiency factors are given in Table 11. The simulation efficiency of CP is uniformly better than NCP across all parameters. ASIS improves upon CP, while BSR again yields the best performance. The CPI inflation exhibits high

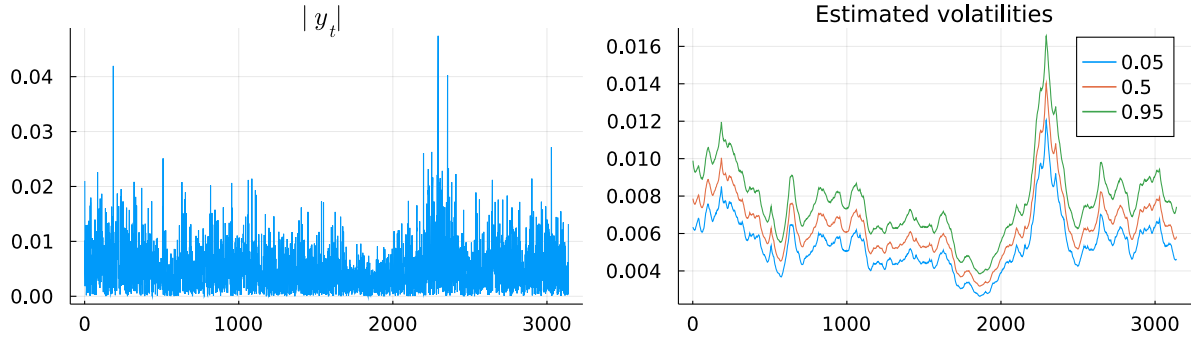


Figure 12: US dollar exchange rates. Plot of  $|y_t|$  and volatilities (0.05, 0.5 and 0.95 quantiles) estimated using BSR.

		NCP	CP	ASIS	BSR
Parameter estimates	$\mu$	$1.558 \pm 0.501$	$1.612 \pm 0.479$	$1.615 \pm 0.466$	$1.614 \pm 0.466$
	$\sigma_\eta$	$0.604 \pm 0.104$	$0.603 \pm 0.105$	$0.594 \pm 0.103$	$0.599 \pm 0.103$
	$\phi$	$0.900 \pm 0.038$	$0.899 \pm 0.038$	$0.901 \pm 0.037$	$0.901 \pm 0.037$
Inefficiency factor	$\mu$	260	2	1	1
	$\sigma_\eta$	50	37	26	19
	$\phi$	37	15	13	8

Table 11: Parameter estimates and inefficiency factors from SV model for CPI data.

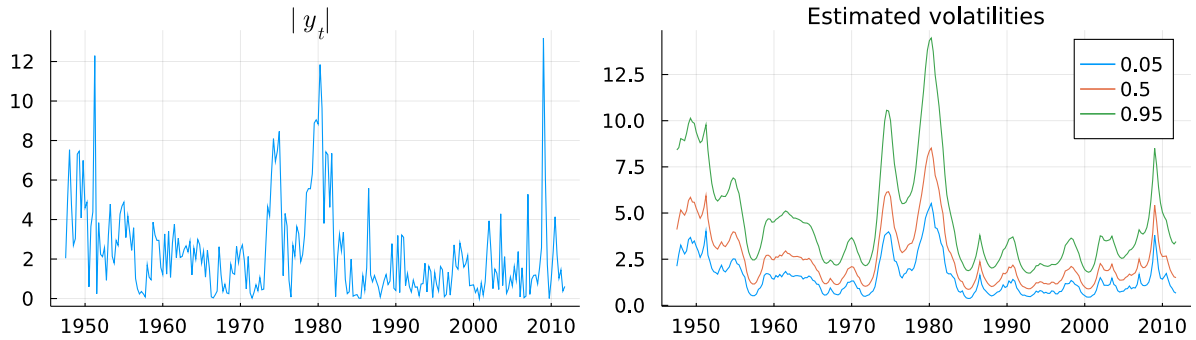


Figure 13: CPI data. Plot of  $|y_t|$  and volatilities (0.05, 0.5 and 0.95 quantiles) estimated using BSR.

persistence, and the plot of volatilities estimated using 20000 samples from BSR in Figure 13 captures the high inflation in the late 1970s to early 1980s. After this period, inflation remains low and stable until the 2008 financial crisis.

The benchmark IBM transactions data is extracted from the TORQ data built by Joel Hasbrouck and NYSE, and is available at <https://faculty.chicagobooth.edu/ruey-s-tsay/research/analysis-of-financial-time-series-3rd-edition>). It has the time of occurrence (measured in seconds from midnight) of each transaction from 1 Nov 1990 to 31 Jan 1991, and we wish to analyze the duration between consecutive transactions,  $d_i$ , using the SCD model. Following Feng et al. (2004), we only consider transactions occurring within normal trading hours (9.30 a.m to 4 p.m.) from 1 Nov to 21 Dec to avoid holiday effects. 23 Nov is also excluded as there is a halt in trading for 1

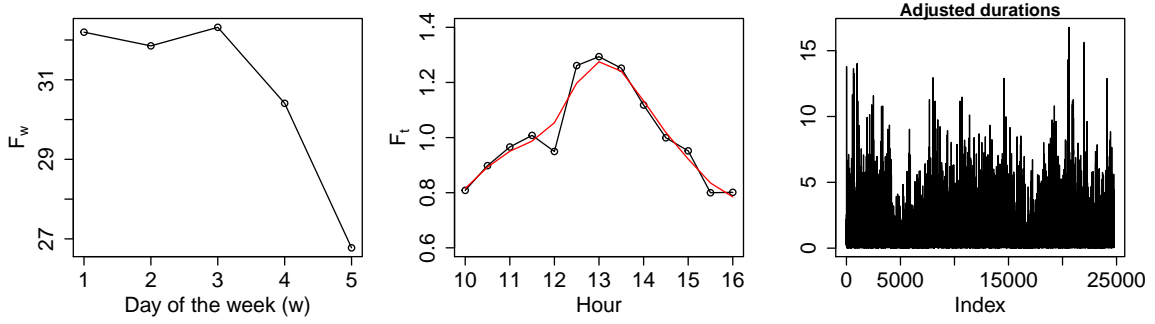


Figure 14: IBM data. Left: Sample average duration  $F_w$  for day  $w$  of the week. Middle: Sample average duration at each knot (black) and smoothed value (red). Right: Adjusted durations.

hour 15 minutes on this day. Due to the unusually high concentration of short durations immediately after opening, Engle and Russell (1998) recommend removing transactions occurring before 10 a.m., and taking the first duration of each day as the average duration of transactions from 9.50 a.m. to 10 a.m. After this procedure and the removal of zero durations, we have  $n = 24765$  observations of  $d_i$ , ranging from 1 to 502 seconds. Following Feng et al. (2004), we remove seasonality due to day-of-week effect (trading increases in frequency towards end of the week) and time-of-day effect (trading is more frequent at the start and end, than in the middle of the day) before analysis. To remove day-of-week effect, we compute the average sample duration  $F_w$  for each weekday,  $w = 1, \dots, 5$ , and set  $\tilde{d}_i = d_i/F_w$  if  $i$  falls in the weekday  $w$ . For time-of-week effect, we construct 13 knots at 30 minutes interval from 10 a.m. to 4 p.m.,  $k_1 = 36000, \dots, k_{13} = 57600$ . The value at knot  $k_s$  is the sample average of durations whose time of transaction falls in  $(k_s - 900, k_s + 900]$ . The smoothed value,  $F_s$ , at  $k_s$  is computed using piecewise cubic splines via the `smooth.spline` function in R, and the adjusted duration is  $\tilde{d}_i/F_s$  if the time of transaction of  $d_i$  falls in  $(k_s - 900, k_s + 900]$ . See Figure 14 for illustration.

Fitting the SCD model to the adjusted durations, the parameter estimates and inefficiency factors are shown in Table 12. The simulation efficiency of the CP is better than NCP for  $\mu$  and  $\phi$ , but worse for  $\sigma_\eta$ . ASIS improves the simulation efficiency for  $\sigma_\eta$  and  $\phi$  significantly but BSR produces even better results. The trace plots in Figure 15 also indicate that there is better mixing in the MCMC chains of  $\sigma_\eta$  and  $\phi$  for BSR than ASIS (the corresponding sample autocorrelations also decay faster).

## 8 Conclusion

This article investigates efficient data augmentation techniques for state space models by considering a linear transformation of the latent states in which working parameters  $(a, \mathbf{w})$  are introduced for simultaneous rescaling and recentering. In the first part, we focus on Gaussian state space models and maximum likelihood estimation via the EM algo-

		NCP	CP	ASIS	BSR
Parameter estimates	$\mu$	$-0.112 \pm 0.022$	$-0.118 \pm 0.023$	$-0.118 \pm 0.023$	$-0.119 \pm 0.023$
	$\sigma_\eta$	$0.150 \pm 0.008$	$0.152 \pm 0.008$	$0.151 \pm 0.008$	$0.152 \pm 0.008$
	$\phi$	$0.957 \pm 0.004$	$0.956 \pm 0.004$	$0.956 \pm 0.004$	$0.956 \pm 0.004$
Inefficiency factor	$\mu$	132	3	2	2
	$\sigma_\eta$	229	289	119	86
	$\phi$	189	172	100	69

Table 12: Parameter estimates and inefficiency factors from SCD model for IBM data.

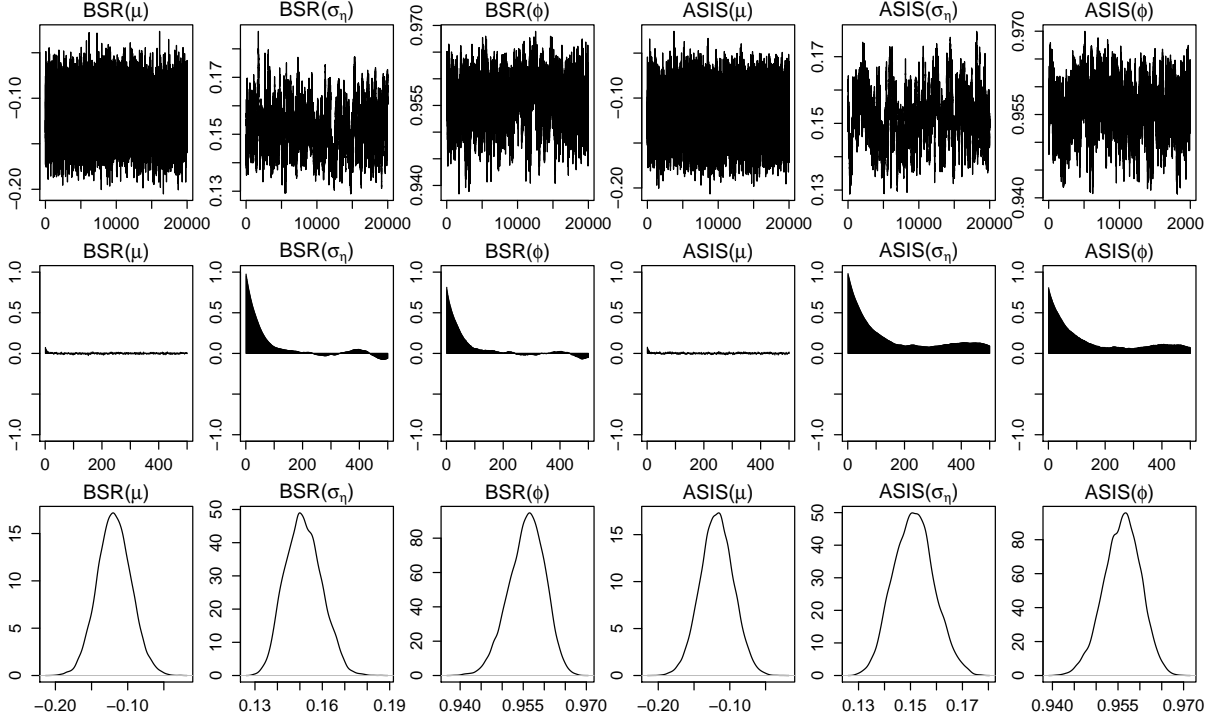


Figure 15: Left: IBM data. First row: Trace plots. Second row: Sample autocorrelation functions up to lag 500. Third row: Estimated marginal posterior densities.

algorithm. By minimizing the amount of missing information, optimal values of  $(a, \mathbf{w})$  which minimize the convergence rate of the EM algorithm, were derived in closed form under different settings. The Gaussian context enabled an in-depth study of the (large sample) properties of these working parameters. As it is not possible to find values of  $(a, \mathbf{w})$  that optimizes the inference of all unknown parameters simultaneously, we designed an AECM algorithm that allows the optimal parametrization for each parameter to be used while conditioning on others. Experimental results indicate that the AECM algorithm always performs better than the worse of CP and NCP, and is often able to outperform both in terms of rate of convergence and maximum likelihood attained. The second part of this article extends these results to non-Gaussian state space models, by developing Bayesian MCMC algorithms for the SV and SCD models. A block-specific reparametrization (BSR) strategy, which allows the data augmentation scheme to be tailored specifically to each block, is proposed for a multi-block MCMC sampler. By using a mixture of normals ap-

proximation and conditioning on the mixture indicators, the SV and SCD models can be expressed as Gaussian state space models. The optimal parametrizations derived in the first part of this article can thus be used for these models. Experimental results indicate that the BSR strategy works very well, surpassing ASIS in all the real applications. The BSR strategy is applicable quite generally and a lot of room remains in the exploration of optimal block-specific reparametrizations, where the “optimal reparametrization” can be derived based on different criteria, such as minimizing of posterior correlation between blocks, besides a straightforward extension of results from the EM algorithm.

## Acknowledgment

The author’s research is supported by the start-up grant (R-155-000-190-133). The author wishes to thank the editor, assistant editor and two referees for their comments and helpful suggestions which have improved this manuscript greatly.

## Supplementary material

Supplementary material available online includes Julia code for all algorithms, extended proofs and other technical details.

## References

- Attias, H. (1999). Inferring parameters and structure of latent variable models by variational Bayes. In K. Laskey and H. Prade (Eds.), *Proceedings of the 15th Conference on Uncertainty in Artificial Intelligence*.
- Bauwens, L. and D. Veredas (2004). The stochastic conditional duration model: a latent variable model for the analysis of financial durations. *Journal of Econometrics* 119, 381–412.
- Benaglia, T., D. Chauveau, D. R. Hunter, and D. Young (2009). mixtools: An R package for analyzing finite mixture models. *Journal of Statistical Software* 32, 1–29.
- Bezanson, J., A. Edelman, S. Karpinski, and V. B. Shah (2017). Julia: A fresh approach to numerical computing. *SIAM review* 59, 65–98.
- Carter, C. K. and R. Kohn (1997). Semiparametric bayesian inference for time series with mixed spectra. *Journal of the Royal Statistical Society: Series B (Statistical Methodology)* 59, 255–268.
- Cryer, J. D. and K.-S. Chan (2008). *Time Series Analysis With Applications in R*. New York, USA: Springer.
- Dempster, A. P., N. M. Laird, and D. B. Rubin (1977). Maximum likelihood from incomplete data via the EM algorithm. *Journal of the Royal Statistical Society, Series B* 39, 1–38.
- Durbin, J. and S. J. Koopman (2012). *Time series analysis by state space methods*. UK: Oxford University Press.

- Engle, R. F. and J. R. Russell (1998). Autoregressive conditional duration: A new model for irregularly spaced transaction data. *Econometrica* 66, 1127–1162.
- Feng, D., G. J. Jiang, and P. X.-K. Song (2004). Stochastic Conditional Duration Models with “Leverage Effect” for Financial Transaction Data. *Journal of Financial Econometrics* 2, 390–421.
- Frühwirth-Schnatter, S. (2004). Efficient Bayesian parameter estimation. In A. Harvey, S. J. Koopman, and N. Shephard (Eds.), *State Space and Unobserved Component Models: Theory and Applications*, pp. 123–151. Cambridge University Press.
- Frühwirth-Schnatter, S. and H. Wagner (2010). Stochastic model specification search for gaussian and partial non-gaussian state space models. *Journal of Econometrics* 154, 85–100.
- Gelfand, A. E., S. K. Sahu, and B. P. Carlin (1995). Efficient parametrisations for normal linear mixed models. *Biometrika* 82, 479–488.
- Gelfand, A. E., S. K. Sahu, and B. P. Carlin (1996). Efficient parametrisations for generalized linear mixed models. In J. M. Bernardo, J. O. Berger, A. P. Dawid, and A. F. M. Smith (Eds.), *Bayesian Statistics* 5.
- Harvey, A., E. Ruiz, and N. Shephard (1994). Multivariate stochastic variance models. *The Review of Economic Studies* 61, 247–264.
- Harvey, A. C. and S. Peters (1990). Estimation procedures for structural time series models. *Journal of Forecasting* 9, 89–108.
- Kalman, R. E. (1960). A new approach to linear filtering and prediction problems. *Journal of Basic Engineering, Transactions of the ASME, Series D* 82, 35–45.
- Kastner, G. and S. Frühwirth-Schnatter (2014). Ancillarity-sufficiency interweaving strategy (asis) for boosting mcmc estimation of stochastic volatility models. *Computational Statistics and Data Analysis* 76, 408–423.
- Kim, S., N. Shephard, and S. Chib (1998). Stochastic volatility: Likelihood inference and comparison with arch models. *The Review of Economic Studies* 65, 361–393.
- Kroese, D. P. and J. C. Chan (2014). *Statistical Modeling and Computation*. New York: Springer-Verlag.
- Liu, C., D. B. Rubin, and Y. N. Wu (1998). Parameter expansion to accelerate EM: The PX-EM algorithm. *Biometrika* 85, 755–770.
- Meng, X.-L. and D. B. Rubin (1993). Maximum likelihood estimation via the ECM algorithm: A general framework. *Biometrika* 80, 267–278.
- Meng, X.-L. and D. van Dyk (1997). The EM algorithm—an old folk-song sung to a fast new tune. *Journal of the Royal Statistical Society, Series B* 59, 511–567.
- Meng, X.-L. and D. van Dyk (1998). Fast EM-type implementations for mixed effects models. *Journal of the Royal Statistical Society, Series B* 60, 559–578.
- Mogensen, P. K. and A. N. Riseth (2018). Optim: A mathematical optimization package for Julia. *Journal of Open Source Software* 3, 615.
- Omori, Y., S. Chib, N. Shephard, and J. Nakajima (2007). Stochastic volatility with leverage: Fast and efficient likelihood inference. *Journal of Econometrics* 140, 425 – 449.
- Ormerod, J. T. and M. P. Wand (2010). Explaining variational approximations. *The American*

- Statistician* 64, 140–153.
- Papaspiliopoulos, O., G. O. Roberts, and M. Sköld (2003). Non-centered parameterisations for hierarchical models and data augmentation. In J. M. Bernardo, M. J. Bayarri, J. O. Berger, A. P. Dawid, D. Heckerman, A. F. M. Smith, and M. West (Eds.), *Bayesian Statistics 7*, pp. 307–326. New York: Oxford University Press.
- Papaspiliopoulos, O., G. O. Roberts, and M. Sköld (2007). A general framework for the parametrization of hierarchical models. *Statist. Sci.* 22, 59–73.
- Pitt, M. K. and N. Shephard (1999). Analytic convergence rates and parameterization issues for the Gibbs sampler applied to state space models. *Journal of Time Series Analysis* 20, 63–85.
- Plummer, M., N. Best, K. Cowles, and K. Vines (2006). Coda: Convergence diagnosis and output analysis for mcmc. *R News* 6, 7–11.
- R Core Team (2020). *R: A Language and Environment for Statistical Computing*. Vienna, Austria: R Foundation for Statistical Computing.
- Roberts, G. O. and S. K. Sahu (1997). Updating schemes, correlation structure, blocking and parameterization for the Gibbs sampler. *Journal of the Royal Statistical Society, Series B* 59, 291–317.
- Sahu, S. K. and G. O. Roberts (1999). On convergence of the EM algorithm and the Gibbs sampler. *Statistics and Computing* 9, 55–64.
- Shumway, R. H. and D. S. Stoffer (1982). An approach to time series smoothing and forecasting using the EM algorithm. *Journal of Time Series Analysis* 3, 253–264.
- Shumway, R. H. and D. S. Stoffer (2017). *Time Series Analysis and Its Applications*. Cham, Switzerland: Springer.
- Strickland, C. M., C. S. Forbes, and G. M. Martin (2006). Bayesian analysis of the stochastic conditional duration model. *Computational Statistics and Data Analysis* 50, 2247–2267.
- Tan, L. S. L. (2019). Explicit inverse of tridiagonal matrix with applications in autoregressive modelling. *IMA Journal of Applied Mathematics* 84, 679–695.
- Tan, M., G.-L. Tian, H.-B. Fang, and K. W. Ng (2007). A fast EM algorithm for quadratic optimization subject to convex constraints. *Statistica Sinica* 17, 945–964.
- Tan, S. L. and D. J. Nott (2014). Variational approximation for mixtures of linear mixed models. *Journal of Computational and Graphical Statistics* 23, 564–585.
- Taylor, S. J. (1982). Financial returns modelled by the product of two stochastic processes – a study of daily sugar prices, 1961–79. In O. D. Anderson (Ed.), *Time Series Analysis: Theory and Practice, Vol 1*, pp. 203–226. North-Holland, Amsterdam: Elsevier.
- Watson, M. W. and R. F. Engle (1983). Alternative algorithms for the estimation of dynamic factor, mimic and varying coefficient regression models. *Journal of Econometrics* 23, 385 – 400.
- Wu, C. F. J. (1983). On the convergence properties of the EM algorithm. *Ann. Statist.* 11, 95–103.
- Yu, Y. and X.-L. Meng (2011). To center or not to center: That is not the question—An ancillarity-sufficiency interweaving strategy (ASIS) for boosting MCMC efficiency. *Journal of Computational and Graphical Statistics* 20, 531–570.

Supplementary material for  
 “Efficient data augmentation techniques for state space models”

Linda S. L. Tan (statsll@nus.edu.sg)

National University of Singapore

## 9 Observed information matrix

The marginal distribution of  $\mathbf{y}$  is  $N(\mu\mathbf{1}, S)$  as

$$\begin{aligned} E(\mathbf{y}) &= E[E(\mathbf{y}|\boldsymbol{\alpha})] = E(\sigma_\eta^2 \boldsymbol{\alpha} + \mu \mathbf{w}) = \mu \bar{\mathbf{w}} + \mu \mathbf{w} = \mu \mathbf{1}, \\ \text{var}(\mathbf{y}) &= \text{var}[E(\mathbf{y}|\boldsymbol{\alpha})] + E[\text{var}(\mathbf{y}|\boldsymbol{\alpha})] = \sigma_\eta^2 \Lambda^{-1} + \sigma_\epsilon^2 I = S. \end{aligned}$$

Hence the log-likelihood of  $\mathbf{y}$  is

$$L(\boldsymbol{\theta}) = \log p(\mathbf{y}|\boldsymbol{\theta}) = -\frac{n}{2} \log(2\pi) - \frac{1}{2} \log |S| - \frac{1}{2} (\mathbf{y} - \mu \mathbf{1})^T S^{-1} (\mathbf{y} - \mu \mathbf{1}).$$

We compute  $L(\boldsymbol{\theta}^{(i)})$  at the end of each iteration in the EM algorithm and the algorithm is terminated when the relative increment in  $L(\boldsymbol{\theta})$  is negligible. We can compute  $L(\boldsymbol{\theta}^{(i)})$  efficiently by finding the  $LDL^T$  decomposition of  $(V_0/\sigma_\epsilon^2)^{-1}$  where  $D$  is a diagonal matrix and  $L$  is a unit lower triangular matrix, and noting that  $S^{-1} = \Lambda V_0/(\sigma_\eta^2 \sigma_\epsilon^2) = (I - V_0/\sigma_\epsilon^2)/\sigma_\eta^2$ . Hence  $\log |S^{-1}| = \log(1 - \phi^2) - n \log(\sigma_\eta^2) - \log |D|$ , and  $S^{-1}(\mathbf{y} - \mu \mathbf{1})$  can be evaluated efficiently using back-substitution.

Recall that  $\mathbf{m}_{01} = V_0(\mathbf{y} - \mu \mathbf{1})/\sigma_\epsilon^2$ , we have

$$\begin{aligned} \frac{\partial L(\theta)}{\partial \mu} &= (\mathbf{y} - \mu \mathbf{1})^T S^{-1} \mathbf{1}, \\ \frac{\partial^2 L(\theta)}{\partial \mu^2} &= -\mathbf{1}^T S^{-1} \mathbf{1}, \\ \frac{\partial L(\theta)}{\partial \sigma_\eta^2} &= -\frac{\text{tr}(S^{-1} \Lambda^{-1})}{2} + \frac{1}{2} (\mathbf{y} - \mu \mathbf{1})^T S^{-1} \Lambda^{-1} S^{-1} (\mathbf{y} - \mu \mathbf{1}), \\ \frac{\partial^2 L(\theta)}{\partial (\sigma_\eta^2)^2} &= \frac{\text{tr}(V_0^2)}{2\sigma_\eta^4 \sigma_\epsilon^4} - \frac{\mathbf{m}_{01}^T S^{-1} \mathbf{m}_{01}}{\sigma_\eta^4}, \\ \frac{\partial^2 L(\theta)}{\partial \mu \partial \sigma_\eta^2} &= -(\mathbf{y} - \mu \mathbf{1})^T S^{-1} \Lambda^{-1} S^{-1} \mathbf{1} = -\frac{\mathbf{m}_{01}^T S^{-1} \mathbf{1}}{\sigma_\eta^2}. \end{aligned}$$

Hence  $I_{\mu, \mu}^{\text{obs}} = \mathbf{1}^T S^{-1} \mathbf{1}$ ,  $I_{\mu, \sigma_\eta^2}^{\text{obs}} = \mathbf{m}_{01}^T S^{-1} \mathbf{1}/\sigma_\eta^2$  and  $I_{\sigma_\eta^2, \sigma_\eta^2}^{\text{obs}} = [2\mathbf{m}_{01}^T S^{-1} \mathbf{m}_{01} - \text{tr}(V_0^2)/\sigma_\epsilon^4]/(2\sigma_\eta^4)$ .

## 10 Updates in EM algorithm

Let  $U = \sigma_\eta^{2a} V_a^{(i)} + (\sigma_\eta^a \mathbf{m}_{a\mathbf{w}}^{(i)} - \mu \bar{\mathbf{w}})(\sigma_\eta^a \mathbf{m}_{a\mathbf{w}}^{(i)} - \mu \bar{\mathbf{w}})^T$ . The first derivative of  $Q(\boldsymbol{\theta}|\boldsymbol{\theta}^{(i)})$  with respect to each parameter is given below.

$$\begin{aligned}\frac{\partial Q(\boldsymbol{\theta}|\boldsymbol{\theta}^{(i)})}{\partial \mu} &= \sigma_\epsilon^{-2}(\mathbf{y} - \mu \mathbf{w} - \sigma_\eta^a \mathbf{m}_{a\mathbf{w}}^{(i)})^T \mathbf{w} + \sigma_\eta^{-2}(\sigma_\eta^a \mathbf{m}_{a\mathbf{w}}^{(i)} - \mu \bar{\mathbf{w}})^T \Lambda \bar{\mathbf{w}}. \\ \frac{\partial Q(\boldsymbol{\theta}|\boldsymbol{\theta}^{(i)})}{\partial \sigma_\eta^2} &= \frac{1}{2\sigma_\eta^4} \left\{ n(a-1)\sigma_\eta^2 - (a-1)\sigma_\eta^{2a} [\text{tr}(\Lambda V_a^{(i)}) + \mathbf{m}_{a\mathbf{w}}^{(i)T} \Lambda \mathbf{m}_{a\mathbf{w}}^{(i)}] + \mu^2 \bar{\mathbf{w}}^T \Lambda \bar{\mathbf{w}} \right. \\ &\quad + (a-2)\mu \sigma_\eta^a \mathbf{m}_{a\mathbf{w}}^{(i)T} \Lambda \bar{\mathbf{w}} + a\sigma_\eta^{a+2} \sigma_\epsilon^{-2} (\mathbf{y} - \mu \mathbf{w})^T \mathbf{m}_{a\mathbf{w}}^{(i)} \\ &\quad \left. - a\sigma_\eta^{2a+2} \sigma_\epsilon^{-2} [\text{tr}(V_a^{(i)}) + \mathbf{m}_{a\mathbf{w}}^{(i)T} \mathbf{m}_{a\mathbf{w}}^{(i)}] \right\}. \\ \frac{\partial Q(\boldsymbol{\theta}|\boldsymbol{\theta}^{(i)})}{\partial \phi} &= -\frac{\text{tr}(\Lambda_1 U)}{2\sigma_\eta^2} - \frac{\phi}{1-\phi^2} = -\frac{1}{\sigma_\eta^2} \left[ \phi \sum_{t=2}^{n-1} U_{tt} - \sum_{t=1}^{n-1} U_{t,t+1} \right] - \frac{\phi}{1-\phi^2}. \\ \frac{\partial Q(\boldsymbol{\theta}|\boldsymbol{\theta}^{(i)})}{\partial \sigma_\epsilon^2} &= \frac{\sigma_\eta^{2a} \text{tr}(V_a^{(i)}) + (\mathbf{y} - \mu \mathbf{w} - \sigma_\eta^a \mathbf{m}_{a\mathbf{w}}^{(i)})^T (\mathbf{y} - \mu \mathbf{w} - \sigma_\eta^a \mathbf{m}_{a\mathbf{w}}^{(i)})}{2\sigma_\epsilon^4} - \frac{n}{2\sigma_\epsilon^2}.\end{aligned}$$

Setting  $\partial Q(\boldsymbol{\theta}|\boldsymbol{\theta}^{(i)})/\partial \theta_s = 0$  then leads to the update for  $\theta_s$ .

## 11 Augmented information matrix

We use  $I_{\text{aug}}(\boldsymbol{\theta}^*)$  to optimize the rate of convergence of the EM algorithm with respect to  $a$  and  $\mathbf{w}$ .

$$\begin{aligned}I_{\text{aug}}(\boldsymbol{\theta}^*) &= - \int p(Y_{\text{mis}}|y_{\text{obs}}, \boldsymbol{\theta}) \nabla_{\boldsymbol{\theta}}^2 \log p(Y_{\text{aug}}|\boldsymbol{\theta}) dY_{\text{mis}}|_{\boldsymbol{\theta}=\boldsymbol{\theta}^*} \\ &= -\nabla_{\boldsymbol{\theta}}^2 \int p(\boldsymbol{\alpha}|\mathbf{y}, \boldsymbol{\theta}^{(i)}) \log p(\mathbf{y}, \boldsymbol{\alpha}|\boldsymbol{\theta}) d\boldsymbol{\alpha}|_{\boldsymbol{\theta}, \boldsymbol{\theta}^{(i)}=\boldsymbol{\theta}^*} = -\nabla_{\boldsymbol{\theta}}^2 Q(\boldsymbol{\theta}|\boldsymbol{\theta}^{(i)})|_{\boldsymbol{\theta}, \boldsymbol{\theta}^{(i)}=\boldsymbol{\theta}^*}.\end{aligned}$$

Note that the 2nd derivative applies only to  $\log p(\mathbf{y}, \boldsymbol{\alpha}|\boldsymbol{\theta})$ . The above expression shows that  $I_{\text{aug}}(\boldsymbol{\theta}^*)$  measures the curvature of  $Q(\boldsymbol{\theta}|\boldsymbol{\theta}^{(i)})$  at the MLE  $\boldsymbol{\theta}^*$ . Let  $\Lambda_2 = \partial^2 \Lambda / \partial \phi^2 = \text{diag}([0, 2, \dots, 2, 0])$ . The diagonal entries of  $\nabla_{\boldsymbol{\theta}}^2 Q(\boldsymbol{\theta}|\boldsymbol{\theta}^{(i)})$  are

$$\begin{aligned}\frac{\partial^2 Q(\boldsymbol{\theta}|\boldsymbol{\theta}^{(i)})}{\partial \mu^2} &= -(\sigma_\epsilon^{-2} \mathbf{w}^T \mathbf{w} + \sigma_\eta^{-2} \bar{\mathbf{w}}^T \Lambda \bar{\mathbf{w}}), \\ \frac{\partial^2 Q(\boldsymbol{\theta}|\boldsymbol{\theta}^{(i)})}{\partial (\sigma_\eta^2)^2} &= -\frac{1}{2\sigma_\eta^4} \left\{ n(a-1) + (a-1)(a-2)\sigma_\eta^{2a-2} [\text{tr}(\Lambda V_a^{(i)}) + \mathbf{m}_{a\mathbf{w}}^{(i)T} \Lambda \mathbf{m}_{a\mathbf{w}}^{(i)}] \right. \\ &\quad - (a-2) \left( \frac{a}{2} - 2 \right) \sigma_\eta^{a-2} \mu \mathbf{m}_{a\mathbf{w}}^{(i)T} \Lambda \bar{\mathbf{w}} - a \left( \frac{a}{2} - 1 \right) \sigma_\eta^a \sigma_\epsilon^{-2} (\mathbf{y} - \mu \mathbf{w})^T \mathbf{m}_{a\mathbf{w}}^{(i)} \\ &\quad \left. + a(a-1)\sigma_\eta^{2a} \sigma_\epsilon^{-2} [\text{tr}(V_a^{(i)}) + \mathbf{m}_{a\mathbf{w}}^{(i)T} \mathbf{m}_{a\mathbf{w}}^{(i)}] + 2\mu^2 \sigma_\eta^{-2} \bar{\mathbf{w}}^T \Lambda \bar{\mathbf{w}} \right\}, \\ \frac{\partial^2 Q(\boldsymbol{\theta}|\boldsymbol{\theta}^{(i)})}{\partial \phi^2} &= -\frac{\text{tr}(\Lambda_2 U)}{2\sigma_\eta^2} - \frac{1+\phi^2}{(1-\phi^2)^2} = -\left( \frac{1}{\sigma_\eta^2} \sum_{t=2}^{n-1} U_{tt} + \frac{1+\phi^2}{(1-\phi^2)^2} \right),\end{aligned}$$

$$\frac{\partial^2 Q(\boldsymbol{\theta}|\boldsymbol{\theta}^{(i)})}{\partial(\sigma_\epsilon^2)^2} = -\frac{\sigma_\eta^{2a}\text{tr}(V_a^{(i)}) + (\mathbf{y} - \mu\mathbf{w} - \sigma_\eta^a \mathbf{m}_{a\mathbf{w}}^{(i)})^T (\mathbf{y} - \mu\mathbf{w} - \sigma_\eta^a \mathbf{m}_{a\mathbf{w}}^{(i)})}{\sigma_\epsilon^6} + \frac{n}{2\sigma_\epsilon^4}.$$

The off-diagonal entries are

$$\begin{aligned} \frac{\partial^2 Q(\boldsymbol{\theta}|\boldsymbol{\theta}^{(i)})}{\partial\mu\partial\sigma_\eta^2} &= -\frac{a}{2}\sigma_\eta^{a-2}\mathbf{m}_{a\mathbf{w}}^{(i)T}(\sigma_\epsilon^{-2}\mathbf{w} - \sigma_\eta^{-2}\Lambda\bar{\mathbf{w}}) - \sigma_\eta^{-4}(\sigma_\eta^a \mathbf{m}_{a\mathbf{w}}^{(i)} - \mu\bar{\mathbf{w}})^T \Lambda\bar{\mathbf{w}}, \\ \frac{\partial^2 Q(\boldsymbol{\theta}|\boldsymbol{\theta}^{(i)})}{\partial\mu\partial\phi} &= -\frac{\text{tr}(\Lambda_1 \frac{\partial U}{\partial\mu})}{2\sigma_\eta^2} = \frac{\bar{\mathbf{w}}^T \Lambda_1 (\sigma_\eta^a \mathbf{m}_{a\mathbf{w}}^{(i)} - \mu\bar{\mathbf{w}})}{\sigma_\eta^2}, \\ \frac{\partial^2 Q(\boldsymbol{\theta}|\boldsymbol{\theta}^{(i)})}{\partial\mu\partial\sigma_\epsilon^2} &= -\frac{(\mathbf{y} - \mu\mathbf{w} - \sigma_\eta^a \mathbf{m}_{a\mathbf{w}}^{(i)})^T \mathbf{w}}{\sigma_\epsilon^4}, \\ \frac{\partial^2 Q(\boldsymbol{\theta}|\boldsymbol{\theta}^{(i)})}{\partial\sigma_\eta^2\partial\phi} &= \frac{\text{tr}[\Lambda_1(U - \sigma_\eta^2 \frac{\partial U}{\partial\sigma_\eta^2})]}{2\sigma_\eta^4} \\ &= \frac{(1-a)\sigma_\eta^{2a}\text{tr}(\Lambda_1 V_a) + (\sigma_\eta^a \mathbf{m}_{a\mathbf{w}}^{(i)} - \mu\bar{\mathbf{w}})^T \Lambda_1 [(1-a)\sigma_\eta^a \mathbf{m}_{a\mathbf{w}}^{(i)} - \mu\bar{\mathbf{w}}]}{2\sigma_\eta^4}, \\ \frac{\partial^2 Q(\boldsymbol{\theta}|\boldsymbol{\theta}^{(i)})}{\partial\sigma_\eta^2\partial\sigma_\epsilon^2} &= \frac{a[\sigma_\eta^{2a}\text{tr}(V_a^{(i)}) - \sigma_\eta^a(\mathbf{y} - \mu\mathbf{w} - \sigma_\eta^a \mathbf{m}_{a\mathbf{w}}^{(i)})^T \mathbf{m}_{a\mathbf{w}}^{(i)}]}{2\sigma_\epsilon^4\sigma_\eta^2}, \quad \frac{\partial^2 Q(\boldsymbol{\theta}|\boldsymbol{\theta}^{(i)})}{\partial\phi\partial\sigma_\epsilon^2} = 0. \end{aligned}$$

Below are some useful identities concerning the conditional distribution  $p(\boldsymbol{\alpha}|\mathbf{y}, \boldsymbol{\theta})$ .

$$\begin{aligned} V_0 &= \sigma_\eta^{2a}V_a = (\frac{I}{\sigma_\epsilon^2} + \frac{\Lambda}{\sigma_\eta^2})^{-1}, & S &= \sigma_\epsilon^2 I + \sigma_\eta^2 \Lambda^{-1} \\ \mathbf{m}_{0\mathbf{w}} &= \sigma_\eta^a \mathbf{m}_{a\mathbf{w}} = \sigma_\epsilon^{-2}V_0(\mathbf{y} - \mu\mathbf{1}) + \mu\bar{\mathbf{w}}, & S^{-1} &= \frac{\Lambda V_0}{\sigma_\eta^2\sigma_\epsilon^2} = \frac{V_0\Lambda}{\sigma_\epsilon^2\sigma_\eta^2} = \frac{I}{\sigma_\epsilon^2} - \frac{V_0}{\sigma_\epsilon^4}, \\ \mathbf{m}_{01} &= \mathbf{m}_{0\mathbf{w}} - \mu\bar{\mathbf{w}} = \sigma_\epsilon^{-2}V_0(\mathbf{y} - \mu\mathbf{1}), & \sigma_\eta^2\Lambda^{-1} &= \frac{V_0 S}{\sigma_\epsilon^2} = \frac{SV_0}{\sigma_\epsilon^2} = V_0 + \frac{V_0 S V_0}{\sigma_\epsilon^4}, \\ \mathbf{m}_{00} &= \mathbf{m}_{0\mathbf{w}} + \mu\mathbf{w} = V_0(\sigma_\epsilon^{-2}\mathbf{y} + \mu\frac{\Lambda}{\sigma_\eta^2}\mathbf{1}), & \frac{\Lambda}{\sigma_\eta^2}V_0\frac{\Lambda}{\sigma_\eta^2} &= \frac{\Lambda}{\sigma_\eta^2}V_0(V_0^{-1} - \frac{I}{\sigma_\epsilon^2}) = \frac{\Lambda}{\sigma_\eta^2} - S^{-1}, \\ \mathbf{y} - \mathbf{m}_{00} &= V_0\frac{\Lambda}{\sigma_\eta^2}(\mathbf{y} - \mu\mathbf{1}), & \frac{\Lambda}{\sigma_\eta^2}\mathbf{m}_{01} &= \frac{\mathbf{y} - \mathbf{m}_{00}}{\sigma_\epsilon^2} = S^{-1}(\mathbf{y} - \mu\mathbf{1}), \end{aligned}$$

For example, when  $\boldsymbol{\theta} = \boldsymbol{\theta}^{(i)}$  (say at convergence),

$$\begin{aligned} \frac{\partial^2 Q(\boldsymbol{\theta}|\boldsymbol{\theta})}{\partial(\sigma_\eta^2)^2} &= -\frac{1}{2\sigma_\eta^4} \left\{ n(a-1) + (a-1)(a-2)[\text{tr}(\frac{\Lambda}{\sigma_\eta^2}V_0) + \mathbf{m}_{0\mathbf{w}}^T \frac{\Lambda}{\sigma_\eta^2} \mathbf{m}_{0\mathbf{w}}] \right. \\ &\quad - (a-2)\left(\frac{a}{2} - 2\right)\mu\mathbf{m}_{0\mathbf{w}}^T \frac{\Lambda}{\sigma_\eta^2} \bar{\mathbf{w}} - a\left(\frac{a}{2} - 1\right)\frac{\mathbf{m}_{0\mathbf{w}}^T(\mathbf{y} - \mu\mathbf{w})}{\sigma_\epsilon^2} \\ &\quad \left. + a(a-1)\sigma_\epsilon^{-2}[\text{tr}(V_0) + \mathbf{m}_{0\mathbf{w}}^T \mathbf{m}_{0\mathbf{w}}] + 2\mu^2\bar{\mathbf{w}}^T \frac{\Lambda}{\sigma_\eta^2} \bar{\mathbf{w}} \right\}, \\ &= -\frac{1}{2\sigma_\eta^4} \left\{ n(1-a)^2 + \frac{a^2}{2}\mathbf{m}_{0\mathbf{w}}^T V_0^{-1} \mathbf{m}_{0\mathbf{w}} - 2a\mu\mathbf{m}_{01}^T \frac{\Lambda}{\sigma_\eta^2} \bar{\mathbf{w}} \right. \\ &\quad \left. + 2(a-1)[\sigma_\epsilon^{-2}\text{tr}(V_0) - \mathbf{m}_{01}^T \frac{\Lambda}{\sigma_\eta^2} \mathbf{m}_{01}] \right\}. \\ \frac{\partial^2 Q(\boldsymbol{\theta}|\boldsymbol{\theta})}{\partial(\sigma_\epsilon^2)^2} &= -\frac{\text{tr}(V_0) + (\mathbf{y} - \mathbf{m}_{00})^T (\mathbf{y} - \mathbf{m}_{00})}{\sigma_\epsilon^6} + \frac{n}{2\sigma_\epsilon^4}. \end{aligned} \tag{19}$$

$$\begin{aligned}
\frac{\partial^2 Q(\boldsymbol{\theta}|\boldsymbol{\theta})}{\partial \mu \partial \sigma_\eta^2} &= -\frac{a \mathbf{m}_{0\mathbf{w}}^T}{2\sigma_\eta^2} \left( V_0^{-1} \mathbf{w} - \frac{\Lambda}{\sigma_\eta^2} \mathbf{1} \right) - \frac{\mathbf{m}_{01}^T \Lambda \bar{\mathbf{w}}}{\sigma_\eta^4}, & \frac{\partial^2 Q(\boldsymbol{\theta}|\boldsymbol{\theta})}{\partial \mu \partial \phi} &= \frac{\mathbf{m}_{01}^T \Lambda_1 \bar{\mathbf{w}}}{\sigma_\eta^2}, \\
\frac{\partial^2 Q(\boldsymbol{\theta}|\boldsymbol{\theta})}{\partial \sigma_\eta^2 \partial \phi} &= \frac{(1-a)[\text{tr}(\Lambda_1 V_0) + \mathbf{m}_{01}^T \Lambda_1 \mathbf{m}_{01}] - a\mu \mathbf{m}_{01}^T \Lambda_1 \bar{\mathbf{w}}}{2\sigma_\eta^4}, & \frac{\partial^2 Q(\boldsymbol{\theta}|\boldsymbol{\theta})}{\partial \mu \partial \sigma_\epsilon^2} &= -\frac{\mathbf{m}_{01}^T \Lambda \mathbf{w}}{\sigma_\eta^2 \sigma_\epsilon^2}, \\
\frac{\partial^2 Q(\boldsymbol{\theta}|\boldsymbol{\theta})}{\partial \sigma_\eta^2 \partial \sigma_\epsilon^2} &= \frac{a[\gamma \text{tr}(V_0) - \mathbf{m}_{01}^T \Lambda \mathbf{m}_{01} - \mathbf{m}_{01}^T \Lambda \bar{\mathbf{w}}]}{2\sigma_\epsilon^2 \sigma_\eta^4},
\end{aligned}$$

Next, we need to evaluate  $\nabla_{\boldsymbol{\theta}}^2 Q(\boldsymbol{\theta}|\boldsymbol{\theta})$  at  $\boldsymbol{\theta} = \boldsymbol{\theta}^*$  (MLE obtained at convergence). To simplify notation, we omit the asterisk below, but the expressions in the remainder of this section are all evaluated at  $\boldsymbol{\theta} = \boldsymbol{\theta}^*$ . Setting  $\partial Q(\boldsymbol{\theta}|\boldsymbol{\theta}^{(i)})/\partial \mu = 0$  at  $\boldsymbol{\theta}, \boldsymbol{\theta}^{(i)} = \boldsymbol{\theta}^*$ :

$$\begin{aligned}
\sigma_\epsilon^{-2}(\mathbf{y} - \mu \mathbf{w} - \mathbf{m}_{0\mathbf{w}})^T \mathbf{w} + (\mathbf{m}_{0\mathbf{w}} - \mu \bar{\mathbf{w}})^T \frac{\Lambda}{\sigma_\eta^2} \bar{\mathbf{w}} &= 0 & \mathbf{m}_{01}^T \frac{\Lambda}{\sigma_\eta^2} \mathbf{1} &= 0 \\
\frac{(\mathbf{y} - \mathbf{m}_{00})^T}{\sigma_\epsilon^2} \mathbf{w} + \mathbf{m}_{01}^T \frac{\Lambda}{\sigma_\eta^2} \bar{\mathbf{w}} &= 0 & (\mathbf{y} - \mu \mathbf{1})^T S^{-1} \mathbf{1} &= 0 \\
\underbrace{\left[ \frac{(\mathbf{y} - \mathbf{m}_{00})}{\sigma_\epsilon^2} - \frac{\Lambda}{\sigma_\eta^2} \mathbf{m}_{01} \right]^T \mathbf{w} + \mathbf{m}_{01}^T \frac{\Lambda}{\sigma_\eta^2} \mathbf{1}}_{=0} &= 0 & \mu &= \frac{\mathbf{y}^T S^{-1} \mathbf{1}}{\mathbf{1}^T S^{-1} \mathbf{1}}.
\end{aligned} \tag{20}$$

Setting  $\partial Q(\boldsymbol{\theta}|\boldsymbol{\theta}^{(i)})/\partial \sigma_\eta^2 = 0$  at  $\boldsymbol{\theta}, \boldsymbol{\theta}^{(i)} = \boldsymbol{\theta}^*$ :

$$n(a-1) - a \text{tr}\left(\frac{V_0}{\sigma_\epsilon^2}\right) + (1-a) \text{tr}\left(V_0 \frac{\Lambda}{\sigma_\eta^2}\right) + \mathbf{m}_{01}^T \frac{\Lambda}{\sigma_\eta^2} \mathbf{m}_{01} + a \mathbf{m}_{0\mathbf{w}}^T \underbrace{\left[ \frac{(\mathbf{y} - \mathbf{m}_{00})}{\sigma_\epsilon^2} - \frac{\Lambda}{\sigma_\eta^2} \mathbf{m}_{01} \right]}_{=0} = 0.$$

Thus

$$\sigma_\eta^2 = \frac{(1-a) \text{tr}(V_0 \Lambda) + \mathbf{m}_{01}^T \Lambda \mathbf{m}_{01}}{n(1-a) + a \text{tr}\left(\frac{V_0}{\sigma_\epsilon^2}\right)}.$$

which leads to

$$n\sigma_\eta^2 = \text{tr}(V_0 \Lambda) + \mathbf{m}_{01}^T \Lambda \mathbf{m}_{01} \quad (a=0) \quad \text{and} \quad \gamma \text{tr}(V_0) = \mathbf{m}_{01}^T \Lambda \mathbf{m}_{01} \quad (a=1). \tag{21}$$

These two formulas are equivalent since  $\gamma \text{tr}(V_0) = \sigma_\eta^2 \text{tr}[(V_0^{-1} - \frac{\Lambda}{\sigma_\eta^2}) V_0] = n\sigma_\eta^2 - \text{tr}(V_0 \Lambda)$ .

Setting  $\partial Q(\boldsymbol{\theta}|\boldsymbol{\theta}^{(i)})/\partial \phi = 0$  at  $\boldsymbol{\theta}, \boldsymbol{\theta}^{(i)} = \boldsymbol{\theta}^*$ :

$$2\phi \sigma_\eta^2 = -(1-\phi^2)[\text{tr}(\Lambda_1 V_0) + \mathbf{m}_{01}^T \Lambda_1 \mathbf{m}_{01}]. \tag{22}$$

Setting  $\partial Q(\boldsymbol{\theta}|\boldsymbol{\theta}^{(i)})/\partial \sigma_\epsilon^2 = 0$  at  $\boldsymbol{\theta}, \boldsymbol{\theta}^{(i)} = \boldsymbol{\theta}^*$ :

$$n\sigma_\epsilon^2 = (\mathbf{y} - \mathbf{m}_{00})^T (\mathbf{y} - \mathbf{m}_{00}) + \text{tr}(V_0). \tag{23}$$

Using these identities, we can simplify  $I_{\text{aug}}(\boldsymbol{\theta}^*)$  so that it is clearer whether there is

any dependence on  $a$  and  $\mathbf{w}$ . The elements in  $I_{\text{aug}}(\boldsymbol{\theta}^*)$  are given by

$$\begin{aligned}
I_{\mu,\mu} &= \frac{\mathbf{w}^T \mathbf{w}}{\sigma_\epsilon^2} + \frac{\bar{\mathbf{w}}^T \Lambda \bar{\mathbf{w}}}{\sigma_\eta^2} = \tau(\mathbf{w}), & I_{\mu,\phi} &= -\frac{\mathbf{m}_{01}^T \Lambda_1 \bar{\mathbf{w}}}{\sigma_\eta^2}, \\
I_{\mu,\sigma_\eta^2} &= \frac{1}{\sigma_\eta^2} \left[ \frac{a \mathbf{m}_{0\mathbf{w}}^T}{2} \left( V_0^{-1} \mathbf{w} - \frac{\Lambda \mathbf{1}}{\sigma_\eta^2} \right) + \frac{\mathbf{m}_{01}^T \Lambda \bar{\mathbf{w}}}{\sigma_\eta^2} \right], & I_{\mu,\sigma_\epsilon^2} &= -\frac{\mathbf{m}_{01}^T \Lambda \bar{\mathbf{w}}}{\sigma_\epsilon^2 \sigma_\eta^2}, \\
I_{\sigma_\eta^2,\sigma_\eta^2} &= \frac{1}{2\sigma_\eta^4} \left[ n(1-a)^2 + \frac{a^2}{2} \mathbf{m}_{0\mathbf{w}}^T V_0^{-1} \mathbf{m}_{0\mathbf{w}} - \frac{2a\mu}{\sigma_\eta^2} \mathbf{m}_{01}^T \Lambda \bar{\mathbf{w}} \right], & I_{\sigma_\eta^2,\sigma_\epsilon^2} &= \frac{a\mu \mathbf{m}_{01}^T \Lambda \bar{\mathbf{w}}}{2\sigma_\eta^4 \sigma_\epsilon^2}, \\
I_{\sigma_\eta^2,\phi} &= \frac{(1-a)\phi}{\sigma_\eta^2(1-\phi^2)} + \frac{a\mu \mathbf{m}_{01}^T \Lambda_1 \bar{\mathbf{w}}}{2\sigma_\eta^4}, & I_{\phi,\sigma_\epsilon^2} &= 0, \\
I_{\phi,\phi} &= \frac{1}{\sigma_\eta^2} \sum_{t=2}^{n-1} (V_0 + \mathbf{m}_{01} \mathbf{m}_{01}^T)_{tt} + \frac{1+\phi^2}{(1-\phi^2)^2}, & I_{\sigma_\epsilon^2,\sigma_\epsilon^2} &= \frac{n}{2\sigma_\epsilon^4}.
\end{aligned}$$

Note that  $\mathbf{m}_{01}^T \frac{\Lambda}{\sigma_\eta^2} \mathbf{w} = -\mathbf{m}_{01}^T \frac{\Lambda}{\sigma_\eta^2} \bar{\mathbf{w}}$  as  $\mathbf{m}_{01}^T \frac{\Lambda}{\sigma_\eta^2} \mathbf{1} = 0$  from (20). Next, we analyze the elements in  $I_{\text{aug}}(\boldsymbol{\theta}^*)$  to identify those that will vary substantially with  $a$  and  $\mathbf{w}$  when  $n$  is large. This is done by considering  $\lim_{n \rightarrow \infty} I_{\theta_i, \theta_j} / n$ . We will use the fact that since  $\mathbf{y} \sim N(\mu \mathbf{1}, S)$ ,  $\mathbf{m}_{01} \sim N(\mathbf{0}, V_0 S V_0 / \sigma_\epsilon^4)$  and Theorem 7 below.

**Lemma 1.** *Let  $X_n \sim N(0, \sigma_n^2)$ , where  $\sigma_n^2 \leq M/n$  with  $M > 0$  being a constant. Then  $X_n \xrightarrow{a.s.} 0$ .*

*Proof.* Since

$$\begin{aligned}
1 - \Phi(x) &= \int_x^\infty \frac{e^{-z^2/2}}{\sqrt{2\pi}} dz \leq \int_x^\infty \frac{ze^{-z^2/2}}{x\sqrt{2\pi}} dz = \frac{e^{-x^2/2}}{x\sqrt{2\pi}}, \\
P(|X_n| > \epsilon) &= 2[1 - \Phi(\epsilon/\sigma_n)] \leq 2[1 - \Phi(\epsilon\sqrt{n/M})] \leq \sqrt{\frac{2M}{n\pi}} \frac{e^{-n\epsilon^2/(2M)}}{\epsilon}.
\end{aligned}$$

Thus

$$\begin{aligned}
\sum_{n=1}^\infty P(|X_n| > \epsilon) &\leq \frac{\sqrt{2M/\pi}}{\epsilon} \sum_{n=1}^\infty \frac{e^{-n\epsilon^2/(2M)}}{\sqrt{n}} \leq \frac{\sqrt{2M/\pi}}{\epsilon} \sum_{n=1}^\infty e^{-n\epsilon^2/(2M)} \\
&= \frac{\sqrt{2M/\pi}}{\epsilon(e^{\epsilon^2/(2M)} - 1)} < \infty.
\end{aligned}$$

Hence  $X_n \xrightarrow{a.s.} 0$ . □

**Theorem 7.** *Suppose  $\mathbf{u} = (u_1, \dots, u_n)^T$  is a bounded constant vector, that is, there exists  $c > 0$  such that  $|u_t| \leq c$  for all  $t = 1, \dots, n$  where  $n > 1$ . Then  $\mathbf{m}_{01}^T \Lambda \mathbf{u} / n$ ,  $\mathbf{m}_{01}^T \Lambda_1 \mathbf{u} / n$  and  $\mathbf{m}_{01}^T S^{-1} \mathbf{u} / n$  converge to zero almost surely.*

*Proof.* Since  $\mathbf{m}_{01}^T \Lambda \mathbf{u} / n$ ,  $\mathbf{m}_{01}^T \Lambda_1 \mathbf{u} / n$  and  $\mathbf{m}_{01}^T S^{-1} \mathbf{u} / n$  are all normally distributed with zero means, from Lemma 1, it suffices to show that  $\text{var}(\mathbf{m}_{01}^T \Lambda \mathbf{u} / n)$ ,  $\text{var}(\mathbf{m}_{01}^T \Lambda_1 \mathbf{u} / n)$  and

$\text{var}(\mathbf{m}_{01}^T S^{-1} \mathbf{u}/n)$  are bounded by  $M/n$  for some  $M > 0$ .

$$\begin{aligned} \text{var}\left(\frac{\mathbf{m}_{01}^T \Lambda \mathbf{u}}{n}\right) &= \frac{\mathbf{u}^T \Lambda V_0 S V_0 \Lambda \mathbf{u}}{n^2 \sigma_\epsilon^4} = \frac{\sigma_\eta^2 \mathbf{u}^T \Lambda V_0 \mathbf{u}}{n^2 \sigma_\epsilon^2} \\ &= \frac{\sigma_\eta^4}{n^2} \mathbf{u}^T \left( \frac{I}{\sigma_\epsilon^2} - \frac{V_0}{\sigma_\epsilon^4} \right) \mathbf{u} \leq \frac{\sigma_\eta^4}{n^2 \sigma_\epsilon^2} \mathbf{u}^T \mathbf{u} \leq \frac{c^2 \sigma_\eta^4}{n \sigma_\epsilon^2}. \end{aligned}$$

$$\begin{aligned} \text{var}\left(\frac{\mathbf{m}_{01}^T \Lambda_1 \mathbf{u}}{n}\right) &= \frac{\mathbf{u}^T \Lambda_1 V_0 S V_0 \Lambda_1 \mathbf{u}}{n^2 \sigma_\epsilon^4} = \frac{1}{n^2} \mathbf{u}^T \Lambda_1 (\sigma_\eta^2 \Lambda^{-1} - V_0) \Lambda_1 \mathbf{u} \\ &\leq \frac{\sigma_\eta^2}{n^2} \mathbf{u}^T \Lambda_1 \Lambda^{-1} \Lambda_1 \mathbf{u} \leq \frac{\sigma_\eta^2}{n^2} \lambda_{\max}(\Lambda^{-1}) \|\Lambda_1 \mathbf{u}\|_2^2 \leq \frac{16 \lambda_{\max}(\Lambda^{-1}) \sigma_\eta^2 c^2}{n}, \end{aligned}$$

where  $\lambda_{\max}(\cdot)$  denotes the maximum eigenvalue. Note that

$$\|\Lambda_1 \mathbf{u}\|_2^2 = u_2^2 + u_{n-1}^2 + \sum_{t=2}^{n-1} (2\phi u_t - u_{t-1} - u_{t+1})^2 \leq 2c^2 + (n-2)(4c)^2 = (16n-30)c^2.$$

Finally,

$$\begin{aligned} \text{var}\left(\frac{\mathbf{m}_{01}^T S^{-1} \mathbf{u}}{n}\right) &= \frac{\mathbf{u}^T S^{-1} V_0 S V_0 S^{-1} \mathbf{u}}{n^2 \sigma_\epsilon^4} = \frac{\mathbf{u}^T V_0^2 S^{-1} \mathbf{u}}{n^2 \sigma_\epsilon^4} = \frac{\mathbf{u}^T V_0^2 (\sigma_\epsilon^{-2} I - \sigma_\epsilon^{-4} V_0) \mathbf{u}}{n^2 \sigma_\epsilon^4} \\ &\leq \frac{\mathbf{u}^T V_0^2 \mathbf{u}}{n^2 \sigma_\epsilon^6} \leq \frac{1}{n^2 \sigma_\epsilon^6} \lambda_{\max}(V_0^2) \|\mathbf{u}\|_2^2 \leq \frac{\lambda_{\max}(V_0^2) c^2}{n \sigma_\epsilon^6}. \end{aligned}$$

□

Thus, assuming  $\mathbf{w}$  (and hence  $\bar{\mathbf{w}}$ ) is bounded,  $\mathbf{m}_{01}^T \Lambda \bar{\mathbf{w}}/n$ ,  $\mathbf{m}_{01}^T \Lambda_1 \bar{\mathbf{w}}/n$  and  $\mathbf{m}_{01}^T S^{-1} \bar{\mathbf{w}}/n$  converge to zero almost surely. As  $\Lambda = I$  if  $\phi = 0$ ,  $\mathbf{m}_{01}^T \bar{\mathbf{w}}/n$  and  $\mathbf{m}_{01}^T \mathbf{w}/n$  also converge to zero almost surely. Thus we have

$$\lim_{n \rightarrow \infty} \frac{I_{\mu, \phi}}{n} = 0, \quad \lim_{n \rightarrow \infty} \frac{I_{\mu, \sigma_\epsilon^2}}{n} = 0, \quad \lim_{n \rightarrow \infty} \frac{I_{\sigma_\eta^2, \phi}}{n} = 0, \quad \lim_{n \rightarrow \infty} \frac{I_{\sigma_\eta^2, \sigma_\epsilon^2}}{n} = 0.$$

## 12 Unknown location parameter

In this section, we consider the location parameter  $\mu$  as the only unknown parameter.

### 12.1 A recurrence relation

Recall that  $v_i = b^{i-1} \kappa_{n-i} / \kappa$  for  $i = 1, \dots, n$ , where

$$\begin{aligned} \kappa &= \varphi_+^2 r_+^{n-1} - \varphi_-^2 r_-^{n-1}, \quad \kappa_i = \varphi_+ r_+^i - \varphi_- r_-^i \quad (i = 0, \dots, n-1), \\ \varphi_\pm &= r_\pm - |\phi|, \quad r_\pm = (c \pm \sqrt{c^2 - 4})/2. \end{aligned}$$

Note that  $r_+ r_- = 1$ ,  $r_+ + r_- = c$  and  $\kappa > 0$ .

**Lemma 2.** If  $0 < \phi < 1$ , then  $cv_i = v_{i-1} + v_{i+1}$  for  $i = 2, \dots, n-1$ .

*Proof.* First,

$$\begin{aligned}\kappa_{i-1} + \kappa_{i+1} &= \varphi_+ r_+^{i-1} - \varphi_- r_-^{i-1} + \varphi_+ r_+^{i+1} - \varphi_- r_-^{i+1} \\ &= \varphi_+ r_+^i (1/r_+ + r_+) - \varphi_- r_-^i (1/r_- + r_-) \\ &= \varphi_+ r_+^i (r_- + r_+) - \varphi_- r_-^i (r_+ + r_-) = c\kappa_i.\end{aligned}$$

As  $b = 1$ , we have  $cv_i = c\kappa_{n-i}/\kappa = (\kappa_{n-i-1} + \kappa_{n-i+1})/\kappa = v_{i-1} + v_{i+1}$ .  $\square$

Recall that the sum of the  $i$ th row of  $Q^{-1}$  is  $s_i = \{1 - b(1 - \phi)(v_i + v_{n-i+1})\}/(c - 2b)$ .

**Lemma 3.** If  $0 < \phi < 1$ , then  $2\phi s_t - s_{t-1} - s_{t+1} < 0$ .

*Proof.* As  $b = 1$ ,  $s_t = \{1 - (1 - \phi)(v_t + v_{n-t+1})\}/(c - 2)$ . From Lemma 2,

$$\begin{aligned}(c - 2)(2\phi s_t - s_{t-1} - s_{t+1}) &= 2\phi - 2 - (1 - \phi)\{2\phi(v_t + v_{n-t+1}) - (v_{t-1} + v_{n-t+2}) - (v_{t+1} + v_{n-t})\} \\ &= 2\phi - 2 - (1 - \phi)(2\phi - c)(v_t + v_{n-t+1}) \\ &= 2\phi - 2 - (2\phi - c)\{1 - (c - 2)s_t\} \\ &= (c - 2)\{1 + (2\phi - c)s_t\}.\end{aligned}$$

From Property 3,  $s_t > 1/(d - \phi)$  implies that  $1 + (2\phi - c)s_t < 1 + (2\phi - c)/(d - \phi) = (d + \phi - c)/(d - \phi) = 0$ . Hence  $2\phi s_t - s_{t-1} - s_{t+1} < 0$ .  $\square$

## 12.2 Assuming $w$ is constant across $t$

**Lemma 4.**  $\lim_{n \rightarrow \infty} \sum_{t=1}^n w_t^{\text{opt}}/n = 1/(1 + u^*)$ , where  $u^* = \gamma/(1 - \phi)^2$ .

*Proof.* From Theorem 2,

$$w_t^{\text{opt}} = \frac{(1 - \phi)^2 + b\gamma(1 - \phi)(v_t + v_{n-t+1})}{(1 - \phi)^2 + \gamma} \quad \text{if } \phi \neq 0.$$

Hence

$$\begin{aligned}\frac{1}{n} \sum_{t=1}^n w_t^{\text{opt}} &= \frac{1}{1 + u^*} + \frac{2b\gamma(1 - \phi)}{n[(1 - \phi)^2 + \gamma]} \sum_{t=1}^n v_t. \\ \kappa \sum_{t=1}^n v_t &= \sum_{t=1}^n b^{t-1} \kappa_{n-t} = \sum_{t=1}^n b^{t-1} (\varphi_+ r_+^{n-t} - \varphi_- r_-^{n-t}) \\ &= \frac{\varphi_+ r_+^n}{b} \sum_{t=1}^n \left(\frac{b}{r_+}\right)^t - \frac{\varphi_- r_-^n}{b} \sum_{t=1}^n \left(\frac{b}{r_-}\right)^t = \frac{\varphi_+(b^n - r_+^n)}{b - r_+} - \frac{\varphi_-(b^n - r_-^n)}{b - r_-} \\ &= \frac{\varphi_+(b^{n+1} - b^n r_- - b r_+^n + r_+^{n+1}) - \varphi_-(b^{n+1} - b^n r_+ - b r_-^n + r_-^{n+1})}{2 - bc}.\end{aligned}$$

Thus

$$\begin{aligned} \frac{1}{n} \sum_{t=1}^n v_t &= \frac{\varphi_+(b^{n+1} - b^n r_- - b r_+^n + r_+^{n-1}) - \varphi_-(b^{n+1} - b^n r_+ - b r_-^n + r_-^{n-1})}{n(2 - bc)(\varphi_+^2 r_+^{n-1} - \varphi_-^2 r_-^{n-1})} \\ &= \frac{\varphi_+(R_1^{n-1} - R_1^{n-2} R_2 - b r_+ + 1) - \varphi_-(R_1^{n-1} - R_1^{n-2} - b r_- R_2^{n-1} + R_2^{n-1})}{n(2 - bc)(\varphi_+^2 - \varphi_-^2 R_2^{n-1})} \end{aligned}$$

where  $R_1 = b/r_+$  and  $R_2 = r_-/r_+$ . Since  $|R_1| < 1$  and  $|R_2| < 1$ ,  $\lim_{n \rightarrow \infty} \sum_{t=1}^n v_t/n = 0$  and  $\lim_{n \rightarrow \infty} \sum_{t=1}^n w_t^{\text{opt}}/n = 1/(1 + u^*)$ .  $\square$

## 13 Unknown scale parameter

Here we assume  $\sigma_\eta^2$  is the only unknown parameter.

$$\begin{aligned} \frac{\partial I_{\sigma_\eta^2, \sigma_\eta^2}}{\partial a} &= \frac{1}{2\sigma_\eta^4} \left\{ 2n(a - 1) + a \mathbf{m}_{0\mathbf{w}}^T V_0^{-1} \mathbf{m}_{0\mathbf{w}} - 2\mu \bar{\mathbf{w}}^T \frac{\Lambda}{\sigma_\eta^2} \mathbf{m}_{01} \right\} = 0 \\ \implies a &= \frac{2n + 2\mu \bar{\mathbf{w}}^T \frac{\Lambda}{\sigma_\eta^2} \mathbf{m}_{01}}{2n + \mathbf{m}_{0\mathbf{w}}^T V_0^{-1} \mathbf{m}_{0\mathbf{w}}} = 1 - \frac{\mathbf{m}_{0\mathbf{w}}^T V_0^{-1} \mathbf{m}_{0\mathbf{w}} - 2\mu \bar{\mathbf{w}}^T \frac{\Lambda}{\sigma_\eta^2} \mathbf{m}_{01}}{2n + \mathbf{m}_{0\mathbf{w}}^T V_0^{-1} \mathbf{m}_{0\mathbf{w}}}. \end{aligned} \quad (24)$$

Note that  $a \leq 1$  for any  $\mathbf{w}$  as

$$\begin{aligned} \mathbf{m}_{0\mathbf{w}}^T V_0^{-1} \mathbf{m}_{0\mathbf{w}} - \frac{2\mu}{\sigma_\eta^2} \mathbf{m}_{01}^T \Lambda \bar{\mathbf{w}} &= (\mathbf{m}_{01} + \mu \bar{\mathbf{w}})^T V_0^{-1} (\mathbf{m}_{01} + \mu \bar{\mathbf{w}}) - \frac{2\mu}{\sigma_\eta^2} \mathbf{m}_{01}^T \Lambda \bar{\mathbf{w}} \\ &= \mathbf{m}_{01}^T V_0^{-1} \mathbf{m}_{01} + 2\mu \mathbf{m}_{01}^T \left( V_0^{-1} - \frac{\Lambda}{\sigma_\eta^2} \right) \bar{\mathbf{w}} + \mu^2 \bar{\mathbf{w}}^T V_0^{-1} \bar{\mathbf{w}} \\ &= \frac{(\mathbf{m}_{01} + \mu \bar{\mathbf{w}})^T (\mathbf{m}_{01} + \mu \bar{\mathbf{w}})}{\sigma_\epsilon^2} + \frac{\mathbf{m}_{01}^T \Lambda \mathbf{m}_{01} + \mu^2 \bar{\mathbf{w}}^T \Lambda \bar{\mathbf{w}}}{\sigma_\eta^2} \geq 0. \end{aligned}$$

$$\frac{\partial I_{\sigma_\eta^2, \sigma_\eta^2}}{\partial \bar{\mathbf{w}}} = \frac{a\mu}{2\sigma_\eta^4} \left\{ a V_0^{-1} \mathbf{m}_{0\mathbf{w}} - 2 \frac{\Lambda}{\sigma_\eta^2} \mathbf{m}_{01} \right\} = \frac{a^2 \mu}{2\sigma_\eta^4} V_0^{-1} \left\{ \mathbf{m}_{01} + \mu \bar{\mathbf{w}} - \frac{2V_0 \Lambda}{a\sigma_\eta^2} \mathbf{m}_{01} \right\}.$$

Setting  $\partial I_{\sigma_\eta^2, \sigma_\eta^2} / \partial \bar{\mathbf{w}} = 0$  leads to

$$\bar{\mathbf{w}} = \frac{1}{\mu} \left( \frac{2V_0 \Lambda}{a\sigma_\eta^2} \mathbf{m}_{01} - \mathbf{m}_{01} \right). \quad (25)$$

Note that (25) implies  $\mathbf{m}_{0\mathbf{w}} = \mathbf{m}_{01} + \mu \bar{\mathbf{w}} = \frac{2V_0 \Lambda}{a\sigma_\eta^2} \mathbf{m}_{01}$ . Solving (24) and (25) simultaneously,

$$\begin{aligned} 2na + \frac{4}{a} \mathbf{m}_{01}^T \frac{\Lambda}{\sigma_\eta^2} V_0 \frac{\Lambda}{\sigma_\eta^2} \mathbf{m}_{01} &= 2n + \frac{4}{a} \mathbf{m}_{01}^T \frac{\Lambda}{\sigma_\eta^2} V_0 \frac{\Lambda}{\sigma_\eta^2} \mathbf{m}_{01} - 2\mathbf{m}_{01}^T \frac{\Lambda}{\sigma_\eta^2} \mathbf{m}_{01} \\ \implies a &= 1 - \frac{\mathbf{m}_{01}^T \Lambda \mathbf{m}_{01}}{n\sigma_\eta^2} = \frac{\text{tr}(V_0 \Lambda)}{n\sigma_\eta^2} = 1 - \frac{\text{tr}(V_0)}{n\sigma_\epsilon^2}, \end{aligned}$$

where the last two equalities follows from (21). The second order derivatives are

$$\begin{aligned}\frac{\partial^2 I_{\sigma_\eta^2, \sigma_\eta^2}}{\partial a^2} &= \frac{1}{2\sigma_\eta^4} (2n + \mathbf{m}_{0\mathbf{w}}^T V_0^{-1} \mathbf{m}_{0\mathbf{w}}), \quad \frac{\partial^2 I_{\sigma_\eta^2, \sigma_\eta^2}}{\partial \bar{\mathbf{w}} \partial \bar{\mathbf{w}}^T} = \frac{a^2 \mu^2}{2\sigma_\eta^4} V_0^{-1}, \\ \frac{\partial^2 I_{\sigma_\eta^2, \sigma_\eta^2}}{\partial \bar{\mathbf{w}} \partial a} &= \frac{\mu}{2\sigma_\eta^4} (2a V_0^{-1} \mathbf{m}_{0\mathbf{w}} - 2 \frac{\Lambda}{\sigma_\eta^2} \mathbf{m}_{01}).\end{aligned}$$

Let  $g = 2 \frac{\Lambda}{\sigma_\eta^2} \mathbf{m}_{01}$ . At  $(a^{\text{opt}}, \bar{\mathbf{w}}^{\text{opt}})$ , the Hessian of  $I_{\sigma_\eta^2, \sigma_\eta^2}$  is

$$\mathcal{H} = \frac{1}{2\sigma_\eta^4} \begin{bmatrix} 2n + (a^{\text{opt}})^{-2} g^T V_0 g & \mu g^T \\ \mu g & \mu^2 (a^{\text{opt}})^2 V_0^{-1} \end{bmatrix},$$

$\mathcal{H}$  is symmetric positive definite because

$$x^T \mathcal{H} x = \frac{1}{2\sigma_\eta^4} \left\{ 2n x_1^2 + \left( \frac{x_1 g}{a^{\text{opt}}} + \mu a^{\text{opt}} V_0^{-1} x_2 \right)^T V_0 \left( \frac{x_1 g}{a^{\text{opt}}} + \mu a^{\text{opt}} V_0^{-1} x_2 \right) \right\} > 0$$

for any  $x = (x_1, x_2)^T \neq 0$ , where the dimensions of  $x_1, x_2$  matches that of  $a$  and  $\mathbf{w}$ .

### 13.1 Large-sample estimate of $a^{\text{opt}}$

The large-sample estimate of  $a^{\text{opt}}$  is  $\hat{a}^{\text{opt}} = 1 - \gamma/\sqrt{d}$ , where

$$d = \{(1 - \phi)^2 + \gamma\} \{(1 + \phi)^2 + \gamma\} = \gamma^2 + 2\gamma(1 + \phi^2) + (1 - \phi^2)^2.$$

$$\begin{aligned}\frac{\partial \hat{a}^{\text{opt}}}{\partial \gamma} &= -\frac{d - \gamma[\gamma + (1 + \phi^2)]}{d^{3/2}} = -\frac{\gamma(1 + \phi^2) + (1 - \phi^2)^2}{d^{3/2}} < 0. \\ \frac{\partial \hat{a}^{\text{opt}}}{\partial |\phi|} &= \frac{2\gamma|\phi|[\gamma + \phi^2 - 1]}{d^{3/2}}.\end{aligned}$$

### 13.2 Augmented information matrix at optimal parametrization

Let  $\xi = \mathbf{m}_{01}^T \Lambda \mathbf{m}_{01} / \sigma_\eta^2 = \text{tr}(V_0) / \sigma_\epsilon^2$ . Suppose  $a = a^{\text{opt}} = 1 - \xi/n$  and  $\bar{\mathbf{w}} = \bar{\mathbf{w}}^{\text{opt}}$ . Note that  $a \mathbf{m}_{0\mathbf{w}} = 2V_0 \Lambda \mathbf{m}_{01} / \sigma_\eta^2$  from (25).

$$\begin{aligned}I_{\mu, \sigma_\eta^2} &= \frac{1}{\sigma_\eta^2} \left\{ \frac{\mathbf{m}_{01}^T \Lambda V_0}{\sigma_\eta^2} \left( V_0^{-1} \mathbf{w} - \frac{\Lambda \mathbf{1}}{\sigma_\eta^2} \right) + \mathbf{m}_{01}^T \frac{\Lambda}{\sigma_\eta^2} \bar{\mathbf{w}} \right\} = \frac{\mathbf{m}_{01}^T S^{-1} \mathbf{1}}{\sigma_\eta^2}. \\ I_{\sigma_\eta^2, \sigma_\eta^2} &= \frac{1}{2\sigma_\eta^4} \left\{ n(a - 1)^2 + \frac{a^2}{2} \mathbf{m}_{0\mathbf{w}}^T V_0^{-1} \mathbf{m}_{0\mathbf{w}} - a[2n(a - 1) + a \mathbf{m}_{0\mathbf{w}}^T V_0^{-1} \mathbf{m}_{0\mathbf{w}}] \right\} \quad (24) \\ &= \frac{1}{2\sigma_\eta^4} \left\{ n(1 - a^2) - \frac{a^2}{2} \mathbf{m}_{0\mathbf{w}}^T V_0^{-1} \mathbf{m}_{0\mathbf{w}} \right\} = \frac{1}{2\sigma_\eta^4} \left\{ 2\xi - \frac{\xi^2}{n} - 2\mathbf{m}_{01}^T \frac{\Lambda}{\sigma_\eta^2} V_0 \frac{\Lambda}{\sigma_\eta^2} \mathbf{m}_{01} \right\} \\ &= \frac{1}{2\sigma_\eta^4} \left\{ 2\xi - \frac{\xi^2}{n} - 2\xi + 2\mathbf{m}_{01}^T S^{-1} \mathbf{m}_{01} \right\} = \frac{1}{2\sigma_\eta^4} \left\{ 2\mathbf{m}_{01}^T S^{-1} \mathbf{m}_{01} - \frac{\xi^2}{n} \right\},\end{aligned}$$

$$\begin{aligned}
I_{\mu,\mu} &= \frac{(\mathbf{1} - \bar{\mathbf{w}})^T(\mathbf{1} - \bar{\mathbf{w}})}{\sigma_\epsilon^2} + \frac{\bar{\mathbf{w}}^T \Lambda \bar{\mathbf{w}}}{\sigma_\eta^2} = \mathbf{1}^T \left( S^{-1} + \frac{V_0}{\sigma_\epsilon^4} \right) \mathbf{1} - \frac{2\mathbf{1}^T \bar{\mathbf{w}}}{\sigma_\epsilon^2} + \bar{\mathbf{w}}^T V_0^{-1} \bar{\mathbf{w}} \\
&= \mathbf{1}^T S^{-1} \mathbf{1} + \left( V_0^{-1} \bar{\mathbf{w}} - \frac{\mathbf{1}}{\sigma_\epsilon^2} \right)^T V_0 \left( V_0^{-1} \bar{\mathbf{w}} - \frac{\mathbf{1}}{\sigma_\epsilon^2} \right).
\end{aligned}$$

Note that  $I_{\mu,\mu} > \mathbf{1}^T S^{-1} \mathbf{1}$  as  $\bar{\mathbf{w}} \neq V_0 \mathbf{1} / \sigma_\epsilon^2$ .

### 13.3 Rate of convergence of Algorithm 2

The rate of convergence of Algorithm 2 at  $(a^{\text{opt}}, \bar{\mathbf{w}}^{\text{opt}})$  is

$$1 - \frac{I_{\sigma_\eta^2, \sigma_\eta^2}^{\text{obs}}}{I_{\sigma_\eta^2, \sigma_\eta^2}} = 1 - \frac{2\mathbf{m}_{01}^T S^{-1} \mathbf{m}_{01} - \text{tr}(V_0^2) / \sigma_\epsilon^4}{2\mathbf{m}_{01}^T S^{-1} \mathbf{m}_{01} - \text{tr}(V_0)^2 / (n\sigma_\epsilon^4)} = \frac{\text{tr}(V_0^2) / (n\sigma_\epsilon^4) - \text{tr}(V_0)^2 / (n^2\sigma_\epsilon^4)}{2\mathbf{m}_{01}^T S^{-1} \mathbf{m}_{01} / n - \text{tr}(V_0)^2 / (n^2\sigma_\epsilon^4)}.$$

This rate is dependent on the observed data and varies even across data sets simulated from the same distribution. We approximate the convergence rate by replacing  $\mathbf{m}_{01}^T S^{-1} \mathbf{m}_{01} / n$  with its mean,  $\text{tr}(V_0^2) / (n\sigma_\epsilon^4)$ . Note that  $\mathbf{m}_{01}^T S^{-1} \mathbf{m}_{01} / n$  converges in mean square to  $\text{tr}(V_0^2) / (n\sigma_\epsilon^4)$  since  $\text{var}(\mathbf{m}_{01}^T S^{-1} \mathbf{m}_{01} / n) = 2\text{tr}(V_0^4) / (n^2\sigma_\epsilon^8) = \mathcal{O}(1/n)$ . From Property 4,

$$\lim_{n \rightarrow \infty} \frac{\text{tr}(V_0^2)}{n\sigma_\epsilon^4} = \frac{\gamma^2 c}{\phi^2 \kappa_0^3}, \quad \lim_{n \rightarrow \infty} \frac{\text{tr}(V_0)^2}{n^2\sigma_\epsilon^4} = \frac{\gamma^2}{\phi^2 \kappa_0^2}$$

where  $\kappa_0 = \sqrt{c^2 - 4} < c$ . Thus the approximate convergence rate of Algorithm 2 when  $n$  is large is

$$\text{DM}_{\text{Alg 2}}^{\text{asympt}} = \lim_{n \rightarrow \infty} \frac{\text{tr}(V_0^2) / (n\sigma_\epsilon^4) - \text{tr}(V_0)^2 / (n^2\sigma_\epsilon^4)}{2\text{tr}(V_0^2) / (n\sigma_\epsilon^4) - \text{tr}(V_0)^2 / (n^2\sigma_\epsilon^4)} = \frac{c - \kappa_0}{2c - \kappa_0} < \frac{1}{2}.$$

Writing  $\text{DM}_{\text{Alg 2}}^{\text{asympt}} = 4(c^2 + c\sqrt{c^2 - 4} + 4)^{-1}$ ,

$$\begin{aligned}
\frac{\partial \text{DM}_{\text{Alg 2}}^{\text{asympt}}}{\partial \gamma} &= -\frac{4(2c + c\sqrt{c^2 - 4} + c^2 / \sqrt{c^2 - 4})}{|\phi|(c^2 + c\sqrt{c^2 - 4} + 4)^2} < 0, \\
\frac{\partial \text{DM}_{\text{Alg 2}}^{\text{asympt}}}{\partial |\phi|} &= \frac{4(2c + c\sqrt{c^2 - 4} + c^2 / \sqrt{c^2 - 4})(1 + \gamma - \phi^2)}{\phi^2(c^2 + c\sqrt{c^2 - 4} + 4)^2} > 0,
\end{aligned}$$

Thus the approximate rate of convergence decreases as  $\gamma$  increases and  $|\phi|$  decreases.

Next, we consider the rate of convergence of Algorithm 2 at some other combinations of  $(a, \mathbf{w})$ , which are necessarily greater than the optimal rate found above. We approximate the term  $\mathbf{m}_{01}^T V_0^{-1} \mathbf{m}_{01}$  by its mean,  $\text{tr}(SV_0) / \sigma_\epsilon^4 = \gamma \text{tr}(\Lambda^{-1}) = n\gamma / (1 - \phi^2) = 2n\zeta$ , where  $\zeta = \gamma / [2(1 - \phi^2)]$ . The approximate rate of convergence is computed as

$$\text{DM}_{\text{Alg 2}} = 1 - \text{E}(I_{\sigma_\eta^2, \sigma_\eta^2}^{\text{obs}}) / \text{E}(I_{\sigma_\eta^2, \sigma_\eta^2}) = 1 - \frac{\text{tr}(V_0^2) / (n\sigma_\epsilon^4)}{B},$$

where the expression for  $B$  is given in the table below.

Parametrization	$a$	$\mathbf{w}$	$2\sigma_\eta^4 I_{\sigma_\eta^2, \sigma_\eta^2}$	$B$
opt	$a^{\text{opt}}$	$\mathbf{w}^{\text{opt}}$	$2\mathbf{m}_{01}^T S^{-1} \mathbf{m}_{01} - \frac{\text{tr}(V_0)^2}{n\sigma_\epsilon^4}$	$\frac{2\text{tr}(V_0^2)}{n\sigma_\epsilon^4} - \frac{\text{tr}(V_0)^2}{n^2\sigma_\epsilon^4}$
*	$\frac{1}{1+\zeta}$	$\mathbf{1}$	$\frac{n\zeta^2 + \mathbf{m}_{01}^T V_0^{-1} \mathbf{m}_{01}/2}{(1+\zeta)^2}$	$\frac{\zeta}{1+\zeta}$
NC	1	$\mathbf{1}$	$\mathbf{m}_{01}^T V_0^{-1} \mathbf{m}_{01}/2$	$\zeta$
C	0	$\mathbf{0}$	$n$	1

The approximate convergence rates follow a hierarchy,

$$\text{DM}_{\text{Alg } 2}^{\text{opt}} \leq \text{DM}_{\text{Alg } 2}^* < \min\{\text{DM}_{\text{Alg } 2}^C, \text{DM}_{\text{Alg } 2}^{\text{NC}}\}.$$

Note that by definition of  $(a^{\text{opt}}, \mathbf{w}^{\text{opt}})$ ,

$$\begin{aligned}
& 2\mathbf{m}_{01}^T S^{-1} \mathbf{m}_{01} - \frac{\text{tr}(V_0)^2}{n\sigma_\epsilon^4} < \frac{n\zeta^2 + \mathbf{m}_{01}^T V_0^{-1} \mathbf{m}_{01}/2}{(1+\zeta)^2} \\
\Rightarrow & \frac{2\text{tr}(V_0^2) - \text{tr}(V_0)^2/n}{\sigma_\epsilon^4} < \frac{n\zeta}{(1+\zeta)}, \quad (\text{taking expectation}) \\
\Rightarrow & \frac{\gamma^2}{\phi^2 \kappa_0^2} \left( \frac{2c}{\kappa_0} - 1 \right) \leq \frac{\zeta}{(1+\zeta)}. \quad (\text{taking } \lim_{n \rightarrow \infty})
\end{aligned}$$

## 14 Kalman Filter and Smoother

Consider the Gaussian state space model specified (with  $a = 0, \mathbf{w} = \mathbf{1}$ ) as

$$\begin{aligned}
y_t &= \alpha_t + \mu + \sigma_\epsilon \epsilon_t, \quad t = 1, \dots, n, \\
\alpha_t &= \phi \alpha_{t-1} + \sigma_\eta \eta_t, \quad t = 2, \dots, n, \\
\alpha_1 &\sim N(0, \sigma_\eta^2/(1-\phi^2)).
\end{aligned} \tag{26}$$

Define  $\hat{\alpha}_{t|j} = \text{E}(\alpha_t | y_{1:j})$  and  $P_{t|j} = \text{var}(\alpha_t | y_{1:j})$  for  $t, j = 1, \dots, n$ , with  $\hat{\alpha}_{1|0} = 0$  and  $P_{1|0} = \sigma_\eta^2/(1-\phi^2)$  being the initial prior values. From (26), the one-step ahead prediction step is given by

$$\hat{\alpha}_{t+1|t} = \phi \hat{\alpha}_{t|t}, \quad P_{t+1|t} = \phi^2 P_{t|t} + \sigma_\eta^2. \tag{27}$$

The joint distribution  $p(\alpha_t, y_t | y_{1:t-1})$  is

$$N \left( \begin{bmatrix} \hat{\alpha}_{t|t-1} \\ \hat{\alpha}_{t|t-1} + \mu \end{bmatrix}, \begin{bmatrix} P_{t|t-1} & P_{t|t-1} \\ P_{t|t-1} & P_{t|t-1} + \sigma_\epsilon^2 \end{bmatrix} \right).$$

Hence, the updating step is given by

$$\begin{aligned}
\hat{\alpha}_{t|t} &= \mathbb{E}(\alpha_t | y_{1:t-1}, y_t) = \hat{\alpha}_{t|t-1} + P_{t|t-1}(P_{t|t-1} + \sigma_\epsilon^2)^{-1}(y_t - \mu - \hat{\alpha}_{t|t-1}) \\
&= \hat{\alpha}_{t|t-1} + P_{t|t-1}F_t^{-1}v_t = \hat{\alpha}_{t|t-1} + K_tv_t, \\
P_{t|t} &= \text{var}(\alpha_t | y_{1:t-1}, y_t) = P_{t|t-1} - P_{t|t-1}^2(P_{t|t-1} + \sigma_\epsilon^2)^{-1} \\
&= P_{t|t-1}(1 - P_{t|t-1}F_t^{-1}) = P_{t|t-1}(1 - K_t),
\end{aligned} \tag{28}$$

where  $F_t = P_{t|t-1} + \sigma_\epsilon^2$ ,  $v_t = y_t - \mu - \hat{\alpha}_{t|t-1}$  and the Kalman gain  $K_t = P_{t|t-1}F_t^{-1}$ . The joint distribution  $p(\alpha_t, \alpha_{t+1} | y_{1:t})$  is

$$N \left( \begin{bmatrix} \hat{\alpha}_{t|t} \\ \hat{\alpha}_{t+1|t} \end{bmatrix}, \begin{bmatrix} P_{t|t} & \phi P_{t|t} \\ \phi P_{t|t} & P_{t+1|t} \end{bmatrix} \right),$$

and  $\alpha_t$  is independent of  $y_{t+1:n}$  given  $\alpha_{t+1}$ . Hence

$$\begin{aligned}
\mathbb{E}(\alpha_t | \alpha_{t+1}, y_{1:n}) &= \mathbb{E}(\alpha_t | \alpha_{t+1}, y_{1:t}) = \hat{\alpha}_{t|t} + \phi P_{t|t}P_{t+1|t}^{-1}(\alpha_{t+1} - \hat{\alpha}_{t+1|t}). \\
\text{var}(\alpha_t | \alpha_{t+1}, y_{1:n}) &= \text{var}(\alpha_t | \alpha_{t+1}, y_{1:t}) = P_{t|t} - \phi^2 P_{t|t}^2 P_{t+1|t}^{-1}.
\end{aligned}$$

Applying the Tower property and law of total variance,

$$\begin{aligned}
\hat{\alpha}_{t|n} &= \mathbb{E}(\alpha_t | y_{1:n}) = \mathbb{E}[\mathbb{E}(\alpha_t | \alpha_{t+1}, y_{1:n}) | y_{1:n}] = \hat{\alpha}_{t|t} + \phi P_{t|t}P_{t+1|t}^{-1}(\hat{\alpha}_{t+1|n} - \hat{\alpha}_{t+1|t}), \\
P_{t|n} &= \text{var}(\alpha_t | y_{1:n}) = \mathbb{E}[\text{var}(\alpha_t | \alpha_{t+1}, y_{1:n}) | y_{1:n}] + \text{var}[\mathbb{E}(\alpha_t | \alpha_{t+1}, y_{1:n}) | y_{1:n}] \\
&= P_{t|t} - \phi^2 P_{t|t}^2 P_{t+1|t}^{-2}(P_{t+1|t} - P_{t+1|n}).
\end{aligned} \tag{29}$$

From (28) and (29),  $\hat{\alpha}_{t|n} = \hat{\alpha}_{t|t-1} + P_{t|t-1}r_{t-1}$ , where

$$r_{t-1} = F_t^{-1}v_t + \phi(1 - K_t)P_{t+1|t}^{-1}(\hat{\alpha}_{t+1|n} - \hat{\alpha}_{t+1|t}) = F_t^{-1}v_t + L_tr_t,$$

where  $L_t = \phi(1 - K_t)$ . Similarly,  $P_{t|n} = P_{t|t-1} - P_{t|t-1}^2N_{t-1}$ ,

$$N_{t-1} = F_t^{-1} + L_t^2 P_{t+1|t}^{-2}(P_{t+1|t} - P_{t+1|n}) = F_t^{-1} + L_t^2 N_t.$$

Hence we obtain the backwards recurrence relations for  $\{r_t\}$  and  $\{N_t\}$  with initial values  $r_n = 0$  and  $N_n = 0$ .

In addition,  $P_{t,t+1|n} = \text{cov}(\alpha_t, \alpha_{t+1} | y_{1:n}) = \mathbb{E}(\alpha_t \alpha_{t+1} | y_{1:n}) - \hat{\alpha}_{t|n} \hat{\alpha}_{t+1|n}$ , where

$$\begin{aligned}
\mathbb{E}(\alpha_t \alpha_{t+1} | y_{1:n}) &= \mathbb{E}[\mathbb{E}(\alpha_t \alpha_{t+1} | \alpha_{t+1}, y_{1:n}) | y_{1:n}] \\
&= \mathbb{E}[\mathbb{E}(\alpha_t | \alpha_{t+1}, y_{1:n}) \alpha_{t+1} | y_{1:n}] \\
&= \mathbb{E}[\{\hat{\alpha}_{t|t} + \phi P_{t|t}P_{t+1|t}^{-1}(\alpha_{t+1} - \hat{\alpha}_{t+1|t})\} \alpha_{t+1} | y_{1:n}] \\
&= \hat{\alpha}_{t|t} \hat{\alpha}_{t+1|n} + \phi P_{t|t}P_{t+1|t}^{-1}\{P_{t+1|n} + \hat{\alpha}_{t+1|n}^2 - \hat{\alpha}_{t+1|t} \hat{\alpha}_{t+1|n}\}.
\end{aligned}$$

Thus

$$\begin{aligned}
P_{t,t+1|n} &= (\hat{\alpha}_{t|t} - \hat{\alpha}_{t|n})\hat{\alpha}_{t+1|n} + \phi P_{t|t} P_{t+1|t}^{-1} \{P_{t+1|n} + (\hat{\alpha}_{t+1|n} - \hat{\alpha}_{t+1|t})\hat{\alpha}_{t+1|n}\} \\
&= P_{t|t-1} (F_t^{-1} v_t - r_{t-1})\hat{\alpha}_{t+1|n} + L_t P_{t|t-1} \{P_{t+1|t}^{-1} P_{t+1|n} + r_t \hat{\alpha}_{t+1|n}\} \\
&= -P_{t|t-1} L_t r_t \hat{\alpha}_{t+1|n} + L_t P_{t|t-1} \{P_{t+1|t}^{-1} P_{t+1|n} + r_t \hat{\alpha}_{t+1|n}\} \\
&= L_t P_{t|t-1} P_{t+1|t}^{-1} P_{t+1|n} = P_{t|t-1} L_t (1 - P_{t+1|t} N_t).
\end{aligned} \tag{30}$$

The algorithm for implementing the Kalman filter and smoother is given below.

---

**Algorithm 7** Kalman Filter and Smoother

---

Set  $\hat{\alpha}_{1|0} = 0$  and  $P_{1|0} = \sigma_\eta^2 / (1 - \phi^2)$ .

For  $t = 1, \dots, n$ ,

1. Compute  $v_t = y_t - \mu - \hat{\alpha}_{t|t-1}$ ,  $F_t = P_{t|t-1} + \sigma_\epsilon^2$  and  $K_t = P_{t|t-1} F_t^{-1}$ .
2. Updating step:  $\hat{\alpha}_{t|t} = \hat{\alpha}_{t|t-1} + K_t v_t$  and  $P_{t|t} = P_{t|t-1} (1 - K_t)$ . (28)
3. Prediction step:  $\hat{\alpha}_{t+1|t} = \phi \hat{\alpha}_{t|t}$  and  $P_{t+1|t} = \phi^2 P_{t|t} + \sigma_\eta^2$ . (27)

Store  $\{v_t\}$ ,  $\{F_t\}$ ,  $\{K_t\}$ ,  $\{\hat{\alpha}_{t+1|t}\}$  and  $\{P_{t+1|t}\}$ . Initialize  $r_n = 0$  and  $N_n = 0$ .

For  $t = n, \dots, 1$ ,

1. Compute  $L_t = \phi(1 - K_t)$ .
  2. If  $t < n$ , compute  $P_{t,t+1|n} = P_{t|t-1} L_t (1 - P_{t+1|t} N_t)$ . (30)
  3. Recurrence relation:  $r_{t-1} = F_t^{-1} v_t + L_t r_t$  and  $N_{t-1} = F_t^{-1} + L_t^2 N_t$ .
  4. Compute  $\hat{\alpha}_{t|n} = \hat{\alpha}_{t|t-1} + P_{t|t-1} r_{t-1}$  and  $P_{t|n} = P_{t|t-1} - P_{t|t-1}^2 N_{t-1}$ .
- 

Note that  $(P_{1|n}, \dots, P_{n|n})^T$  and  $(P_{1,2|n}, \dots, P_{n-1,n|n})^T$  are respectively the diagonal and first diagonal of  $V_0 = (I/\sigma_\epsilon^2 + \Lambda/\sigma_\eta^2)^{-1}$  and  $(\hat{\alpha}_{1|n}, \dots, \hat{\alpha}_{n|n})^T = \mathbf{m}_{0\mathbf{1}} = V_0(\mathbf{y} - \mu\mathbf{1})/\sigma_\epsilon^2$ . We can also use the Kalman filter to compute  $\bar{\mathbf{w}}^{\text{opt}} = V_0 \mathbf{1}/\sigma_\epsilon^2$  and  $a^{\text{opt}} = 1 - \text{tr}(V_0)/\sigma_\epsilon^2$  by setting  $\mathbf{y} = \mathbf{0}$ ,  $\mu = -1$ ,  $\sigma_\epsilon^2 = 1$  and  $\sigma_\eta^2 = \gamma$  in the above algorithm. If  $\sigma_\epsilon$  is not constant across  $t$ , we only need to replace  $\sigma_\epsilon$  by  $\sigma_{\epsilon_t}$  in the Kalman filter.

## 15 EM Algorithm for finding posterior mode (unknown scale parameter)

Suppose a prior  $p(\sigma_\eta^2)$  has been specified on  $\sigma_\eta^2$ . Then at convergence,

$$\begin{aligned}
\frac{\partial Q(\boldsymbol{\theta}|\boldsymbol{\theta})}{\partial \sigma_\eta^2} &= \frac{1}{2\sigma_\eta^2} \left\{ (1-a) \left[ \text{tr} \left( \frac{\Lambda}{\sigma_\eta^2} V_0 \right) + \mathbf{m}_{0\mathbf{w}}^T \frac{\Lambda}{\sigma_\eta^2} \mathbf{m}_{0\mathbf{w}} - n \right] + \mu^2 \bar{\mathbf{w}}^T \frac{\Lambda}{\sigma_\eta^2} \bar{\mathbf{w}} + a \sigma_\epsilon^{-2} (\mathbf{y} - \mu \mathbf{w})^T \mathbf{m}_{0\mathbf{w}} \right. \\
&\quad \left. + (a-2) \mu \mathbf{m}_{0\mathbf{w}}^T \frac{\Lambda}{\sigma_\eta^2} \bar{\mathbf{w}} - a \sigma_\epsilon^{-2} \left[ \text{tr}(V_0) + \mathbf{m}_{0\mathbf{w}}^T \mathbf{m}_{0\mathbf{w}} \right] \right\} + \nabla_{\sigma_\eta^2} \log p(\sigma_\eta^2) = 0.
\end{aligned}$$

If we set  $a = 1$  and  $\mathbf{w} = \mathbf{1}$ , we obtain

$$\mathbf{m}_{01} \frac{\Lambda}{\sigma_\eta^2} \mathbf{m}_{01} - \sigma_\epsilon^{-2} \text{tr}(V_0) + 2\sigma_\eta^2 \nabla_{\sigma_\eta^2} \log p(\sigma_\eta^2) = 0. \quad (31)$$

Thus, the posterior mode  $\sigma_\eta^2$  satisfies (31). Substituting (31) into (19), we obtain

$$\begin{aligned} I_{\sigma_\eta^2, \sigma_\eta^2}^B &= \frac{1}{2\sigma_\eta^4} \left\{ n(a-1)^2 + \frac{a^2}{2} \mathbf{m}_{0\mathbf{w}}^T V_0^{-1} \mathbf{m}_{0\mathbf{w}} - 2a\mu \mathbf{m}_{01}^T \frac{\Lambda}{\sigma_\eta^2} \bar{\mathbf{w}} + 4(a-1)\sigma_\eta^2 \nabla_{\sigma_\eta^2} \log p(\sigma_\eta^2) \right\}, \\ \frac{\partial I_{\sigma_\eta^2, \sigma_\eta^2}^B}{\partial a} &= \frac{1}{2\sigma_\eta^4} \left\{ 2n(a-1) + a\mathbf{m}_{0\mathbf{w}}^T V_0^{-1} \mathbf{m}_{0\mathbf{w}} - 2\mu \mathbf{m}_{01}^T \frac{\Lambda}{\sigma_\eta^2} \bar{\mathbf{w}} + 4\sigma_\eta^2 \nabla_{\sigma_\eta^2} \log p(\sigma_\eta^2) \right\}, \\ \frac{\partial I_{\sigma_\eta^2, \sigma_\eta^2}^B}{\partial \bar{\mathbf{w}}} &= \frac{a\mu}{2\sigma_\eta^4} (aV_0^{-1} \mathbf{m}_{0\mathbf{w}} - 2\frac{\Lambda}{\sigma_\eta^2} \mathbf{m}_{01}). \end{aligned}$$

Solving  $\partial I_{\sigma_\eta^2, \sigma_\eta^2}^B / \partial a$  and  $\partial I_{\sigma_\eta^2, \sigma_\eta^2}^B / \partial \bar{\mathbf{w}} = \mathbf{0}$  simultaneously, we obtain

$$a^{\text{opt}} = 1 - \frac{\mathbf{m}_{01}^T \frac{\Lambda}{\sigma_\eta^2} \mathbf{m}_{01} + 2\sigma_\eta^2 \nabla_{\sigma_\eta^2} \log p(\sigma_\eta^2)}{n} = 1 - \frac{\text{tr}(V_0)}{n\sigma_\epsilon^2}, \quad \mathbf{w}^{\text{opt}} = \frac{1}{\mu} \left( \frac{2V_0\Lambda}{a^{\text{opt}}\sigma_\eta^2} - I \right) \mathbf{m}_{01}.$$

Thus we obtain the same expressions of  $(a^{\text{opt}}, \mathbf{w}^{\text{opt}})$  as in Section 2.2.

## 16 Gibbs sampler and variational Bayes

Suppose  $\mu$  is the only unknown parameter and  $p(\mu) \propto 1$ .

$$\begin{aligned} p(\mu, \boldsymbol{\alpha} \mid \mathbf{y}) &\propto p(\mathbf{y} \mid \boldsymbol{\alpha}, \mu) p(\boldsymbol{\alpha} \mid \mu) \\ &\propto \exp \left\{ -\frac{(\mathbf{y} - \sigma_\eta^a \boldsymbol{\alpha} - \mu \mathbf{w})^T (\mathbf{y} - \sigma_\eta^a \boldsymbol{\alpha} - \mu \mathbf{w})}{2\sigma_\epsilon^2} - \frac{(\sigma_\eta^a \boldsymbol{\alpha} - \mu \bar{\mathbf{w}})^T \Lambda (\sigma_\eta^a \boldsymbol{\alpha} - \mu \bar{\mathbf{w}})}{2\sigma_\eta^2} \right\} \\ &\propto \exp \left\{ -\frac{\sigma_\eta^{2a} \boldsymbol{\alpha}^T V_0^{-1} \boldsymbol{\alpha} - 2\sigma_\eta^a \boldsymbol{\alpha}^T \mathbf{y} / \sigma_\epsilon^2 + \mu^2 \tau(\mathbf{w}) - 2\mu \mathbf{w}^T \mathbf{y} / \sigma_\epsilon^2 + 2\mu \sigma_\eta^a \boldsymbol{\alpha}^T \rho(\mathbf{w})}{2} \right\} \end{aligned}$$

where  $\tau(\mathbf{w}) = \sigma_\epsilon^{-2} \mathbf{w}^T \mathbf{w} + \sigma_\eta^{-2} \bar{\mathbf{w}}^T \Lambda \bar{\mathbf{w}}$  and  $\rho(\mathbf{w}) = V_0^{-1} \mathbf{w} - \sigma_\eta^{-2} \Lambda \mathbf{1}$ . Hence

$$\begin{aligned} \begin{bmatrix} \mu \\ \boldsymbol{\alpha} \end{bmatrix} \mid \mathbf{y} &\sim \text{N} \left( \begin{bmatrix} \frac{\mathbf{y}^T S^{-1} \mathbf{1}}{\mathbf{1}^T S^{-1} \mathbf{1}} \\ \sigma_\eta^{-a} V_0 \left\{ \frac{\mathbf{y}}{\sigma_\epsilon^2} - \rho(\mathbf{w}) \frac{\mathbf{y}^T S^{-1} \mathbf{1}}{\mathbf{1}^T S^{-1} \mathbf{1}} \right\} \end{bmatrix}, \begin{bmatrix} \tau(\mathbf{w}) & \sigma_\eta^a \rho(\mathbf{w})^T \\ \sigma_\eta^a \rho(\mathbf{w}) & \sigma_\eta^{2a} V_0^{-1} \end{bmatrix}^{-1} \right) \\ p(\mu \mid \boldsymbol{\alpha}, \mathbf{y}) &\propto \exp \left\{ -\frac{\mu^2 \tau(\mathbf{w}) - 2\mu \{\mathbf{w}^T \mathbf{y} / \sigma_\epsilon^2 - \sigma_\eta^a \boldsymbol{\alpha}^T \rho(\mathbf{w})\}}{2} \right\}. \end{aligned}$$

Hence

$$\mu \mid \boldsymbol{\alpha}, \mathbf{y} \sim \text{N}(\tau(\mathbf{w})^{-1} \{\sigma_\epsilon^{-2} \mathbf{y}^T \mathbf{w} - \sigma_\eta^a \boldsymbol{\alpha}^T \rho(\mathbf{w})\}, \tau(\mathbf{w})^{-1}),$$

$$p(\boldsymbol{\alpha} \mid \mu, \mathbf{y}) \propto \exp \left\{ -\frac{\sigma_\eta^{2a} \boldsymbol{\alpha}^T V_0^{-1} \boldsymbol{\alpha} - 2\boldsymbol{\alpha}^T \sigma_\eta^a \{\mathbf{y}/\sigma_\epsilon^2 - \mu \rho(\mathbf{w})\}}{2} \right\}$$

Hence

$$\boldsymbol{\alpha} \mid \mu, \mathbf{y} \sim N(\sigma_\eta^{-a} V_0 \{\mathbf{y}/\sigma_\epsilon^2 - \mu \rho(\mathbf{w})\}, \sigma_\eta^{-2a} V_0),$$

Let  $CC^T = \sigma_\eta^{-2a} V_0$  and  $Z_s \stackrel{iid}{\sim} N(0, 1)$  for  $s = 1, 2, 3$ . We can write

$$\begin{aligned} \boldsymbol{\alpha}^{(i)} &= \sigma_\eta^{-a} V_0 \{\mathbf{y}/\sigma_\epsilon^2 - \mu^{(i-1)} \rho(\mathbf{w})\} + CZ_1 \\ \mu^{(i)} &= \frac{\sigma_\epsilon^{-2} \mathbf{y}^T \mathbf{w} - \sigma_\eta^a \boldsymbol{\alpha}^{(i)T} \rho(\mathbf{w})}{\tau(\mathbf{w})} + \frac{Z_2}{\sqrt{\tau(\mathbf{w})}} \\ &= \frac{\sigma_\epsilon^{-2} \mathbf{y}^T \mathbf{w} - \rho(\mathbf{w})^T V_0 \{\mathbf{y}/\sigma_\epsilon^2 - \mu^{(i-1)} \rho(\mathbf{w})\}}{\tau(\mathbf{w})} + \frac{Z_2}{\sqrt{\tau(\mathbf{w})}} + \frac{\sigma_\eta^a \rho(\mathbf{w})^T CZ_1}{\tau(\mathbf{w})} \\ &= \frac{\mathbf{y}^T S^{-1} \mathbf{1} + \mu^{(i-1)} \rho(\mathbf{w})^T V_0 \rho(\mathbf{w})}{\tau(\mathbf{w})} + \frac{\sqrt{\tau(\mathbf{w}) + \rho(\mathbf{w})^T V_0 \rho(\mathbf{w})}}{\tau(\mathbf{w})} Z_3. \end{aligned}$$

For variational Bayes,

$$\begin{aligned} q(\mu) &\propto \exp[\mathbb{E}_{q(\boldsymbol{\alpha})} \{\log p(\mu, \boldsymbol{\alpha}, \mathbf{y})\}] \\ &\propto \exp \left[ -\frac{\mu^2 \tau(\mathbf{w}) - 2\mu \{\mathbf{w}^T \mathbf{y}/\sigma_\epsilon^2 - \sigma_\eta^a \rho(\mathbf{w})^T \mathbf{m}_\alpha^q\}}{2} \right]. \end{aligned}$$

Hence  $q(\mu)$  is  $N(\tau(\mathbf{w})^{-1} \{\mathbf{w}^T \mathbf{y}/\sigma_\epsilon^2 - \sigma_\eta^a \rho(\mathbf{w})^T \mathbf{m}_\alpha^q\}, \tau^{-1})$ .

$$\begin{aligned} q(\boldsymbol{\alpha}) &\propto \exp[\mathbb{E}_{q(\mu)} \{\log p(\mu, \boldsymbol{\alpha}, \mathbf{y})\}] \\ &\propto \exp \left[ -\frac{\sigma_\eta^{2a} \boldsymbol{\alpha}^T V_0^{-1} \boldsymbol{\alpha} - 2\sigma_\eta^a \boldsymbol{\alpha}^T \{\mathbf{y}/\sigma_\epsilon^2 - m_\mu^q \rho(\mathbf{w})\}}{2} \right]. \end{aligned}$$

Hence  $q(\boldsymbol{\alpha})$  is  $N(\sigma_\eta^{-a} V_0 \{\mathbf{y}/\sigma_\epsilon^2 - m_\mu^q \rho(\mathbf{w})\}, \sigma_\eta^{-2a} V_0)$ . In the updating,

$$\begin{aligned} \mathbf{m}_\alpha^{q(i)} &= \sigma_\eta^{-a} V_0 \{\mathbf{y}/\sigma_\epsilon^2 - m_\mu^{q(i-1)} \rho(\mathbf{w})\} \\ m_\mu^{q(i)} &= \tau(\mathbf{w})^{-1} \{\mathbf{w}^T \mathbf{y}/\sigma_\epsilon^2 - \sigma_\eta^a \rho(\mathbf{w})^T \mathbf{m}_\alpha^{q(i)}\} \\ &= \tau(\mathbf{w})^{-1} \{\mathbf{w}^T \mathbf{y}/\sigma_\epsilon^2 - \rho(\mathbf{w})^T V_0 [\mathbf{y}/\sigma_\epsilon^2 - m_\mu^{q(i-1)} \rho(\mathbf{w})]\} \\ &= \tau(\mathbf{w})^{-1} \{\mathbf{y}^T S^{-1} \mathbf{1} + m_\mu^{q(i-1)} \rho(\mathbf{w})^T V_0 \rho(\mathbf{w})\}. \end{aligned}$$

## 17 Allowing $\sigma_\epsilon^2$ to vary with time

Suppose  $\sigma_\epsilon^2$  is replaced by  $\sigma_{\epsilon_t}^2$  at time  $t$  in the Gaussian state space model. Let  $\boldsymbol{\sigma}_\epsilon^2 = (\sigma_{\epsilon_1}^2, \dots, \sigma_{\epsilon_n}^2)^T$ . Then in matrix notation, the model can be expressed as

$$\mathbf{y} \mid \boldsymbol{\alpha}, \boldsymbol{\theta} \sim N(\sigma_\eta^a \boldsymbol{\alpha} + \mu \mathbf{w}, D_\epsilon), \quad \sigma_\eta^a \boldsymbol{\alpha} \mid \boldsymbol{\theta} \sim N(\mu \bar{\mathbf{w}}, \sigma_\eta^2 \Lambda^{-1}),$$

where  $D_\epsilon = \text{diag}(\boldsymbol{\sigma}_\epsilon^2)$ . The marginal distribution of  $\mathbf{y}$  is  $N(\mu \mathbf{1}, S)$  where  $S = D_\epsilon + \sigma_\eta^2 \Lambda^{-1}$  and the conditional distribution  $p(\boldsymbol{\alpha} \mid \mathbf{y}, \boldsymbol{\theta})$  is  $N(\mathbf{m}_{\text{aw}}, V_a)$ , where

$$V_a = \sigma_\eta^{-2a} (D_\epsilon^{-1} + \sigma_\eta^{-2} \Lambda)^{-1}, \quad \mathbf{m}_{\text{aw}} = \sigma_\eta^a V_a [D_\epsilon^{-1} (\mathbf{y} - \mu \mathbf{w}) + \mu \sigma_\eta^{-2} \Lambda \bar{\mathbf{w}}].$$

When  $a = 0$  and  $\mathbf{w} = \mathbf{1}$ ,  $V_0 = (D_\epsilon^{-1} + \sigma_\eta^{-2} \Lambda)^{-1}$  and  $\mathbf{m}_{01} = V_0 D_\epsilon^{-1} (\mathbf{y} - \mu \mathbf{1})$ . It can be derived that

$$\begin{aligned} Q(\boldsymbol{\theta} \mid \boldsymbol{\theta}^{(i)}) &= \frac{1}{2} [\log(1 - \phi^2) - (\mathbf{y} - \mu \mathbf{w} - \sigma_\eta^a \mathbf{m}_{\text{aw}}^{(i)})^T D_\epsilon^{-1} (\mathbf{y} - \mu \mathbf{w} - \sigma_\eta^a \mathbf{m}_{\text{aw}}^{(i)}) \\ &\quad - \sigma_\eta^{2a} \text{tr}(D_\epsilon^{-1} V_a^{(i)}) - \log |D_\epsilon| - n(1 - a) \log(\sigma_\eta^2) - \sigma_\eta^{2(a-1)} \text{tr}(\Lambda V_a^{(i)}) \\ &\quad - \sigma_\eta^{-2} (\sigma_\eta^a \mathbf{m}_{\text{aw}}^{(i)} - \mu \bar{\mathbf{w}})^T \Lambda (\sigma_\eta^a \mathbf{m}_{\text{aw}}^{(i)} - \mu \bar{\mathbf{w}})] - n \log(2\pi). \end{aligned}$$

$$\nabla_\mu Q(\boldsymbol{\theta} \mid \boldsymbol{\theta}^{(i)}) = (\mathbf{y} - \mu \mathbf{w} - \sigma_\eta^a \mathbf{m}_{\text{aw}}^{(i)})^T D_\epsilon^{-1} \mathbf{w} + \sigma_\eta^{-2} (\sigma_\eta^a \mathbf{m}_{\text{aw}}^{(i)} - \mu \bar{\mathbf{w}})^T \Lambda \bar{\mathbf{w}}.$$

$$\nabla_\mu^2 Q(\boldsymbol{\theta} \mid \boldsymbol{\theta}^{(i)}) = -(\mathbf{w}^T D_\epsilon^{-1} \mathbf{w} + \sigma_\eta^{-2} \bar{\mathbf{w}}^T \Lambda \bar{\mathbf{w}}),$$

$$\begin{aligned} \nabla_{\sigma_\eta^2} Q(\boldsymbol{\theta} \mid \boldsymbol{\theta}^{(i)}) &= \frac{1}{2\sigma_\eta^4} \left\{ n(a-1)\sigma_\eta^2 - (a-1)\sigma_\eta^{2a} [\text{tr}(\Lambda V_a^{(i)}) + \mathbf{m}_{\text{aw}}^{(i)T} \Lambda \mathbf{m}_{\text{aw}}^{(i)}] + \mu^2 \bar{\mathbf{w}}^T \Lambda \bar{\mathbf{w}} \right. \\ &\quad + (a-2)\mu \sigma_\eta^a \mathbf{m}_{\text{aw}}^{(i)T} \Lambda \bar{\mathbf{w}} + a\sigma_\eta^{a+2} (\mathbf{y} - \mu \mathbf{w})^T D_\epsilon^{-1} \mathbf{m}_{\text{aw}}^{(i)} \\ &\quad \left. - a\sigma_\eta^{2a+2} [\text{tr}(D_\epsilon^{-1} V_a^{(i)}) + \mathbf{m}_{\text{aw}}^{(i)T} D_\epsilon^{-1} \mathbf{m}_{\text{aw}}^{(i)}] \right\}. \end{aligned}$$

$$\begin{aligned} \nabla_{\sigma_\eta^2}^2 Q(\boldsymbol{\theta} \mid \boldsymbol{\theta}^{(i)}) &= -\frac{1}{2\sigma_\eta^4} \left\{ n(a-1) + (a-1)(a-2)\sigma_\eta^{2a-2} [\text{tr}(\Lambda V_a^{(i)}) + \mathbf{m}_{\text{aw}}^{(i)T} \Lambda \mathbf{m}_{\text{aw}}^{(i)}] \right. \\ &\quad - (a-2) \left( \frac{a}{2} - 2 \right) \sigma_\eta^{a-2} \mu \mathbf{m}_{\text{aw}}^{(i)T} \Lambda \bar{\mathbf{w}} - a \left( \frac{a}{2} - 1 \right) \sigma_\eta^a (\mathbf{y} - \mu \mathbf{w})^T D_\epsilon^{-1} \mathbf{m}_{\text{aw}}^{(i)} \\ &\quad \left. + a(a-1)\sigma_\eta^{2a} [\text{tr}(D_\epsilon^{-1} V_a^{(i)}) + \mathbf{m}_{\text{aw}}^{(i)T} D_\epsilon^{-1} \mathbf{m}_{\text{aw}}^{(i)}] + 2\mu^2 \sigma_\eta^{-2} \bar{\mathbf{w}}^T \Lambda \bar{\mathbf{w}} \right\}. \end{aligned}$$

We have the following identities:

$$\begin{aligned} V_0 &= \sigma_\eta^{2a} V_a = (D_\epsilon^{-1} + \frac{\Lambda}{\sigma_\eta^2})^{-1}, & S &= D_\epsilon + \sigma_\eta^2 \Lambda^{-1} \\ \mathbf{m}_{0\mathbf{w}} &= \sigma_\eta^a \mathbf{m}_{\text{aw}} = V_0 D_\epsilon^{-1} (\mathbf{y} - \mu \mathbf{1}) + \mu \bar{\mathbf{w}}, & S^{-1} &= \frac{\Lambda}{\sigma_\eta^2} V_0 D_\epsilon^{-1} = D_\epsilon^{-1} V_0 \frac{\Lambda}{\sigma_\eta^2} = D_\epsilon^{-1} - D_\epsilon^{-1} V_0 D_\epsilon^{-1}, \\ \mathbf{m}_{01} &= \mathbf{m}_{0\mathbf{w}} - \mu \bar{\mathbf{w}} = V_0 D_\epsilon^{-1} (\mathbf{y} - \mu \mathbf{1}), & \sigma_\eta^2 \Lambda^{-1} &= V_0 D_\epsilon^{-1} S = S D_\epsilon^{-1} V_0 = V_0 + V_0 D_\epsilon^{-1} S D_\epsilon^{-1} V_0, \\ \mathbf{m}_{00} &= \mathbf{m}_{0\mathbf{w}} + \mu \mathbf{w} = V_0 (D_\epsilon^{-1} \mathbf{y} + \mu \frac{\Lambda}{\sigma_\eta^2} \mathbf{1}), & \frac{\Lambda}{\sigma_\eta^2} V_0 \frac{\Lambda}{\sigma_\eta^2} &= \frac{\Lambda}{\sigma_\eta^2} V_0 (V_0^{-1} - D_\epsilon^{-1}) = \frac{\Lambda}{\sigma_\eta^2} - S^{-1}, \\ & & \frac{\Lambda}{\sigma_\eta^2} \mathbf{m}_{01} &= D_\epsilon^{-1} (\mathbf{y} - \mathbf{m}_{00}) = S^{-1} (\mathbf{y} - \mu \mathbf{1}), \end{aligned}$$

Setting  $\nabla_{\mu}Q(\boldsymbol{\theta} \mid \boldsymbol{\theta}^{(t)}) = 0$  at  $\boldsymbol{\theta}, \boldsymbol{\theta}^{(t)} = \boldsymbol{\theta}^*$ :

$$\begin{aligned}
(\mathbf{y} - \mu \mathbf{w} - \mathbf{m}_{0\mathbf{w}})^T D_{\epsilon}^{-1} \mathbf{w} + (\mathbf{m}_{0\mathbf{w}} - \mu \bar{\mathbf{w}})^T \frac{\Lambda}{\sigma_{\eta}^2} \bar{\mathbf{w}} &= 0 \\
(\mathbf{y} - \mathbf{m}_{00})^T D_{\epsilon}^{-1} \mathbf{w} + \mathbf{m}_{01}^T \frac{\Lambda}{\sigma_{\eta}^2} \bar{\mathbf{w}} &= 0 \\
[D_{\epsilon}^{-1}(\mathbf{y} - \mathbf{m}_{00}) - \frac{\Lambda}{\sigma_{\eta}^2} \mathbf{m}_{01}]^T \mathbf{w} + \mathbf{m}_{01}^T \frac{\Lambda}{\sigma_{\eta}^2} \mathbf{1} &= 0 \quad \implies \mu = \frac{\mathbf{y}^T S^{-1} \mathbf{1}}{\mathbf{1}^T S^{-1} \mathbf{1}}. \\
\mathbf{m}_{01}^T \frac{\Lambda}{\sigma_{\eta}^2} \mathbf{1} &= 0 \\
(\mathbf{y} - \mu \mathbf{1})^T S^{-1} \mathbf{1} &= 0
\end{aligned}$$

Setting  $\nabla_{\sigma_{\eta}^2}Q(\boldsymbol{\theta} \mid \boldsymbol{\theta}^{(t)}) = 0$  at  $\boldsymbol{\theta}, \boldsymbol{\theta}^{(t)} = \boldsymbol{\theta}^*$ :

$$n(a-1) - a \text{tr}(D_{\epsilon}^{-1} V_0) - (a-1) \text{tr}(V_0 \frac{\Lambda}{\sigma_{\eta}^2}) + \mathbf{m}_{01}^T \frac{\Lambda}{\sigma_{\eta}^2} \mathbf{m}_{01} + a \mathbf{m}_{0\mathbf{w}}^T [D_{\epsilon}^{-1}(\mathbf{y} - \mathbf{m}_{00}) - \frac{\Lambda}{\sigma_{\eta}^2} \mathbf{m}_{01}] = 0.$$

Thus

$$\sigma_{\eta}^2 = \frac{(1-a) \text{tr}(V_0 \Lambda) + \mathbf{m}_{01}^T \Lambda \mathbf{m}_{01}}{n(1-a) + a \text{tr}(D_{\epsilon}^{-1} V_0)}.$$

Setting  $a = 0$  or  $a = 1$ , we obtain

$$\mathbf{m}_{01}^T \Lambda \mathbf{m}_{01} = \sigma_{\eta}^2 \text{tr}(D_{\epsilon}^{-1} V_0) = n \sigma_{\eta}^2 - \text{tr}(V_0 \Lambda).$$

The elements in the augmented information matrix are given by

$$\begin{aligned}
I_{\mu, \mu} &= \mathbf{w}^T D_{\epsilon}^{-1} \mathbf{w} + \sigma_{\eta}^{-2} \bar{\mathbf{w}}^T \Lambda \bar{\mathbf{w}}, \\
I_{\sigma_{\eta}^2, \sigma_{\eta}^2} &= \frac{1}{2\sigma_{\eta}^4} \left\{ n(a-1)^2 + \frac{a^2}{2} \mathbf{m}_{0\mathbf{w}}^T V_0^{-1} \mathbf{m}_{0\mathbf{w}} - 2a\mu \bar{\mathbf{w}}^T \frac{\Lambda}{\sigma_{\eta}^2} \mathbf{m}_{01} \right\}.
\end{aligned}$$

Since  $\nabla_{\mu} I_{\mu, \mu} = 2[D_{\epsilon}^{-1} \mathbf{w} - \frac{\Lambda}{\sigma_{\eta}^2} \bar{\mathbf{w}}]$  and  $\nabla_{\mu} I_{\mu, \mu} = 2V_0^{-1}$ , the rate of convergence of Algorithm 1 is minimized at

$$\mathbf{w}^{\text{opt}} = \sigma_{\eta}^{-2} V_0 \Lambda \mathbf{1} \quad \text{or} \quad \bar{\mathbf{w}} = V_0 D_{\epsilon}^{-1} \mathbf{1}.$$

For Algorithm 2, setting  $\nabla_a I_{\sigma_{\eta}^2, \sigma_{\eta}^2} = 0$  and  $\nabla_{\sigma_{\eta}^2} I_{\sigma_{\eta}^2, \sigma_{\eta}^2} = 0$  if  $\mu \neq 0$  yields

$$a = \frac{2n + 2\mu \bar{\mathbf{w}}^T \frac{\Lambda}{\sigma_{\eta}^2} \mathbf{m}_{01}}{2n + \mathbf{m}_{0\mathbf{w}}^T V_0^{-1} \mathbf{m}_{0\mathbf{w}}}, \quad \bar{\mathbf{w}} = \frac{1}{\mu} \left( \frac{2}{a} V_0 \frac{\Lambda}{\sigma_{\eta}^2} \mathbf{m}_{01} - \mathbf{m}_{01} \right).$$

Solving these two equations simultaneously,

$$a = 1 - \frac{\mathbf{m}_{01}^T \frac{\Lambda}{\sigma_{\eta}^2} \mathbf{m}_{01}}{n} = \frac{\text{tr}(V_0 \Lambda)}{n \sigma_{\eta}^2} = 1 - \frac{\text{tr}(V_0 D_{\epsilon}^{-1})}{n}.$$

It can be verified similarly that the Hessian of  $I_{\sigma_{\eta}^2, \sigma_{\eta}^2}$  is symmetric positive definite.